For Reference

NOT TO BE TAKEN FROM THIS ROOM

For Reference

NOT TO BE TAKEN FROM THIS ROOM

Ex libris
universitatis
albertaensis

UNIVERSITY OF ALBERTA
QUAECUMQUE VERA

University of Albe
Printing Departme

Digitized by the Internet Archive
in 2019 with funding from
University of Alberta Libraries

https://archive.org/details/kineticsofdissol00howa

THE UNIVERSITY OF ALBERTA

THE KINETICS OF THE DISSOLUTION OF CRYSTALLINE QUARTZ IN WATER AT HIGH TEMPERATURES AND HIGH PRESSURES

A THESIS
SUBMITTED TO THE FACULTY OF GRADUATE STUDIES IN
PARTIAL FULFILMENT OF THE REQUIREMENTS FOR THE
DEGREE OF MASTER OF SCIENCE

DEPARTMENT OF MINING AND METALLURGY

by

Howard Siebert
Edmonton, Alberta
July 1964

UNIVERSITY OF ALBERTA

FACULTY OF GRADUATE STUDIES

The undersigned certify that they have read and recommend to the Faculty of Graduate Studies for acceptance, a thesis titled "The Kinetics of the Dissolution of Crystalline Quartz in Water at High Temperatures and High Pressures" submitted by Howard Siebert, B. Sc., in partial fulfilment of the requirements for the degree of Master of Science.

TABLE OF CONTENTS

PAGE

INTRODUCTION 1

REVIEW OF LITERATURE 3

Kinetics Data 3

Mechanism of Quartz Dissolution and the State of the Dissolved Species 4

The Effect of Surface Treatments on the Rate of Dissolution of Quartz Powders 8

Beilby Layer 8

Incomplete Monolayer or Multilayer of Silicic Acid 10

The Effect of Crystallographic Orientation on the Rate of Dissolution 12

The Solubility of Quartz in Water at High Temperatures and High Pressures 13

THEORY 16

Derivation of Rate Equation 16

EXPERIMENTAL 20

Equipment 20

Platelet Tests 20

Powder Tests 22

The Solution Used 25

Preparation of Quartz Samples 25

Platelet Tests 25

Powder Tests 27

PAGE

Preparation of the Autoclave for an Experiment .. 28
  Platelet Tests 28
  Powder Tests 28
Sampling Procedure 29
  Platelet Tests 29
  Powder Tests 30
Analytical Technique 30
EXPERIMENTAL RESULTS 48
Stirring Speed 48
  Platelet Tests 48
  Powder Tests 49
Sampling 50
High Solubility Layer 53
Accuracy of the Colorimetric Method as Compared to Weight Loss Determinations for Dissolved Silica 55
State of the Dissolved Species 56
Adsorption of Silica on Stainless Steel 57
Surface Area of the Quartz Powder 61
The Data as Expressed by the First Order Rate Equation 63
Surface Phenomena Observed on the Platelets 64
Experimental Errors 64
DISCUSSION OF RESULTS 68
CONCLUSIONS 84

PAGE

REFERENCES 87

APPENDIX I:

Calculation of Data 89

Rate Equation Calculations 89

Calculation of Activation Energy 91

APPENDIX II:

Tables VIII-XIII 93

ABSTRACT

Dissolution of quartz discs (cut parallel to basal (0001) plane) and quartz powders (-200#, +270#) in double distilled water, at 233°C - 301°C and 3000 psi, was found to proceed as a first order reaction, involving an activation energy of 18.7 kcal/mole; i.e. of the same magnitude as dissolution of quartz in alkaline media. The basal (0001) plane of quartz appears to dissolve seventy times faster than the randomly oriented planes of the powder. The molybdate determinations for dissolved silica suggest that the monomeric form of silicic acid is formed in solution,

$$SiO_2(\text{quartz}) + 2H_2O_{(1)} \rightleftharpoons Si(OH)_4(\text{solution})$$

ACKNOWLEDGEMENTS

The investigations described in this thesis were carried out in the laboratories of the Department of Mining and Metallurgy under the supervision of Professor E.O. Lilge and Dr. J. Leja. It has been the author's pleasure to work under and be associated with these two people.

The author also wishes to thank the other members of the Department of Mining and Metallurgy, particularly Dr. W. V. Youdelis for his assistance in the field of rate theory, Mr. L. Perry for his advice and assistance in overcoming the many mechanical difficulties encountered, Mrs. S. Kobusiak, Mrs. M. Stingley, Mr. R. M. Scott, Mr. J. Cahoon, and Mr. J. Wojno for their help and advice in preparing the thesis.

Grateful acknowledgement is made to Eldorado Mining and Refining Limited for the financial assistance given to the writer during his Master's program.

LIST OF TABLES

TABLE PAGE

I Relative Value of Rate Constant 4

II-A Verification of the Sampling Method Adopted for the Platelet Tests 51

II-B Verification of the Sampling Method Adopted for the Powder Tests 52

III Comparison of Colorimetric and Weight Loss Methods for Total Silica 55

IV The State of the Dissolved Species 56

V Rate of Desorption of Silica from Stainless Steel at 470°F 58

VI Sources of Systematic Error 66

VII Comparison of Activation Energies Determined by Other Investigators 70

VIII (1-17) Experimental Data and Calculations for a First Order Reaction 93

IX Least Squares Computer Program 110

X-A Compilation of Data from Least Squares Computer Analysis of Experimental Data for Dissolution of Quartz Plates in Water 112

X-B Compilation of Data from Least Squares Computer Analysis of Experimental Data for Dissolution of Quartz Powder in Water 113

XI Slopes, Specific Rate Constants and Reciprocal Kelvin Temperatures for Each Experiment ... 114

TABLE PAGE

XII Standard Deviation of Slope Computed as Per Cent 115

XIII Standard Deviation of C_s Compared to Maximum Deviation of C_s 116

LIST OF FIGURES

FIGURE PAGE

1 Isobaric Solubility Curves for the Quartz-Water System 15

2 Cross Section of a 1-Litre Autoclave Modified for Magnetically Coupled Stirring. 33

3 1-Litre Autoclave Assembled for Operation ... 34

4-A Component Parts of the Dismantled Autoclave.. 35

4-B View Showing the Arrangement of the Working Parts Inside the Autoclave 35

4-C Exploded View of the Magnetic Coupling 35

5-A Schematic Flow Diagram of Gas Compression and Measuring System to Autoclave 36

5-B Schematic Flow Diagram of the Autoclave, Transducer and Associated Electrical Controls 37

6 Plan and Layout of the Gas Compression and Measuring System 38

7-A Electrical Circuits of Transducer and Associated Electrical Equipment 39

7-B Electrical Circuit of Overset-Underset Heater Control System 40

8 Exploded View of the Stainless Steel Holder and Its Disposition Within the Autoclave 41

9 Sample Dropping Mechanism 42

FIGURE PAGE
10 Sampling Apparatus 43
11 Cross Sectional View of the Stainless Steel Filter Used Within the Autoclave 44
12 Calibration Curve for Variacs Used in Overset-Underset Heater Control System 45
13 Photomicrographs of the (-200#, +270#) Quartz Powder 46
14 Bausch and Lomb Spectronic-20 Colorimeter Calibration Curve 47
15 The Effect of Stirring on the Rate of Dissolution of a Quartz Plate in Water 72
16 The Effect of Stirring Speed on the Rate of Dissolution of Quartz Powder 73
17 A Study of the Effect of Varying Volume (Due to Sampling) on Rate 74
18 Typical Plot of Concentration vs. Time Exhibiting the Three Reaction Zones for the Reaction of Quartz in Water 75
19 Adsorption Isotherm for the Soluble Silica/Stainless Steel Interface 76
20 Model of SiO_4 Tetrahedron in the Plan View .. 77
21 Reproducibility Test 78
22 Relation Between Rate and Surface Area of Quartz Available for Reaction 79

FIGURE PAGE

23-A Effect of Temperature on Rate as Expressed by the First Order Rate Equation for the Reaction of a Quartz Plate with Water 80

23-B Effect of Temperature on Rate as Expressed by the First Order Rate Equation for the Reaction of a Quartz Plate with Water 81

24 Effect of Temperature on Rate as Expressed by the First Order Rate Equation for the Reaction of Quartz Powder with Water 82

25-A Quartz Surface After Polishing Before Dissolution, 380X 83

25-B Quartz Surface After Dissolution at 315°C, 380X 83

25-C Quartz Surface After Dissolution at 219°C, 137X 83

26 Arrhenius Plot for Activation Energy 86

INTRODUCTION

In 1961 a research program on the dissolution of non-metallic minerals in alkaline leach liquors was initiated under a grant from Eldorado Mining and Refining, in order to examine the variables affecting the solubility and dissolution rates of silica and silicates in alkaline leach liquors. The object of these investigations was to determine the factors which contributed to the sodium carbonate consumption in alkaline leaching of uranium ores. Since the bulk of the ores is made up of silica and silicates, it was thought that part of the consumption could be attributed to the dissolution of these non-metallics.

To pursue such an investigation to its final conclusion involves a study of the dissolution of each of the silica and silicate minerals, a problem considered to be too comprehensive to be undertaken at the time. However, since quartz comprises an appreciable portion of the feed to the alkaline leach process, this mineral was singled out as a basis for study and then only in a quartz-water system. Specifically in this thesis, a literature survey and results of investigations related to the "Kinetics of the Dissolution of Crystalline Quartz in Water at High Temperatures and High Pressures" are discussed. This will form a basis for further study of the more complex systems: quartz-sodium hydroxide, quartz-sodium carbonate and sodium bicarbonate.

A survey of the literature concerning the quartz-water

system suggested that the reaction should be studied at temperatures above 150°C in order that kinetic data can be obtained in a reasonable period of time, and in order that the rate is not masked by slight inconsistencies of the quartz surfaces. Further, the rate of dissolution for basal (0001) plane was studied in the first series of tests since quartz dissolves most rapidly from this plane. This work has already been published in a paper (38). Once the kinetics of dissolution for the basal (0001) plane was established, further studies of the rate of dissolution of randomly oriented planes (powders) were studied for comparison. The higher surface areas (and therefore lower reaction interval) and convenience in handling the powders facilitated a thorough study of all the factors that might affect the rate of dissolution of crystalline quartz.

REVIEW OF LITERATURE

Kinetics Data

Although there are abundant thermodynamic data for the quartz-water system (1,3,5-9), very few kinetics data exist for this system (10-12). The work of Hooley (11) is mainly concerned with dissolution of silica glass and quartz by hydroxides of Group I at temperatures below 100°C, while that of Greenberg and O'Connor (12) is primarily concerned with the dissolution of amorphous silica in water at temperatures below 100°C. Greenberg and O'Connor (12) propose a rate equation for the dissolution of quartz in water;

i.e. $$\log\left[\frac{Ce - C}{Ce}\right] = kSt$$

where: Ce = equilibrium solubility of quartz in water,

C = concentration of monosilicic acid in solution at time t,

k = rate constant,

S = surface area of the quartz.

Unfortunately, they lack sufficient reliable data to verify this rate equation.

Kitahara (10) has carried out some rate studies on pure crystalline quartz in water under supercritical conditions (i.e. 400-480°C and specific volumes of water ranging from 1.6 to 3.0 ml/gm). He applied the rate equation proposed by Greenberg (12) to his data and plotted $\log\left[(Ce - C)/Ce\right]$

against time for each temperature and specific volume and obtained straight lines. The relative values of rate constant "k" were obtained from the slopes of these lines.

TABLE I

RELATIVE VALUE OF RATE CONSTANT(10)

Temp. °C	Specific Volume mg/g	Ce Wt. %	Relative Value of Rate Constant
400	3	0.046	6.8
440	3	0.053	4.0
480	3	0.075	3.6
400	2	0.080	3.8
440	2	0.110	2.8
480	2	0.158	2.8
440	1.6	0.130	2.6

Although the bombs and contents were not agitated (probably this was not necessary since the solvent is in the gaseous phase), the results indicate that the mechanism of solution is not diffusion controlled.

Mechanism of Quartz Dissolution and the State of the Dissolved Species

There is some doubt as to whether the nature of the dissolved species is a colloidal polyelectrolyte, monomeric silicic acid or monomeric silicate.

Frederickson and Cox(29) carried out tests on the solubility of quartz in water at temperatures ranging from 200-370°C. Electron micrographs of the reaction products and the leached quartz surfaces led them to conclude that the dissolution of quartz involves a disintegration of mosaic elements (cemented together by weaker O-O bonds than Si-O bonds within the mosaic) to give a suspension of colloidal particles, the average size of which they calculate to be of the order of 800Å.

Hooley(11) proposes that the dissolution of quartz in hydroxide solutions is a two-step mechanism:

$$(1) \quad SiO_{2\,(solid)} + 2H_2O \rightleftharpoons SiO_2.2H_2O_{(s)}$$

$$(2) \quad SiO_2.2H_2O + 2OH^- \rightleftharpoons Si(OH)_6^{2-} \text{ (in solution)}$$

The first step is an adsorption of water followed by reaction with the hydroxyl ion to produce soluble products. Hooley states that if the pH of the solution is 7, as in NaCl solutions, no attack of crystalline quartz will take place. Work by Van Lier(1) shows that solubility of quartz in NaCl solutions of 10^{-1} N NaCl is the same as the solubility in H_2O, and at higher concentrations of NaCl there is a strong accelerating effect on the rate of dissolution. This seems to rule out the basis for Hooley's theory and the existence of a monomeric silicate in the quartz-water system. Iler(13) considers that "the dissolution of solid silica in water involves a simultaneous hydration and depolymerization:

$$(3)\quad (SiO_2)_n + 2n(H_2O) \rightleftharpoons n\ Si(OH)_4$$

When silica passes into solution, there must be a chemical reaction on the surface of the solid phase with water, whereby the surface layer of SiO_2 is hydrated; then as each silicon atom with its surrounding oxygen atom is detached from the surface, further reaction with water occurs and soluble monosilicic acid is formed."

According to Franck(15) the solution of quartz in pure water may be represented by the reaction

$$Q + n.H_2O \rightleftharpoons SiO_2.nH_2O$$

where Q represents solid crystalline quartz. In a thermodynamic treatment of Kennedy's solubility data for quartz in water(9), Mosebach(16) and Franck(15) have both deduced the association constant n as equal to 2. Wood(8) set up a theoretical equation for the solubility of quartz in supercritical water, the chemical potentials of the participating components being evaluated by methods of statistical mechanics. Upon fitting the equation to the experimental quartz solubility data of Kennedy(9) he deduced that complex hydrated molecules (probably polymers of H_4SiO_4) are involved at pressures greater than 500 bars. These molecules dissociate at lower pressures and further polymerize at higher pressures.

Jander and Jahr(33) have measured the diffusion coefficient of silica from silica gel. (In the formation

of quartz veins(13) it is suspected that deposition of silica sometimes precedes the development of quartz crystals.) They have deduced that in all cases where amorphous silica is reacted with water, the SiO_2 is dissolved "crystalloidally, not colloidally." They believe it to be present in "true" solution since it goes through membrane filters of small pore size. A diffusion coefficient of 0.53 was determined which, according to Jander, is an almost conclusive evidence of monomolecular silicic acid.

Morey(3) in his solubility measurements of quartz powders in water found that the colorimetric analysis for monomeric silica and the colorimetric analysis for total silica were identical, provided that the analysis were started immediately after the samples had been collected. This provides further evidence that the species in aqueous solution is either monomeric or that it reacts stoichiometrically with molybdate in the same fashion as does the monomer.

On reviewing this information it might be concluded that the reaction mechanism is:

(a) Disintegration of the mosaic elements due to the dissolution of the higher solubility material cementing them together.

(b) The appearance in solution of colloidal particles 800Å in diameter (from the elements forming the mosaic) and monomeric silica

(from the material cementing the elements of the mosaic).

(c) Further disintegration of the colloid to polysilicic acid and monomeric silicic acid.

The Effect of Surface Treatments on the Rate of Dissolution of Quartz Powders

The existence of a high solubility (H.S.) layer on the surface of ground quartz particles has been established by various workers(18-24), though the nature of this layer is a subject of considerable controversy. This layer is thought to be either

(a) a Beilby type layer consisting only of mechanically "disturbed" amorphous silica, or

(b) an incomplete monolayer or multilayer of silicic acid.

Beilby Layer. Kitto and Patterson(18) were among the first to suggest the existence of the high solubility "Beilby" type layer. Ritchie and co-workers(19-23) proposed that the high solubility layer is composed of "a thin outer skin" (0.02-0.03μ) of high solubility, blending via a thicker and less soluble transitional layer into a resistant crystalline matrix. About one-fifth of the layer is supposedly amorphous. The nature of this "graded" structure has been investigated extensively by Ritchie and co-workers and is the subject of a series of papers(19-23).

Clelland, Cumming and Ritchie(21) demonstrated the existence of a high solubility layer by extractive solubility methods. Clelland and Ritchie(22) further showed that this high solubility layer is not a surface layer of hydrated silica, but rather is a vitreous silica layer produced during mechanical grinding which can be removed by a solvent (e.g. NaOH solution) and can be regenerated by a purely mechanical polishing process. Gibb, Ritchie and Sharpe(23) using electron optical methods showed that the original surface layer is amorphous (estimated mean thickness about 0.03-0.06μ) and that there is some evidence of an intermediate layer of very minute crystallites between the amorphous layer and the crystalline matrix. In a final paper in the series Dempster and Ritchie(19) present physical evidence consistent with the concept of a disturbed surface layer, containing non-quartz silica:

(1) Differential thermal analysis of quartz dusts is markedly affected by the presence of this layer on fine particles.

(2) A densiometric X-ray diffraction method is similarly influenced by the disturbed layer on fine particles, line intensity being markedly increased by etching the finely ground dusts.

Other workers such as Van Lier(1) and Morey(3) investigated the solubility of quartz powders in water at lower temperatures and found it necessary to remove the "disturbed"

layer in order to obtain true solubility values for crystalline quartz in water. Van Lier completely removed this layer by pretreating the quartz powder with dilute HF, successively with progressively weaker solutions of NaOH and finally with water. Van Lier estimates the thickness of the layer to be 300Å, which is consistent with the work of Ritchie.

Incomplete Monolayer or Multilayer of Silicic Acid. Holt and King$^{(24)}$ argue that if the high solubility layer were a true Beilby layer it would not be possible to regenerate it by chemical means. They have been able to regenerate this layer by equilibrating the powder with silicic acid solution after the high solubility layer has been leached off with sodium hydroxide solution. Further, they have been able to identify the layer as silicic acid by following the exchange reaction between a quartz surface and dissolved, labelled (31 Si) silicic acid. They therefore conclude that the high solubility layer is an incomplete monolayer or multilayer of silicic acid. Holt and King have calculated that one-sixth of the surface of a quartz particle is covered by a monolayer of silicic acid (assuming that 12.3$Å^2$ is the area of a silica unit).

Liberti$^{(2)}$ by the use of infrared absorption to identify quartz and other silica modifications was able to reach some fairly conclusive results with regard to the nature of the high solubility layer and possibly justify

both points of view as regards the nature of the high solubility layer.

(1) Quartz particles always have an easily solubilized layer around the surface which should be considered as a "disturbed" or semicrystalline state. The thickness of the layer depends on the grinding time (e.g. in the case where quartz is ground to $<2\mu$ in 50 hours in an agate mortar, about 50% of the quartz particle is affected).

(2) Dry grinding may cause such a friction that the external region of the particle melts and assumes the vitreous phase on cooling. By extensive grinding the interior parent structure is gradually disturbed and the thickness of the vitreous layer increases to the point that the skeletal structure of the quartz can no longer be identified.

(3) Wet grinding of quartz never causes the formation of a vitreous phase, but only that of a disturbed layer.

Heavens(33) obtained sharp Kikuchi patterns on electron-diffractograms of an acid washed quartz crystal, proving the absence of any thick layer of non-crystalline material (a 5Å layer of amorphous silica would completely obliterate the Kikuchi pattern). This shows that an amorphous layer of more

than monomolecular thickness can only result from a grinding operation.

In view of Liberti's work, we might conclude:

(1) Dry ground quartz will have a vitreous layer, the depth of which will be dependent on the length of time it was ground. This powder could also have a partial monolayer of silicic acid on the vitreous surface.

(2) Wet ground quartz will have an easily solubilized layer around the surface. The thickness of the layer depends on the grinding time. (Presumably the vitreous phase is solubilized by the water as it forms and a high solubility layer of silicic acid adsorbs on the quartz particle surfaces.

(3) A freshly fractured but unground quartz particle will not have a vitreous layer, but could possibly have on its surface a monolayer of silicic acid.

The Effect of Crystallographic Orientation on the Rate of Dissolution

Work by Landise(25) shows that in quartz crystallization the order of growth rates is under all conditions arranged in the following sequence:

basal (0001) face $>(01\bar{1}1)$ face $>(10\bar{1}1)$ face $\gg$ prism $(10\bar{1}0)$ face.

The order of dissolution rates is also the same and according to Kennedy(9), plates cut parallel to basal (0001) appear to reach equilibrium with water in one-quarter to one-half the time required by a plate cut parallel to the rhombohedral face. Mugge(31) etched various crystallographic planes of quartz with 40% HF and found that the rate of dissolution for (0001) basal plane was one hundred times that of the hexagonal face.

The Solubility of Quartz in Water at High Temperatures and High Pressures

Many researchers have investigated the solubility of quartz in water at high temperatures and high pressures(1,3,5-9,29) and it is generally acknowledged that the investigations of Kennedy(9) provide the most reliable data. He determined the solubility of quartz in water by placing carefully weighed plates of quartz in a bomb with known amounts of distilled water. The bomb was then sealed and heated for a time sufficient to insure equilibrium. The bomb was quenched, the quartz plate removed, dried and reweighed. The loss in weight of the quartz plate independent of time once equilibrium between quartz and the solution was established, coupled with knowledge of the amount of water in the bomb, gave the solubility value for the temperature and pressure involved. At a given temperature, the pressure was varied by varying the amount of water in the bomb (the

solid/liquid ratio must have also been varied). The solubility values were plotted vs. temperature as isobaric curves, as shown in Fig. 1.

Determinations have been made along the three phase (liquid-vapor-quartz) region at the vapor pressure of water, as well as determinations at higher pressures. In the three phase region the solubility of quartz rises to a maximum of 0.075 wt.% at 332°C and falls off sharply until the critical temperature of 374.11°C is reached. As pressure is increased the maximum solubility is progressively shifted to higher temperatures until 400 bars is reached, when the maximum solubility occurs above the critical temperature. At 1000 bars pressure the isobaric solubility curve remains linear below the critical temperature.

Kennedy's determinations are of high accuracy, most points lie within 0.001 wt.% of smooth isobaric curves. Duplicate runs agree with ± 0.001%.

As can be seen from Fig. 1, the solubility of quartz in water is dependent on the pressure (i.e. specific volume of the system). Since a plot of solubility against the logarithm of specific volume gives nearly linear curves, Kennedy proposes an equation for the solubility of quartz of the form:

$$S = -Af(t) \log \frac{1}{d}$$

where: S = solubility; A = constant;

t = temperature; d = density of solution.

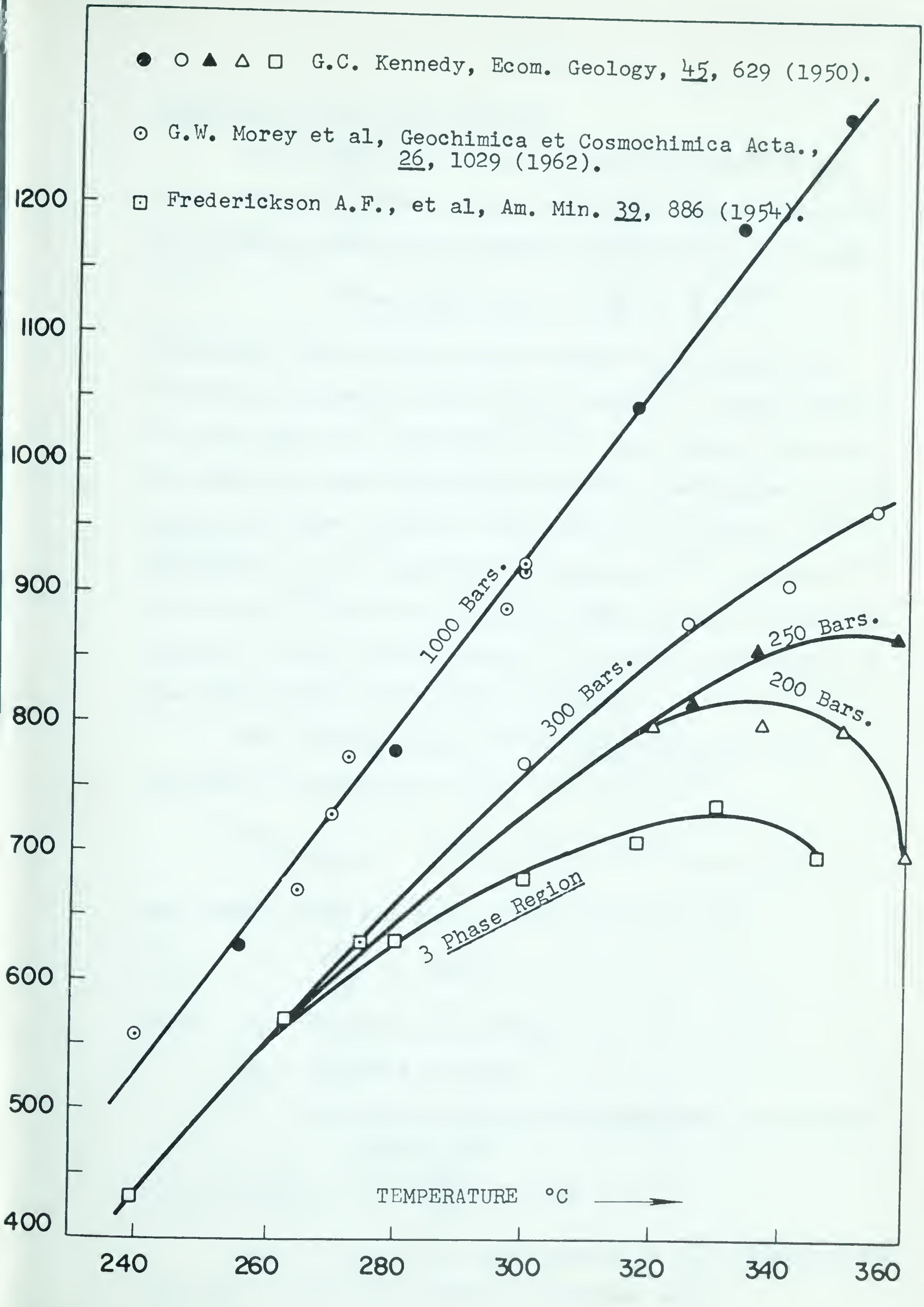

FIG. 1 ISOBARIC SOLUBILITY CURVES FOR THE QUARTZ - WATER SYSTEM

THEORY

Derivation of the Rate Equation

Data tabulated in Figs. 15 and 18 suggest a zero order reaction between quartz and water (there appears to be a linear relationship between concentration and time):

$$\text{Dissolution rate} = \frac{dc}{dt} = k \quad (38)$$

during the initial time period before equilibrium and saturation of water with SiO_2 is reached. If the reaction is zero order, it continues at the same rate ad infinitum and does not reach equilibrium as described by the various people who have worked on the solubility of quartz (1,3,5-9,29). Therefore, it was suggested by Greenberg (12), Kitahara (10) and Puxley (34) that the reaction might be more validly considered a first order reaction. A rigorous derivation of the first order rate equation follows:

The simplest suggested and probably most valid reaction of quartz with water is (13,15,16,18):

$$SiO_{2\,(solid)} + 2H_2O_{(l)} \rightleftharpoons Si(OH)_{4\,(solution)}$$

The general rate equation for this reaction is:

$$\frac{dM_s}{dt} = kM_w{}^nA^n$$

where: M_s = grammols of $Si(OH)_4$

M_w = grammols of water

A = concentration of quartz expressed as surface area in cm^2.

If we consider n = 1, $\frac{dM_s}{dt} = kM_wA$

i.e. First order with respect to H_2O concentration and first order with respect to surface area.

Rate of forward reaction is:

$$\frac{dM'_s}{dt} = k_1 M_w A = k_1 A \left[M'_w - 2M_s \right]$$

where: M'_w = initial concentration of water in grammols,

and k_1 = rate constant for forward reaction.

Rate of reverse reaction is:

$$\frac{dM''_s}{dt} = k_{-1} A M_s$$

where: k_{-1} = rate constant for reverse reaction.

Overall rate is then:

$$\frac{dM_s}{dt} = k_1 A \left[M'_w - 2M_s \right] - k_{-1} A M_s$$

but at equilibrium the rate of the forward reaction must be equal to the rate of the reverse reaction.

$$\therefore \quad k_1 A \left[M'_w - 2M^e_s \right] = k_{-1} A M^e_s$$

$$\text{and} \quad k_{-1} = k_1 \left[\frac{M'_w - 2M^e_s}{M^e_s} \right]$$

where: M^e_s = equilibrium concentration of $Si(OH)_4$

$$\therefore \quad \frac{dM_s}{dt} = k_1 A \left[M^1_w - 2M_s \right] - k_1 A M_s \left[\frac{M'_w - 2M^e_s}{M^e_s} \right]$$

$$= k_1 A M'_w \left[\frac{M^e_s - M_s}{M^e_s} \right]$$

Integrating:

$$\int \frac{dM_s}{M^e_s - M_s} = k_1 A \frac{M'_w}{M^e_s} \int dt$$

we get

$$- \ln \left[M^e_s - M_s \right] = k_1 A \left[\frac{M'_w}{M^e_s} \right] t + k'$$

at $t = 0$

$M_s = 0$

$$\therefore \quad k' = \ln M^e_s$$

and $$\ln \left[\frac{M^e_s - M_s}{M^e_s} \right] = k_1 (t) \left[\frac{M'_w}{M^e_s} \right] A$$

or $$k_1 = - \frac{M^e_s}{M'_w} \cdot \ln \left[1 - \frac{M_s}{M^e_s} \right] \cdot \frac{1}{t} \cdot \frac{1}{A} \quad \mathrm{Sec}^{-1} \mathrm{cm}^{-2}$$

For the rate equation that has been derived to be valid, the following conditions must be met:

(i) There must be a linear relationship between "A" and $\ln \left[1 - \frac{M_s}{M^e_s} \right]$ at constant temperature. (A plot of A vs. $\ln \left[1- \frac{M_s}{M^e_s} \right]$ must yield a straight line.)

(ii) There must be a linear relationship between $\ln\left[1 - \frac{M_s}{M^e_s}\right]$ and time for constant temperature and surface area. (A plot of $\ln\left[1 - \frac{M_s}{M^e_s}\right]$ vs. t must yield a straight line.)

(iii) The half-life must be constant with regard to surface to volume ratio. (The concentration of solubilized species at any time "t" will be the same for any surface to volume ratio.)

EXPERIMENTAL

Kinetics data for this thesis were collected from two series of experiments:

(a) dissolution of silica from quartz platelets, and

(b) dissolution of silica from quartz powders.

Since the equipment and techniques for the second series were radically different from the first series, it is necessary to describe them separately under the sub-headings of

1. Platelet tests
2. Powder tests

Equipment

Platelet Tests. An electrically heated autoclave of one litre capacity was used for the series of experiments. It is essentially the same unit as is shown on Figs. 2, 3 and 4 except that the stirring system was the original direct drive stirrer. This unit was sealed from leaking around the stirring shaft by the use of lubricated, teflon-asbestos packing in the stuffing box where the stainless steel spacers are now located. Some modifications to the original commercial unit were made, viz.

(a) The balanced oil lubrication system was removed because of continual leakage of oil to the reaction chamber and because of increased internal volume caused by this system. Lubrication of the stirring shaft was effected by

periodically coating the teflon-asbestos packing with molybdenum disulfide grease.

(b) A six-inch pencil thermocouple was installed immediately below the threads on the autoclave beaker so that the temperature of the liquid was measured at the point two inches above the bottom of the stirring shaft. A Honeywell Brown Electronik recorder was used in conjunction with this thermocouple to continuously record temperature during an experiment.

(c) All the existing tubing and valves on the autoclave were replaced by smaller, 21-gauge stainless steel tubing and smaller stainless steel valves.

(d) Measurements of pressure were made on a 4½" Bourdon-type Ashcroft laboratory test gauge (7,500 psi range) attached to the autoclave by an isolation valve. The Bourdon tube of the gauge and the adjoining pressure tubing were vacuum filled with distilled water to eliminate trapped air bubbles, and the isolation valve closed before attachment to the rest of the assembly. In this way, pressure in the autoclave could be brought to bear on the gauge when desired by opening the

isolation valve. The compressibility of water in the Bourdon tube was considered negligible under the test conditions.

A "Sym-ply-trol" temperature controller in conjunction with a "Powerstat" variable transformer was used to control the temperature of the solution within the autoclave. Temperature control within ± 2°C was obtained by placing the control thermocouple next to the autoclave wall and by setting the variac to give the minimum energy required for each temperature setting.

The gas compression and measuring system illustrated on Figs. 5 and 6 was used to pressurize the autoclave to the required 3000 psi working pressure and maintain it at that value. Bottled gas was let into the grooved liner compression cylinder and compressed to the desired value using the displacement pump. An oil water emulsion was used as a compressing fluid in the system.

Powder Tests. It was found, during the platelet tests, that a slight loss in pressure (along with a resultant loss in fluid as vapor) occurred between the packing and the upper stirring shaft of the autoclave. This loss of pressure and water vapor was small and could be tolerated as long as the working temperature did not exceed 600°F, the length of the run did not exceed 12 hours at high temperatures, and the stirring speed did not exceed 247 rpm. During the preliminary powder runs, when the stirring speed was

necessarily higher than 247 rpm, it was impossible to maintain a constant pressure for very long. For these reasons, the autoclave stirring system was modified to the magnetically coupled, totally enclosed stirring system illustrated on Figs. 2 and 4. The original motor supplied with the autoclave was used to drive the outer magnet as shown in Fig. 3, since the laboratory motor drive shown on Fig. 4 lacked sufficient torque to run the stirrer at more than 300 rpm.

Some details of the magnetic drive are:

(a) The speed of the stirrer is varied by the use of appropriately paired step pulleys on the drive motor and the magnet drive.

(b) To ensure that the inner and outer magnets remain coupled, the power is transmitted from the pulley to the outer magnet through a friction clutch. The clutch is set to slip at a torque less than the torque required to break the couple between the two magnets, Fig. 2.

(c) A 1000-turn winding has been attached to the outside of the rotor housing at the level of the inner magnet. The generator effect of the magnet turning next to the coil gives off a small current that can be measured on an A.C. micro-ammeter. This gives positive proof

as to whether or not the inner magnet is rotating (twice as much current is generated when the magnets are uncoupled as is generated when they are coupled), Fig. 5B.

With the magnetically coupled drive, leakage ceased to be a problem.

The autoclave was further modified, viz.

(a) The Bourden-type Ashcroft laboratory test gauge was replaced with a pressure measuring transducer since it decreased the dead volume between the reaction chamber and pressure measuring instrument. The transducer was used in conjunction with a power supply, zero adjust circuit and calitration circuit, Figs. 5B and 7A. A Honeywell Brown Electronik multipoint recorder automatically records the output of the transducer in pounds per square inch.

(b) The temperature control system was further modified to an overset-underset heater control system, the circuit of which is illustrated on Fig. 7B. In this system, the controller instead of switching to on or off, switches to high or low energy settings on either of a pair of variacs. The energy settings are preselected for the required temperature from

Fig. 12. The median curve on Fig. 12 is obtained by determining equilibrium temperature of the autoclave heaters for a series of variac settings. With this system, control of better than ± 0.5°C is obtained.

The rest of the equipment is identical to that used for the platelet runs.

The Solution Used. The dissolution tests were carried out in doubly distilled water, the second distillation being from a very dilute potassium permanganate solution. To remove any dissolved carbon dioxide or oxygen, nitrogen was bubbled through the water immediately before its use in a dissolution test.

Preparation of Quartz Samples

Platelet Tests. The quartz plates used in this experiment were cut from large crystals obtained from the Murray-American Corporation. These crystals were optically clear and very pure and were sufficiently large to yield plates three inches in diameter from any crystallographic plane.

The steps used in the preparation of a sample were as follows:

(1) A 6 mm thick plate was cut perpendicularly to the c-axis to yield a plate whose surface was parallel to the (0001) basal plane.

(2) The plate was then rounded to have a disc of 2.550 inches in diameter.

(3) The surfaces of the disc were ground flat and polished using 600 R.A. size of silicon tetracarbide grinding powder.

(4) After thorough rinsing, the disc was treated with hot 50% HCl solution for one hour to remove any iron and was again rinsed with distilled water.

(5) The acid treated disc was then held at 400°C in a furnace for one-half hour to remove any adsorbed organic matter and water, cooled in a dessicator and weighed.

Steps (4) and (5) were repeated on the disc following the completion of a reaction (traces of iron oxide were deposited from the stainless steel holder onto the disc, presumably due to galvanic action of Pt-stainless steel).

In order to study the rate of dissolution of a single crystallographic plane at a time and in order to avoid the high surface free energies of edges, a special stainless steel holder (Fig. 8) was constructed to hold the prepared plate. The sample and holder were constructed to expose a large surface area of quartz to solution in order to decrease the time of experiment.

The quartz disc mounted in its holder was placed directly beneath the autoclave stirrer and was fastened to

the bottom of the autoclave beaker by means of a bolt through the bottom of the autoclave.

Powder Tests. Large optically clear quartz crystals were reduced to less than 0.25 inches with a hammer. The material was then repeatedly cleaned with hot 50% HCl and washed free from HCl with distilled water. The final grinding was carried out in an alumina mortar. The ground quartz was then sized dry through Tyler sieves and the size fraction chosen for these experiments (-200#, +270#), was wet screened to remove any fines. The powder was again cleaned with dilute HCl and washed with water. After drying, the powder was heated and held at 400°C for one hour, cooled and stored.

The surface area of the powder was calculated from photomicrographs, such as shown on Fig. 13 (the particles are very closely sized and a microscopic count shows that the photomicrographs shown on Fig. 13 are very representative of the whole sample).

A device for dropping the powder sample into the solution after the autoclave reaches working temperatures has been devised and is illustrated on Figs. 4, 6 and 9. The bucket is held to the cover of the autoclave by a rod which extends through one of the service fittings on the cover to the gland, where a pressure sealed rod pins it. The bucket is prevented from accidentally tipping by the locating pin which fits into a hole on the cover. When

working temperature is reached, the sample is dropped into the solution by withdrawing the retaining rod; this allows the bucket and rod assembly to slide to the bottom of the guide tube which is just above the stirrer blades. The assembly is positioned so that the currents caused by the stirrer tips the bucket. The bucket holds a maximum of 2.8 grams of powder.

Preparation of the Autoclave for an Experiment

Platelet Tests. Once the sample was placed in the autoclave and the autoclave assembled, the whole system was flushed with nitrogen and subsequently evacuated with a vacuum pump. The flushing and evacuation were repeated three times with evacuation as the final step. Distilled water previously purged from CO_2 was then siphoned into the autoclave through the sampling assembly, and the pressure within the autoclave increased to 500-900 psi using the gas compression pump, the required overpressure being supplied by compressed nitrogen gas. Following the removal of each sample, the pressure was readjusted to 3,000 psi. On completion of an experiment, the autoclave was quenched from working temperature to room temperature in a bucket of water, the time for quenching being of the order of twenty minutes.

Powder Tests. It was found through experience that the amount of CO_2 in the atmosphere dissolving in the water

did not noticeably affect the rate of quartz dissolution. Other investigators have had the same experience with quartz solubility measurements(3). Furthermore, evacuating the autoclave previous to a run would have sucked the quartz powder from the storage bucket. Therefore, the solution was charged into the autoclave while it was dismantled and the area above the water was flushed with nitrogen gas. Other than this, the start up and shutdown procedures were identical to those outlined for the platelet tests.

Sampling Procedure

Platelet Tests. A sampling apparatus (Fig. 10) was designed so that liquid samples could be taken from the interior of the autoclave at working temperatures of 205-344°C and be quenched to room temperature for determinations of volume and silica content. A capillary tube (a) which extended well below the liquid level in the autoclave was connected to a three-way valve (b) on the exterior of the autoclave. To take a sample, beaker (c), quenched in liquid nitrogen, was screwed to the three-way valve at (d) and evacuated with a vacuum pump through (e). After the beaker had been evacuated, valve (f) was closed and valve (g) opened to admit a sample, then closed after the beaker had filled. Valve (f) was then opened and the sample was forced out by the residual pressure into a flask for weighing and analysis. Two samples of five millilitres each

were taken, the first one being a blank sample to draw off the stagnant liquid from the tubing of the sampling system.

Powder Tests. The sampling technique used in the platelet tests was modified to reduce the volume of solution removed from the autoclave and to filter the fluid from the solids inside the autoclave. The sample was filtered through a stainless steel filter arrangement illustrated on Fig. 11. The sample was reduced by:

(a) Forcing the stagnant fluid in the sampling tubing into the autoclave with nitrogen from the compression system via the three-way valve shown on Fig. 10. The gas from the compressor had to be at working pressure plus 300 psi. The pressure recorder indicated whether the tubing had been cleared (higher pressure reading). Also, if the first sample contained no fluid, the clearing operation was known to be successful. Consecutive samples verified the validity of these assumptions. (The pressure build-up was slight.)

(b) Reducing the volume of the sample bomb to 1.7 ml, two consecutive samples were combined to give 3.0-3.5 ml of sample.

Analytical Technique

Three methods of analysis were used in this work:

(a) weight loss of quartz disc;

(b) the molybdate colorimetric method for silica determination;

(c) the evaporation of the sample, after treatment with a sodium hydroxide solution followed by by fusion and redissolution of the melt in doubly distilled water. This sample was then analyzed by the colorimetric method.

The colorimetric method, outlined by Alexander, Heston and Iler$^{(26)}$ is useful for determining the monomeric dissolved silica acid and the amounts of monosilicate and dislicate ions in solution. Alexander$^{(27)}$ has reported that monosilicic acid forms a yellow silicomolybdate complex with molybdic acid within 75 seconds (at 20°C), while disilicic acid requires 10 minutes.

The colorimetric method is based on the reaction of silica with ammonium molybdate at a pH of 1.5$^{(28)}$ to form the yellow silicomolybdic acid. Calibration tests (Fig.13) and recent literature$^{(28)}$, indicate that the ratio of molybdic acid to silica should be such that an optical density not greater than 0.5 is obtained. If the ratio is smaller, then insufficient molybdic acid is present to react with all of the silica.

The color intensity of the silicomolybdate complex was measured with Bausch and Lomb Spectronic 20 colorimeter at 400 mμ. The readings were taken two, five and ten minutes after the sample aliquot had been added to the

molybdate reagent. The readings were converted to concentrations of SiO_2 by means of a calibration curve (Fig. 13).

Method (b) outlined above is useful for determining the concentrations of monosilic and disilicic acid while method (c) is useful for determining any polymerized and colloidal silica as well after conversion, to a sodium monosilicate.

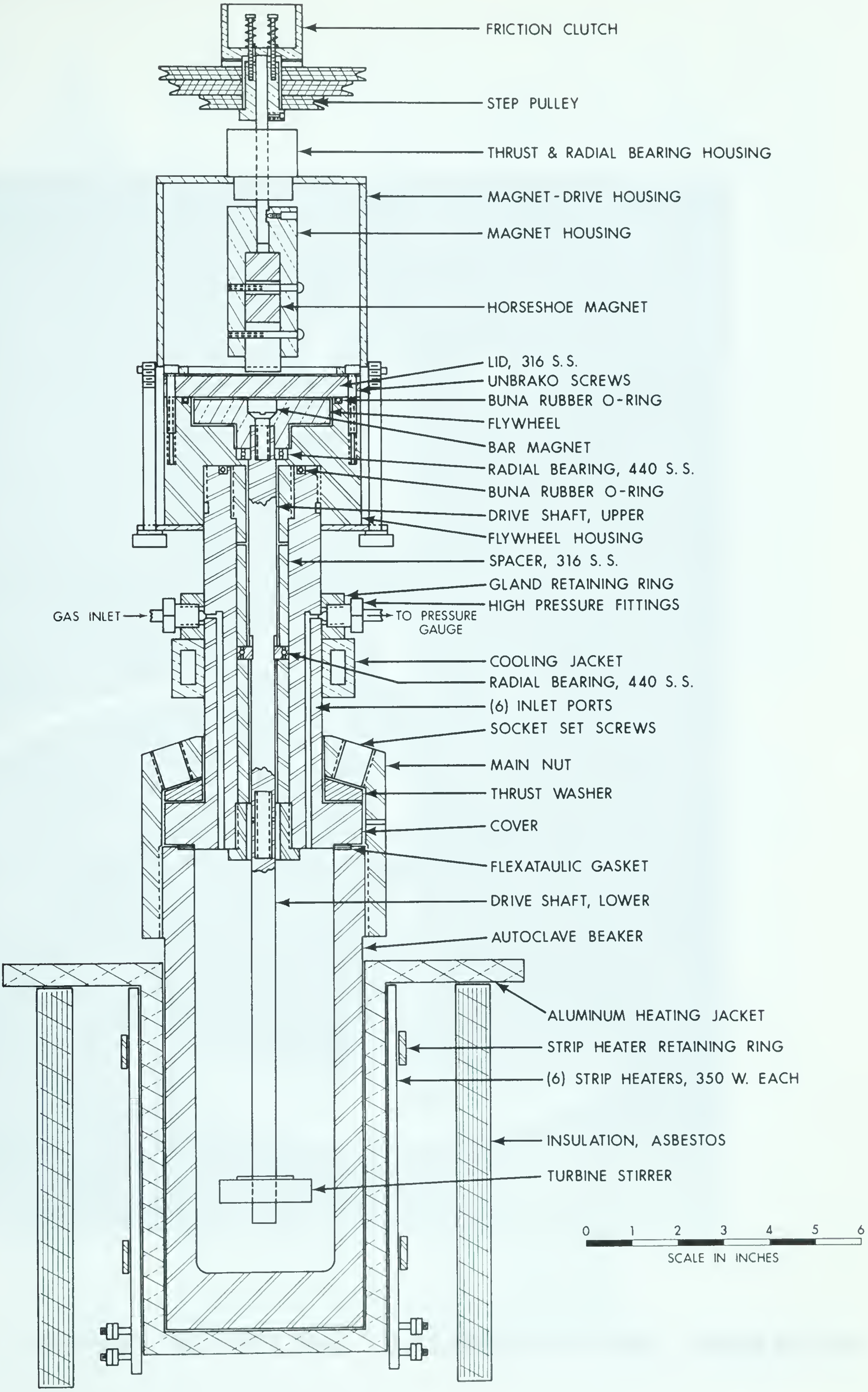

FIG. 2 CROSS SECTION OF A 1-LITRE AUTOCLAVE MODIFIED FOR MAGNETICALLY COUPLED STIRRING

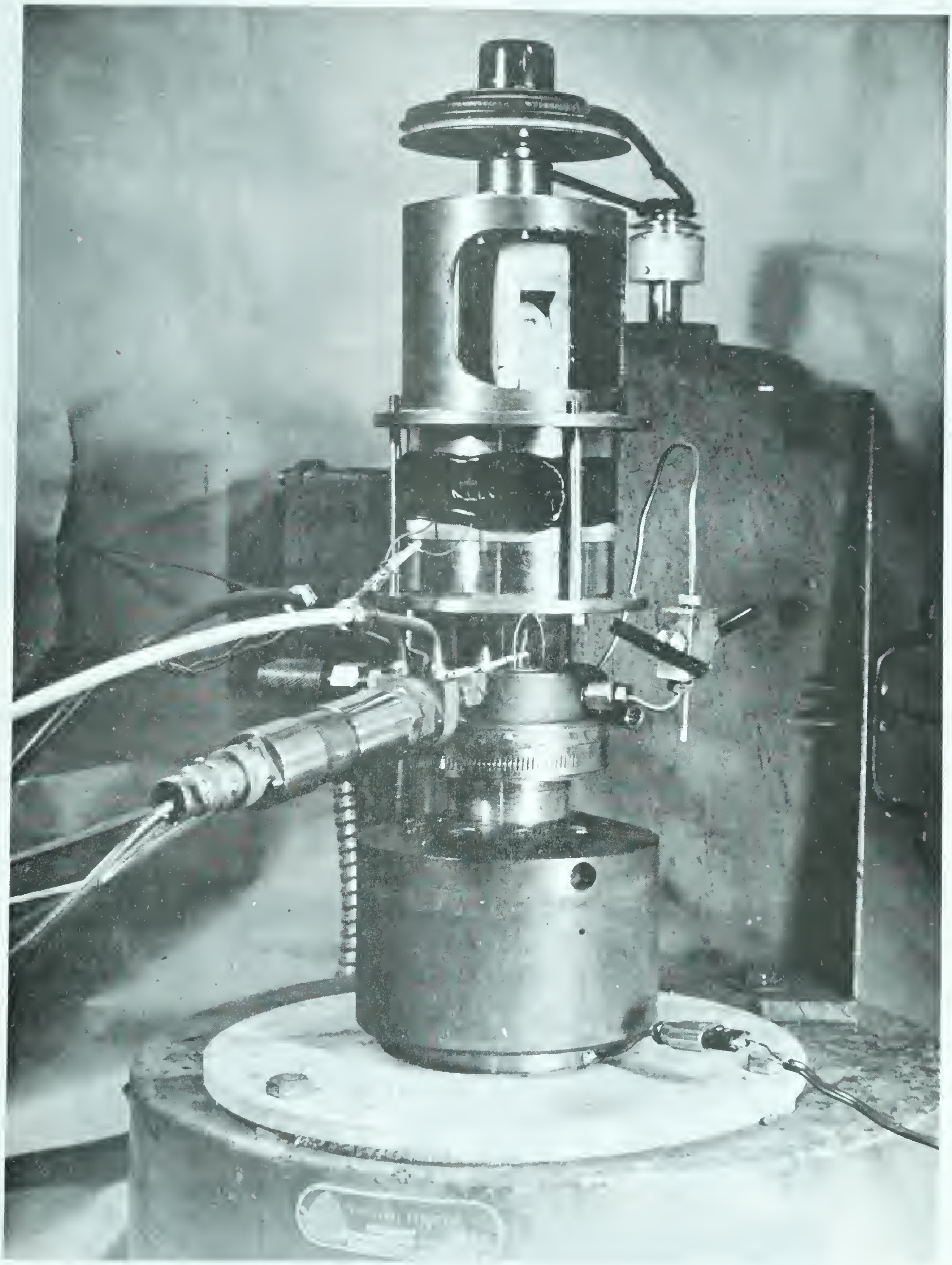

FIG. 3 1—LITRE AUTOCLAVE ASSEMBLED FOR OPERATION

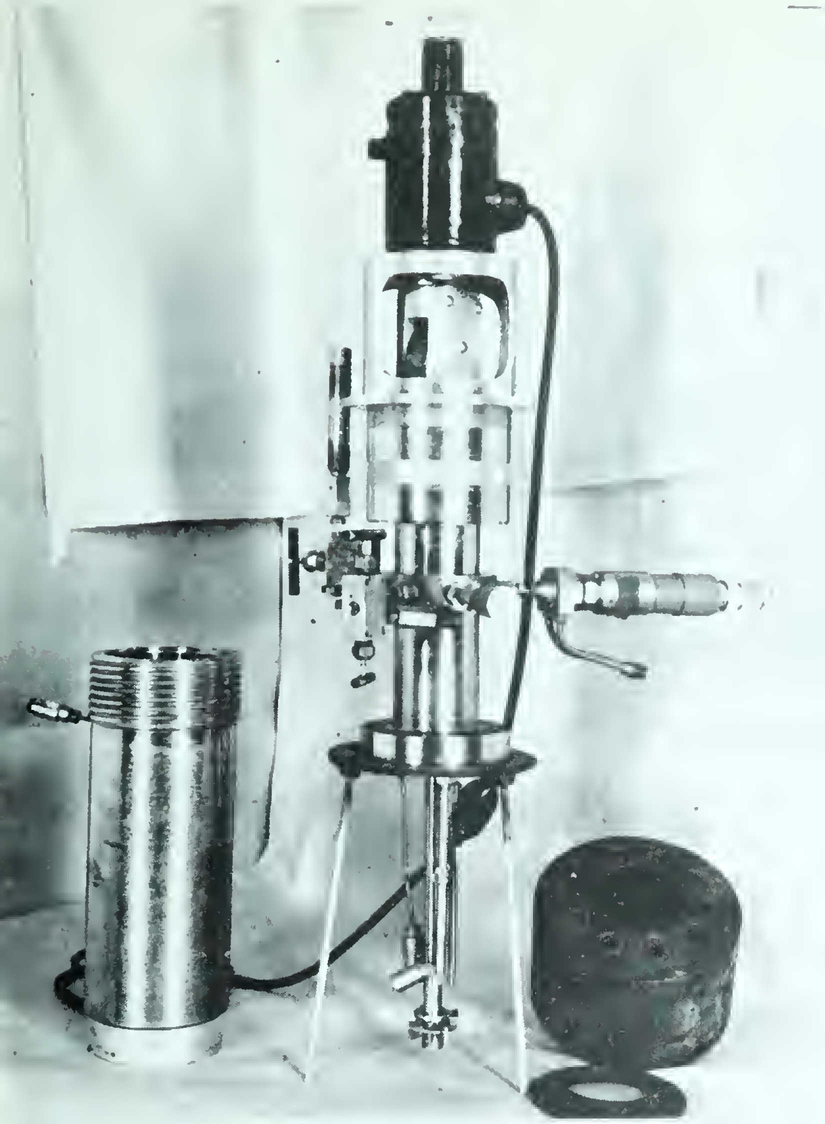

IG.4A COMPONENT PARTS OF THE DISMANTLED AUTOCLAVE

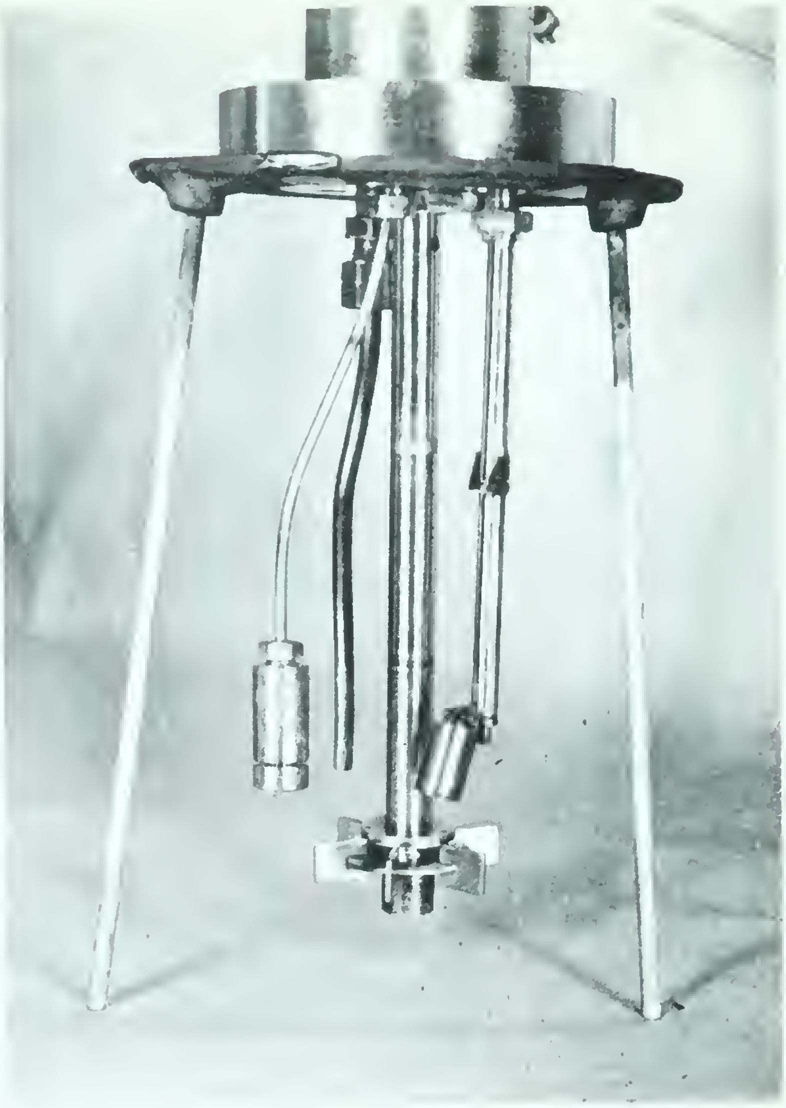

FIG.4B VIEW SHOWING THE ARRANGEMENT OF THE WORKING PARTS INSIDE THE AUTOCLAVE

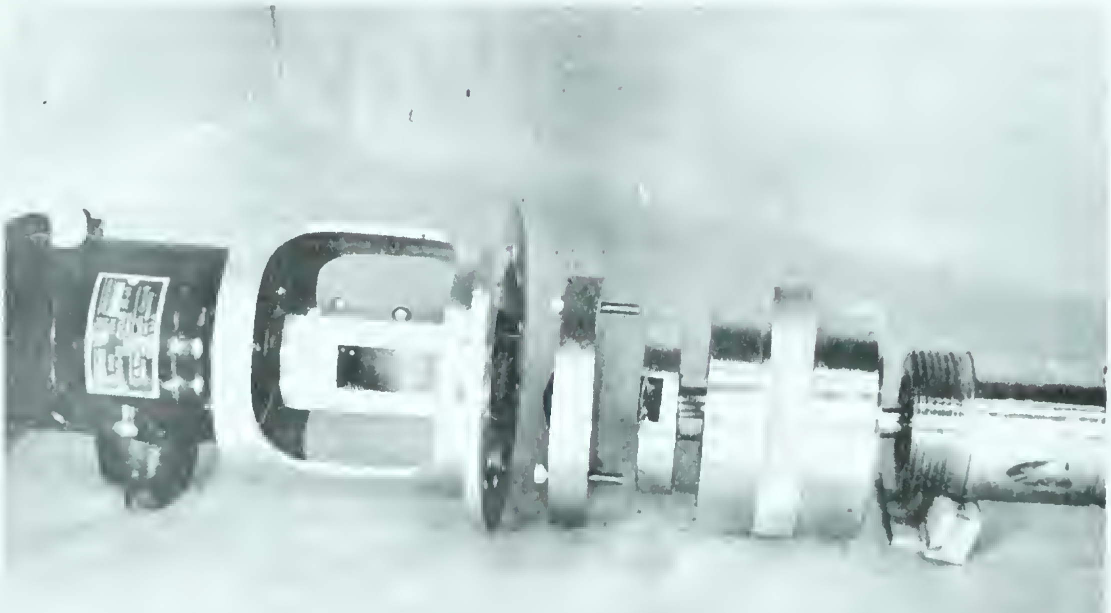

FIG.4C EXPLODED VIEW OF THE MAGNETIC COUPLING

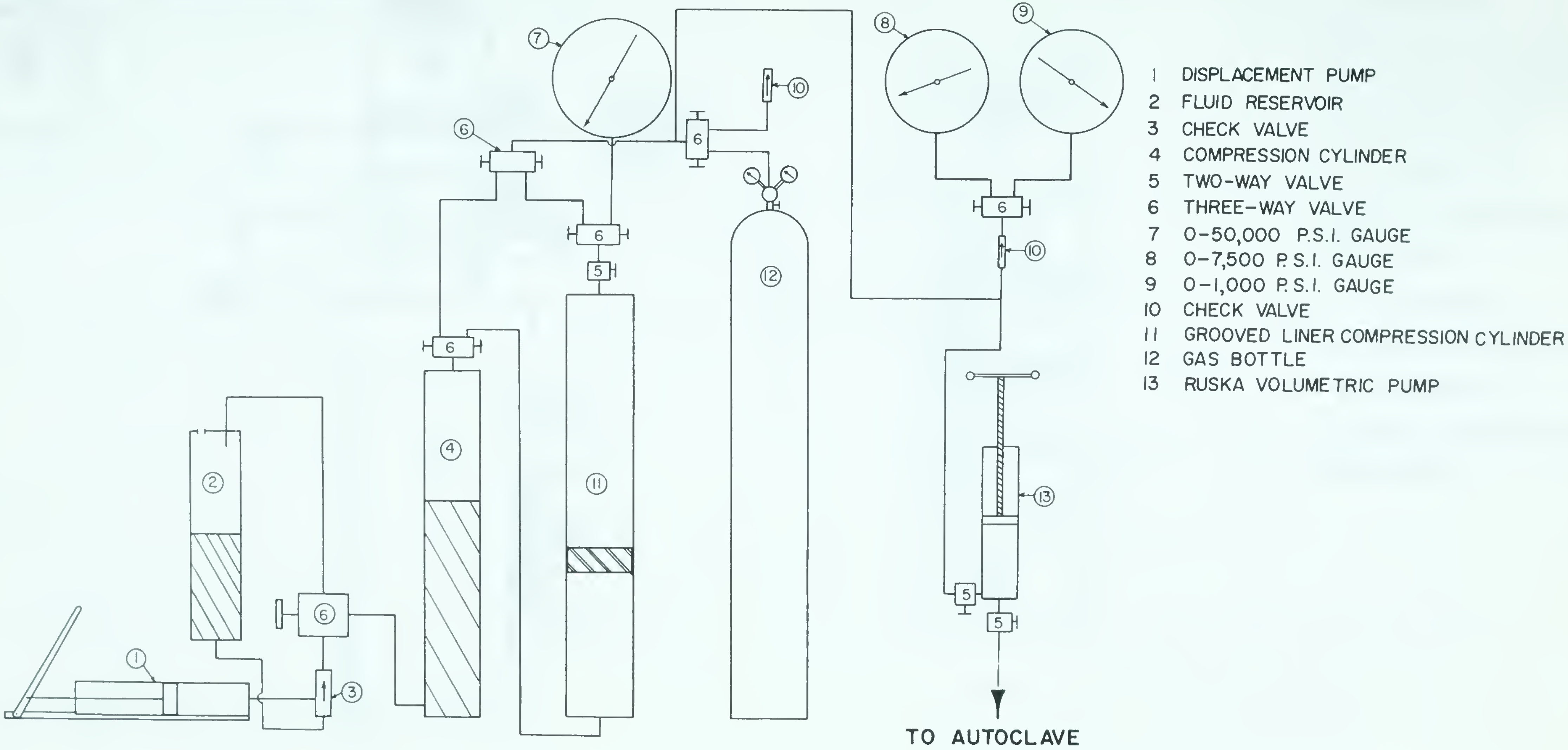

FIG. 5A SCHEMATIC FLOW DIAGRAM OF GAS COMPRESSION AND MEASURING SYSTEM TO AUTOCLAVE

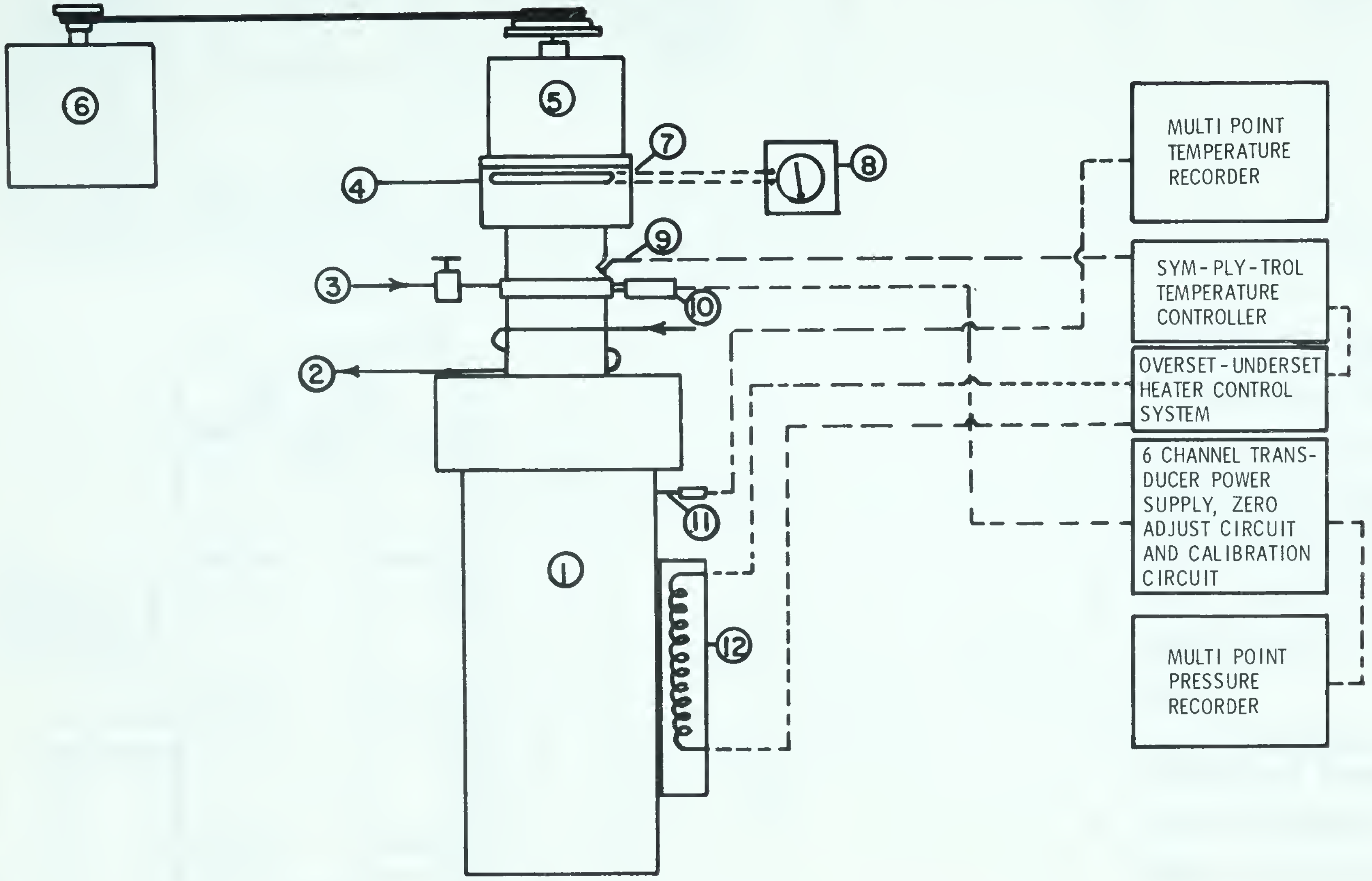
⑥
⑤
⑦
④
⑧
⑨
③
⑩
②
⑪
①
⑫
MULTI POINT TEMPERATURE RECORDER
SYM-PLY-TROL TEMPERATURE CONTROLLER
OVERSET-UNDERSET HEATER CONTROL SYSTEM
6 CHANNEL TRANSDUCER POWER SUPPLY, ZERO ADJUST CIRCUIT AND CALIBRATION CIRCUIT
MULTI POINT PRESSURE RECORDER

1 - 1-LITRE AUTOCLAVE
2 - STUFFING BOX COOLING JACKET
3 - INLET FROM GAS COMPRESSION SYSTEM
4 - INNER-MAGNET HOUSING
5 - OUTER-MAGNET HOUSING
6 - EXPLOSION-PROOF DRIVE MOTOR
7 - DETECTION COIL
8 - A. C. MICRO-AMMETER
9 - TEMPERATURE CONTROLLING THERMOCOUPLE
10 - PRESSURE TRANSDUCER
11 - TEMPERATURE RECORDING THERMOCOUPLE
12 - AUTOCLAVE HEATER

FIG. 5B SCHEMATIC FLOW DIAGRAM OF THE AUTOCLAVE, TRANSDUCER AND ASSOCIATED ELECTRIC CONTROLS

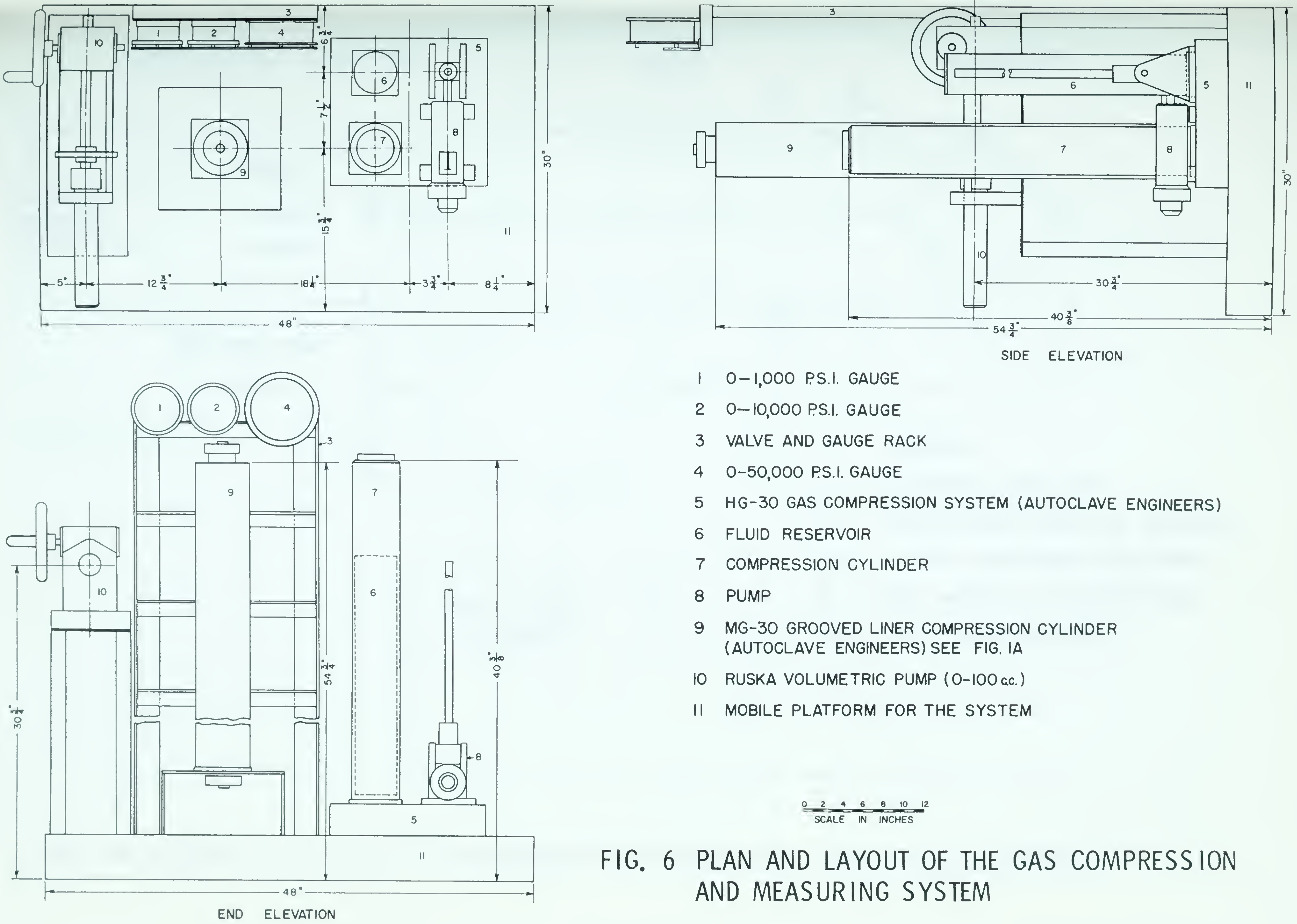

1 0–1,000 P.S.I. GAUGE
2 0–10,000 P.S.I. GAUGE
3 VALVE AND GAUGE RACK
4 0-50,000 P.S.I. GAUGE
5 HG-30 GAS COMPRESSION SYSTEM (AUTOCLAVE ENGINEERS)
6 FLUID RESERVOIR
7 COMPRESSION CYLINDER
8 PUMP
9 MG-30 GROOVED LINER COMPRESSION CYLINDER (AUTOCLAVE ENGINEERS) SEE FIG. 1A
10 RUSKA VOLUMETRIC PUMP (0-100 cc.)
11 MOBILE PLATFORM FOR THE SYSTEM

FIG. 6 PLAN AND LAYOUT OF THE GAS COMPRESSION AND MEASURING SYSTEM

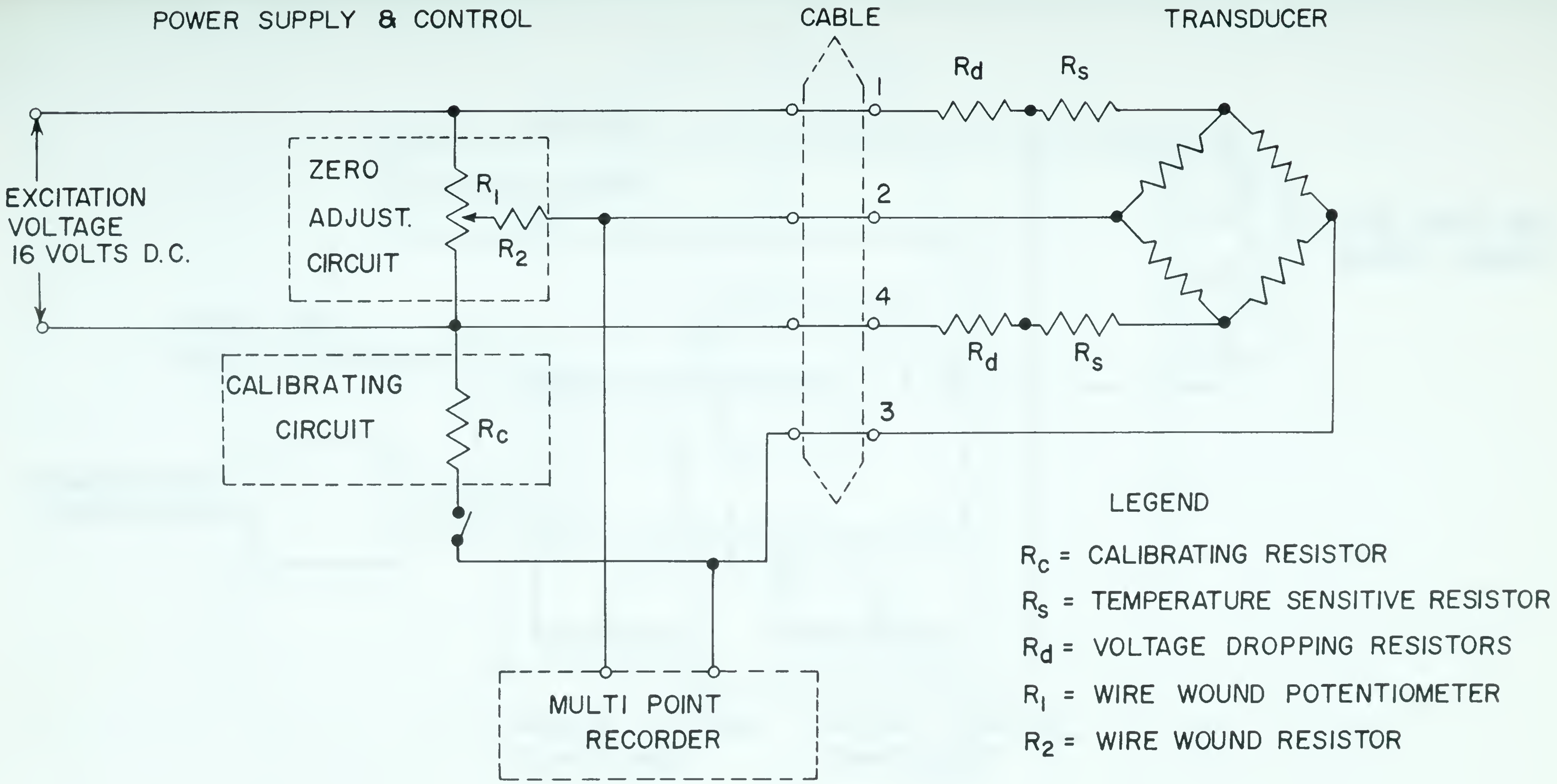
POWER SUPPLY & CONTROL
CABLE
TRANSDUCER
EXCITATION VOLTAGE 16 VOLTS D.C.
ZERO ADJUST. CIRCUIT
R_1
R_2
CALIBRATING CIRCUIT
R_c
1
2
4
3
R_d
R_s
R_d
R_s
MULTI POINT RECORDER
LEGEND
R_c = CALIBRATING RESISTOR
R_s = TEMPERATURE SENSITIVE RESISTOR
R_d = VOLTAGE DROPPING RESISTORS
R_1 = WIRE WOUND POTENTIOMETER
R_2 = WIRE WOUND RESISTOR

FIG. 7A ELECTRICAL CIRCUIT OF TRANSDUCER AND ASSOCIATED ELECTRICAL EQUIPMENT

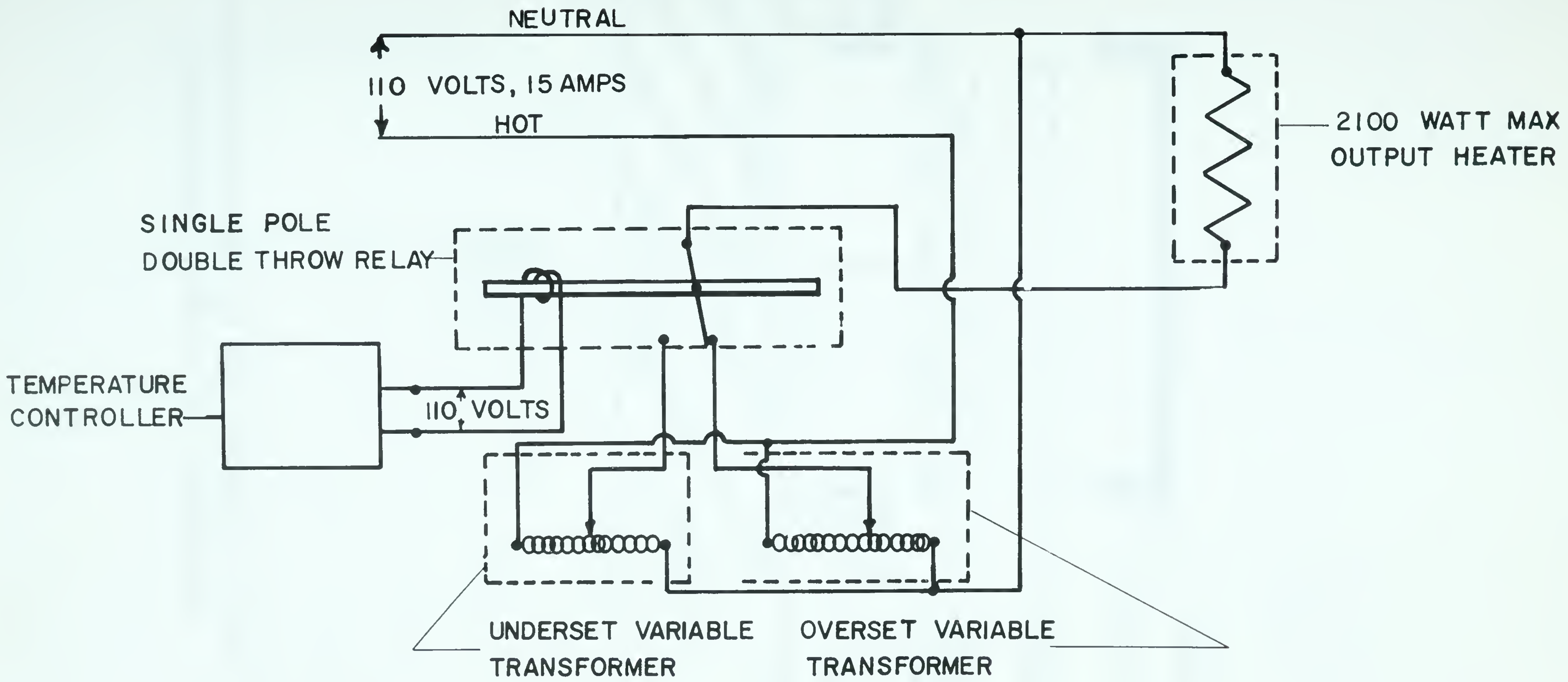

FIG. 7B ELECTRICAL CIRCUIT OF OVERSET-UNDERSET HEATER CONTROL SYSTEM

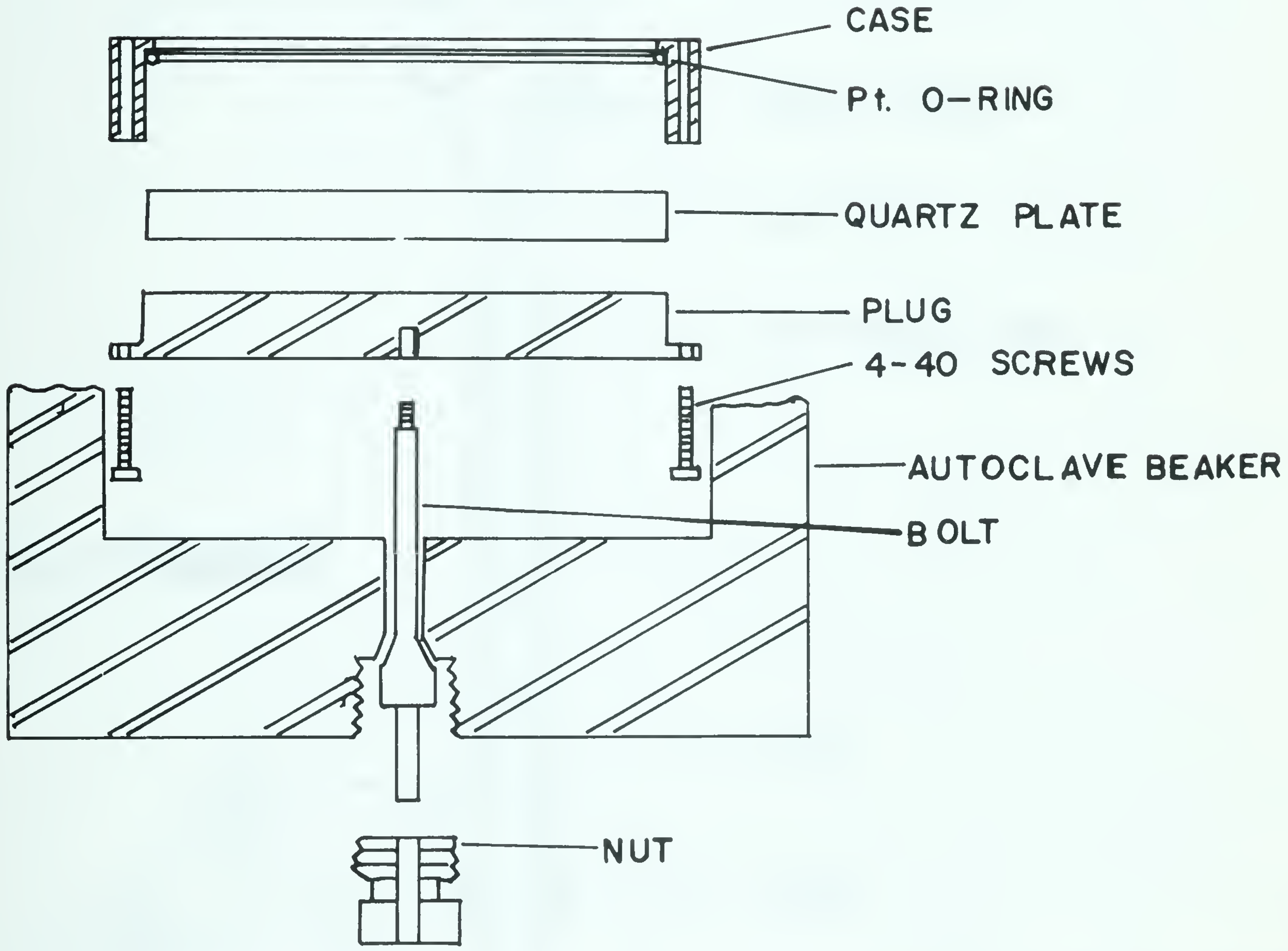

FIG. 8 EXPLODED VIEW OF THE STAINLESS STEEL HOLDER AND ITS DISPOSITION WITHIN THE AUTOCLAVE

[illegible]

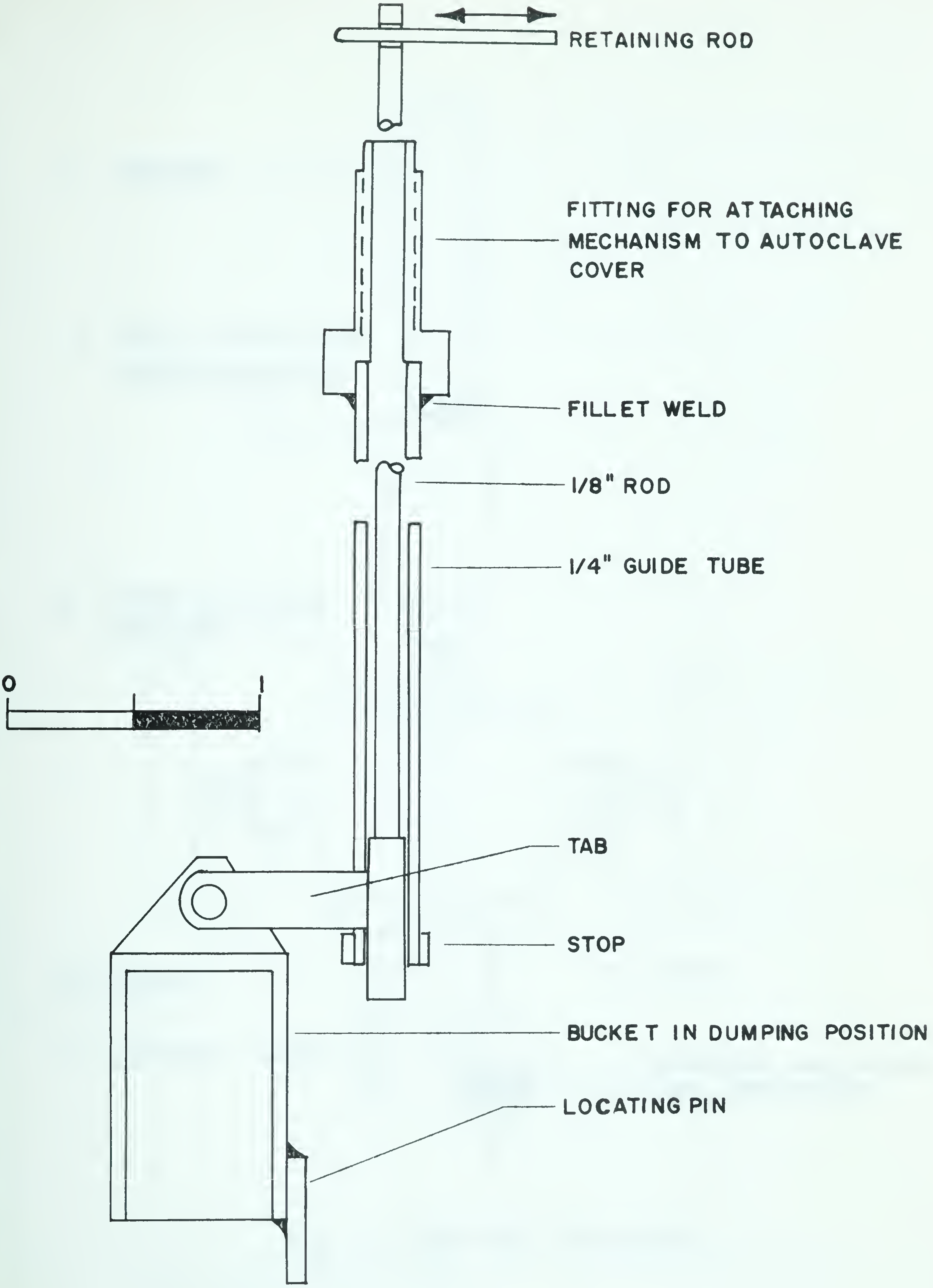
RETAINING ROD
FITTING FOR ATTACHING MECHANISM TO AUTOCLAVE COVER
FILLET WELD
1/8" ROD
1/4" GUIDE TUBE
0
1
TAB
STOP
BUCKET IN DUMPING POSITION
LOCATING PIN

FIG. 9 SAMPLE DROPPING MECHANISM

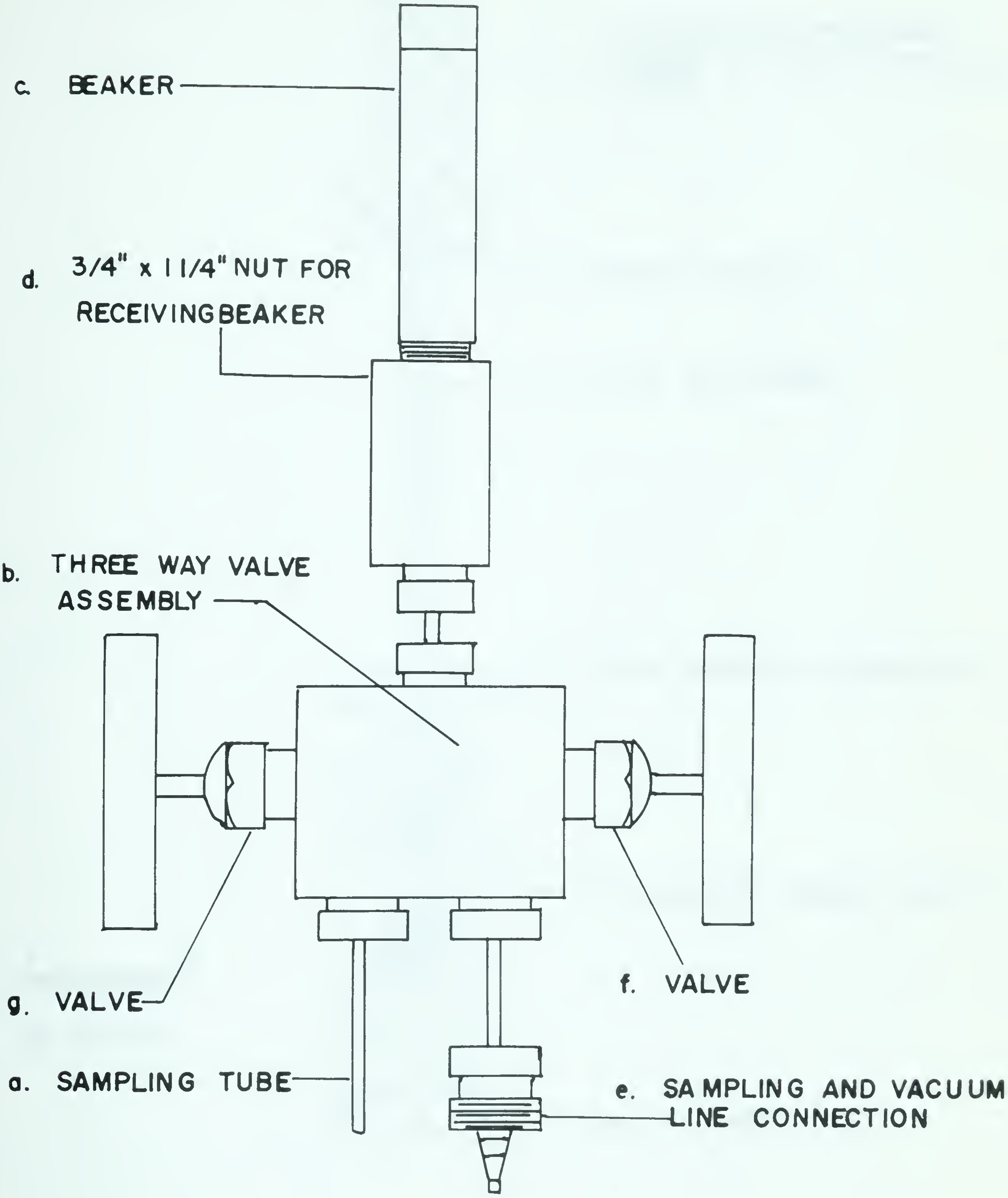
c. BEAKER
d. 3/4" x 1 1/4" NUT FOR RECEIVING BEAKER
b. THREE WAY VALVE ASSEMBLY
g. VALVE
f. VALVE
a. SAMPLING TUBE
e. SAMPLING AND VACUUM LINE CONNECTION

FIG. 10 SAMPLING APPARATUS

[illegible]

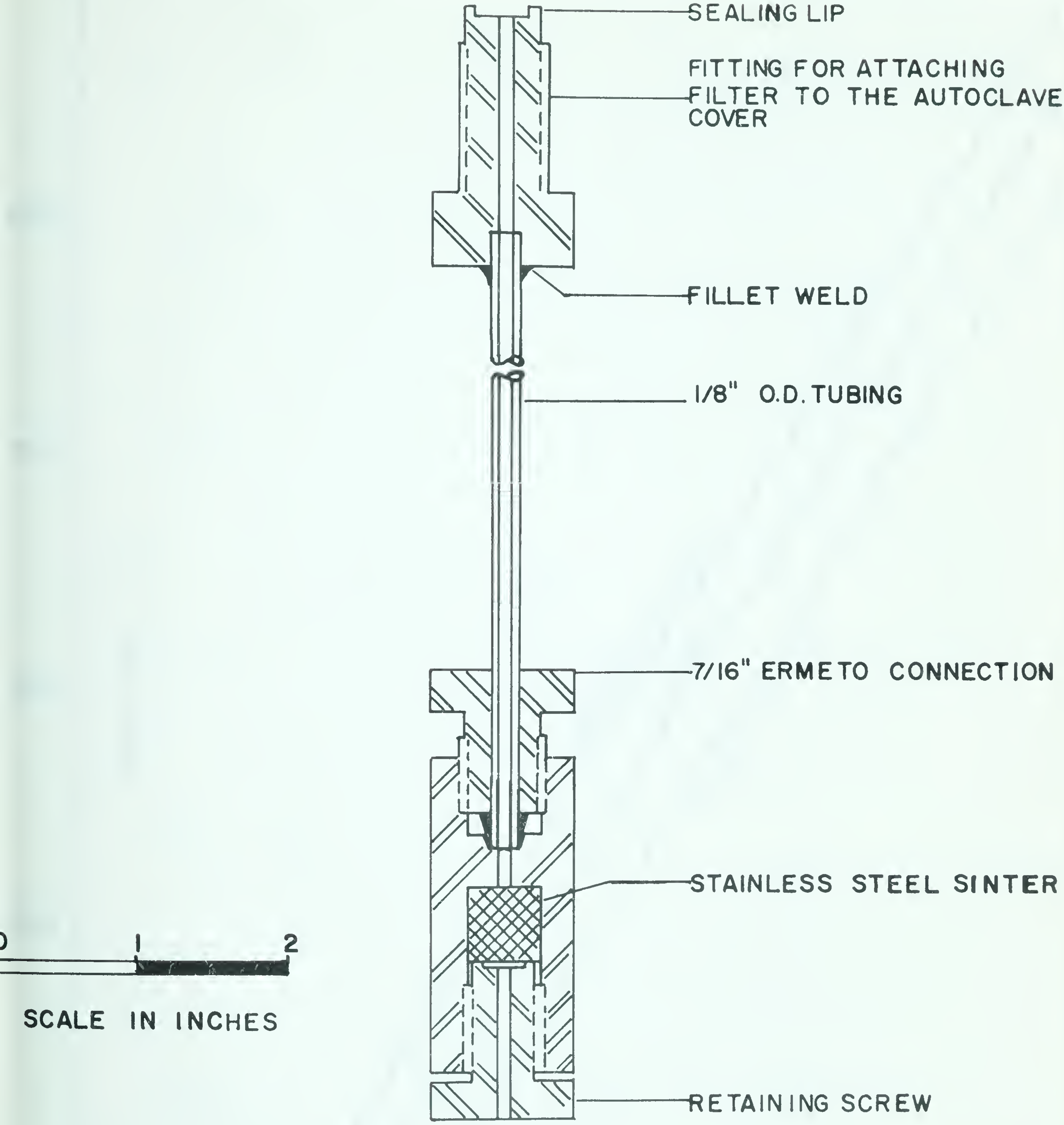

FIG. 11 CROSS SECTIONAL VIEW OF THE STAINLESS STEEL FILTER USED WITHIN THE AUTOCLAVE.

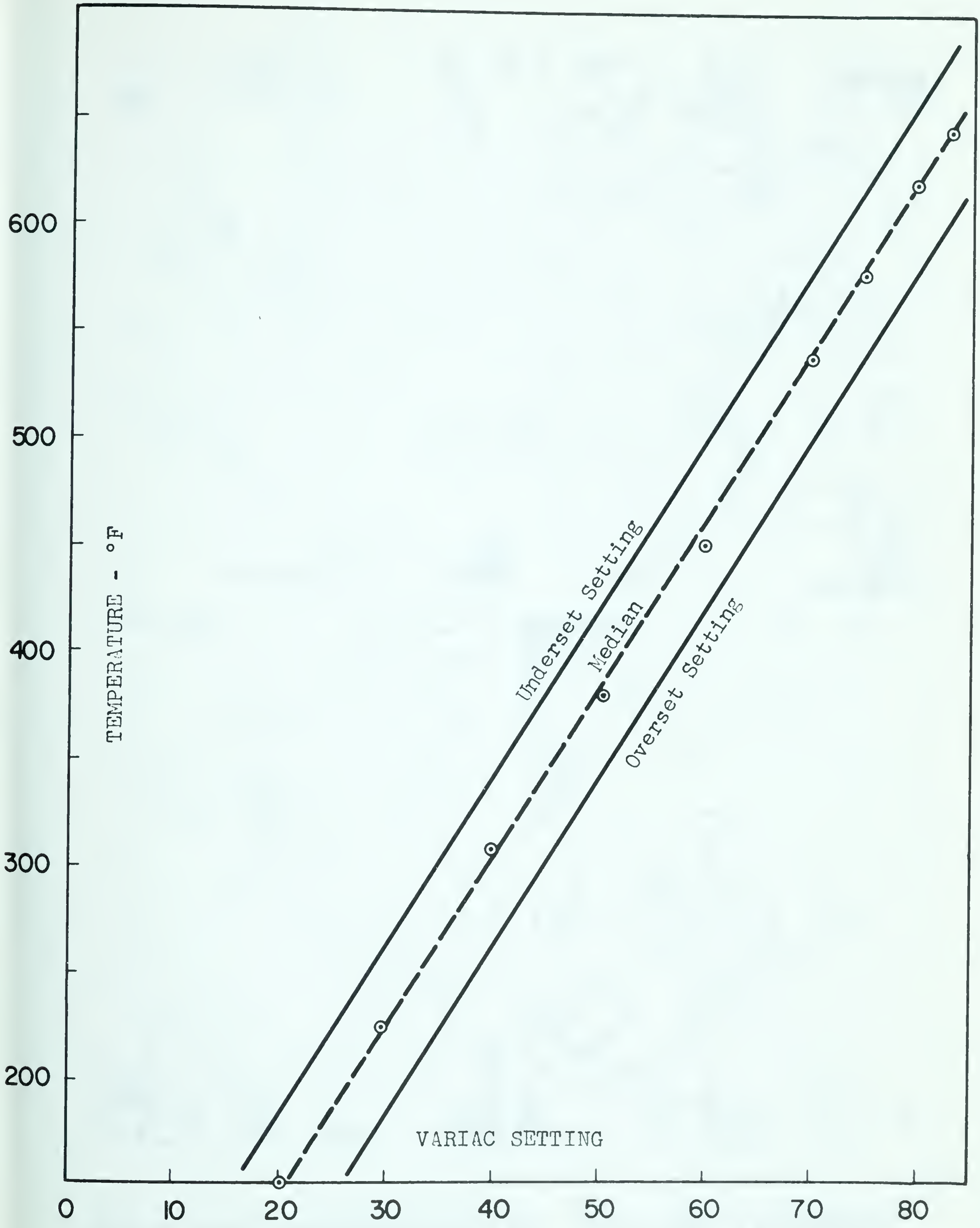

FIG. 12 CALIBRATION CURVE FOR VARIACS USED IN OVERSET - UNDERSET HEATER CONTROL SYSTEM

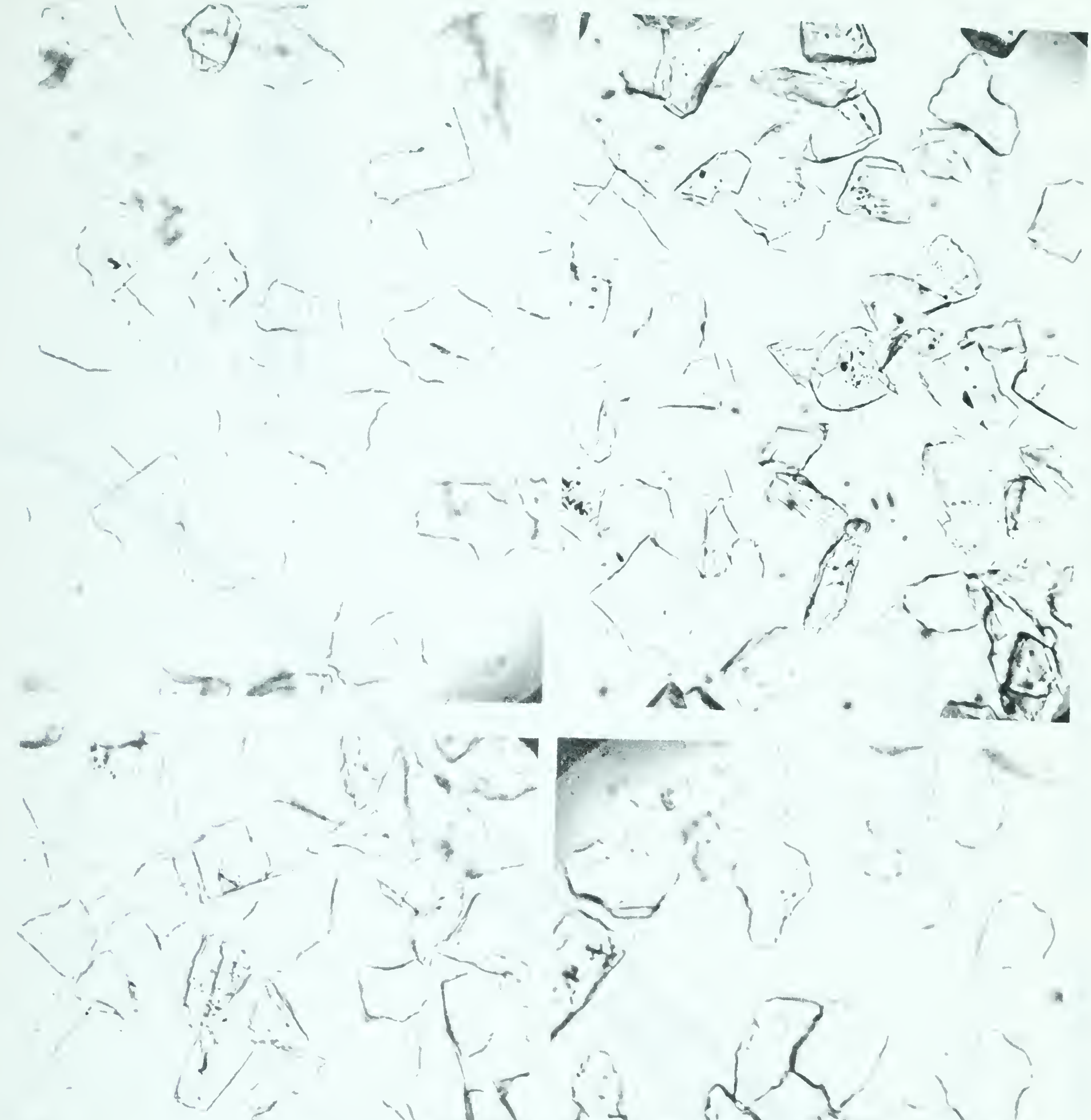

FIG. 13 PHOTOMICROGRAPHS OF THE (-200 + 270) MESH QUARTZ POWDER, 120 X.

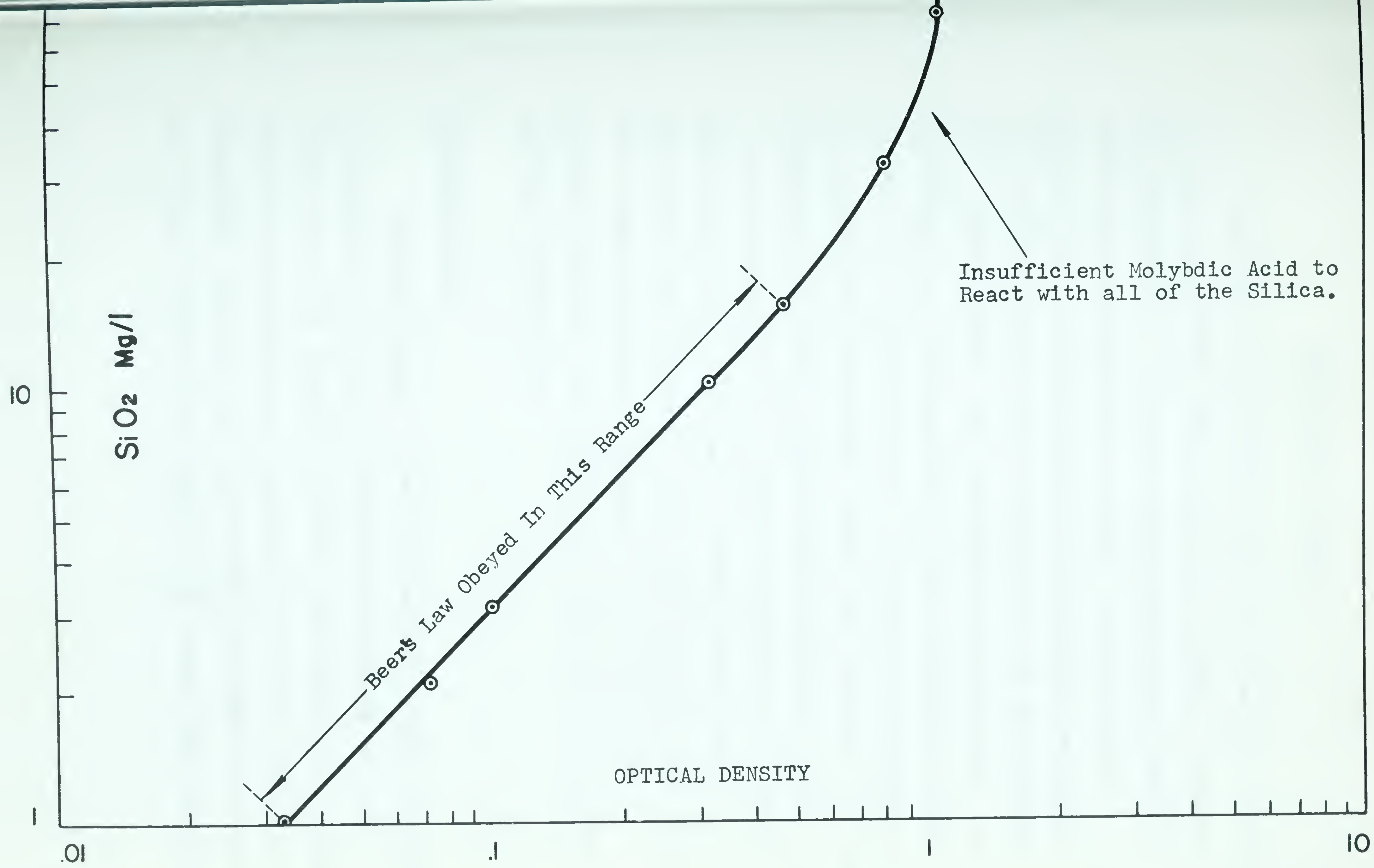

FIG. 14 BAUSCH AND LOMB SPECTRONIC - 20 COLORIMETER CALIBRATION CURVE

[illegible]

EXPERIMENTAL RESULTS

The data for this thesis were collected from thirty-one experiments which were culled from a total of seventy-five experiments. The high rate of experimental failure was mainly due to the ease in which the quartz-water reaction could be inhibited or accelerated by the appearance of minute quantities of impurities, the abrasiveness of the quartz powder, and the technical problems that are encountered in a hyper-pressure, hyper-temperature system. The first two difficulties were overcome by manipulation of the experimental conditions, whereas the third one required a complete rebuilding of the original equipment as well as a radical approach to the problem of maintaining a dynamic seal around a stirring shaft. The data that were used in this thesis are thought to be of good accuracy since pains were taken to eliminate systematic errors and since the standard deviation was always much less than the maximum possible random error.

Stirring Speed

Platelet Tests. It was necessary to study the effect of stirring on the rate of dissolution because too high a speed would have created a vortex, thus reducing the surface area of quartz/solution interface and creating quartz/vapor interface, while too low a stirring speed might allow diffusion from the bulk of the solution to become rate controlling,

thus masking the kinetics of the surface reactions. Fig. 15 shows the effect of three stirring speeds: 247 rpm, 512 rpm, and 666 rpm, for 201 bars pressure and 248-250°C. The concentration versus time curves remain straight lines for all three stirring speeds, the small variation in slope being mainly due to slight differences in temperature for the reactions. Therefore, 247 rpm was used for the stirring speed in the remaining tests, since leakage along the shaft at low speed was less frequent than at the higher speeds.

Powder Tests. In the powder tests, two criteria had to be observed in selecting the correct stirring speed, viz.

(a) Quartz is very hard in comparison to stainless steel (H = 7 on Moh's scale) and at high speeds quartz removes the passive oxide film on the autoclave walls, exposing iron for reaction with water. The resulting iron-water complex, alone or in combination with soluble silica, reprecipitates on the quartz particles and thus seriously inhibits the quartz water reaction. This effect was evidenced by the non-linear dissolution rate and the bright brown stain on the quartz powder.

(b) The agitation must be sufficiently vigorous to ensure that diffusion from the bulk of the solution does not become rate controlling,

The abrasion effect was found to be very difficult to combat and until the baffles were removed from the autoclave, it did not diminish with decreased stirring speed. Fortunately, a range of stirring speeds was discovered (200-400 rpm) where agitation was sufficiently vigorous to eliminate diffusion from the bulk and yet was not so vigorous that abrasion occurred, Fig. 16, and powders removed from the autoclave under these conditions were as pure white as the unleached sample. (Even trace amounts of iron oxide are noticeable when the sample is wetted and inspected under a strong light.) For the remainder of the tests the solutions were stirred at 352 rpm.

Sampling

Even though elaborate precautions were taken to ensure that the sample removed from the autoclave did not contain "stagnant" solution retained in the sampling tubes, it was necessary to check the sampling technique by taking successive samples to verify that the initial sample was truly representative of the solution within the autoclave. Table IIA shows the validity of the sampling method adopted for the platelet tests, since it gives the variations in SiO_2 content on comparison of:

(a) a previously taken sample;

(b) a blank; i.e. mixture of new solution and

"stagnant" solution retained in the sampling tubes;

(c) a sample of the new solution, and

(d) a subsequent duplicate of the new solution.

TABLE IIA

VERIFICATION OF SAMPLING METHOD ADOPTED FOR PLATELET TESTS

(a) Preceding Sample mg/1 SiO_2	(b) "Blank" mg/1 SiO_2	(c) New Sample mg/1 SiO_2	(d) Check mg/1 SiO_2
70.1	121.5	150.0	149.0
150.0	150.0	181.0	181.0
181.0	183.0	187.0	186.0

It is seen that the analyses of the two samples (c) and (d) agree very well, indicating that the sampling method whereby the first blank sample of 5 ml is rejected and the second 5 ml portion is used is reliable. The analysis of the "blank" shows that it is a mixture of the preceding solution retained in the sampling tubing and the new solution.

The sampling technique employed for the powder tests was verified in a like manner with the exception that, as explained previously, the blank sample consisted of

compressed gas. Table IIB shows some consecutive samples taken during the powder tests.

TABLE IIB

VERIFICATION OF SAMPLING METHOD ADOPTED FOR POWDER TESTS

Run	Sample mg/1 SiO_2	Consecutive Sample mg/1 SiO_2
2	27.9	27.3
3	19.4	20.5
4	23.7	22.5
5	27.3	27.0

Removal of samples from the autoclave during a reaction makes the system one of changing volume. As mentioned in the theoretical derivation, the rate equation should account for this effect; to verify this assumption two parallel tests were run in which:

(a) a standard experiment was run in which 30 ml samples were taken at 60 minute intervals to represent a system of varying volume, and

(b) four separate tests were run for successively increasing intervals of 60, 120, 180 and 240 minutes and were sampled at the end of the

test interval to represent a system of constant volume.

The data for these tests are compiled in graphical form as shown on Fig. 17, and we see that even though very large samples were taken from the varying-volume system, the slopes agree within 4.2%, which is within the standard deviation of the slope for run 6 (±4.5%).

High Solubility Layer

In the platelet tests the high solubility layer was not apparent because it was leached off the small surface area of the platelet (30.20 cm^2) while the solution was being brought to working temperature. During the powder tests, however, a more extensive study of the high solubility layer was facilitated because of the large surface area on the powder (1080 cm^2 for 2.7000 gms) and because it was possible to hold the sample out of the solution until working temperature was reached. The first concern of the investigations in this regard was to discover how much of the quartz powder this layer comprised and to confirm that it did not interfere with the kinetic study of the dissolution of the crystalline matrix once this layer was leached off.

The rate at which a "fresh" quartz powder dissolves in water can be delineated into three arbitrary zones, Fig. 18:

Zone A: High solubility layer of adsorbed silicic acid and the rapidly dissolving portion of the vitreous layer.

Zone B: Transition layer of vitreous silica between the H.S. vitreous layer and the crystalline matrix, the dissolution rate being intermediate to the outer layer and the inner crystalline matrix.

Zone C: Crystalline matrix which dissolves at the lowest rate and which begins dissolving at 60 minutes after the reaction has begun at 245°C. The rate data for this investigation were taken from Zone C.

The presence of these three zones is consistent with the findings of others(1-3, 18-24) and agrees with the conclusions made in the literature survey. Obviously, the previous history of the powder and the size fraction used will determine the extent of each layer. For instance, the -200, +270 mesh fraction of powder used in these experiments would be expected to have a fairly shallow high solubility and vitreous layer since less than one hour was required to grind each batch of powder to pass a 200 mesh screen. From the graphs of C_s vs. t, such as Figs. 18 and 20, it was possible to obtain a fairly accurate estimate of the amount of silica comprising Zones A and B. Using this information, we can perform a simple calculation to estimate the depth of the layer, i.e.

Zone A + Zone B = 5.9 mg

Wt. of layer = Density x surface area x depth

Using Density = $2.65\ \text{gm/cm}^3$

S.A. = $400\ \text{cm}^2 \times 2.7$

w = 5.9×10^{-3} gm

x = depth

$$x = \frac{w}{d \times \text{S.A.}}$$

$$= \frac{5.9 \times 10^{-3}}{2.65 \times 400 \times 2.7}$$

$$= 206 \times 10^{-8}\ \text{cm}$$

or $x = 206$ Å

which is slightly less than estimated by Ritchie and Sharpe^(23)^ and Van Lier^(1)^ (i.e. 300-600 Å).

In order to confirm the existence of the high solubility layer and in order to confirm that the rate in Zone C is due to the dissolution of the crystalline matrix, a test was run in which the powder had been previously leached for 12 hours to remove all traces of the high solubility and vitreous layers. According to the data plotted on Fig. 18, the high solubility and vitreous layers were completely removed (as evidenced by linear results from zero time) and the rate agrees with that in Zone C of the previous run. The slopes of the first order plots of the data for these

two experiments agree within 5.4% and although this is not within the standard deviation of the slope, ±2.5%, the comparison is quite good since the temperatures were different by 0.8°C.

Accuracy of the Colorimetric Method as Compared to Weight Loss Determinations for Dissolved Silica

As stated earlier, a comparison of the weight loss method with the colorimetric method for the total amount of silica dissolved should give a good check on the analytical method used. Table III gives a comparison of these two methods.

TABLE III

COMPARISON OF COLORIMETRIC AND WEIGHT LOSS METHODS
FOR TOTAL SILICA

mg SiO_2 Colorimetric F (b)	mg SiO_2 Weight Loss F (a)	% Diff.
70.5	66.2	- 6.5
28.7	29.2	+ 1.7
70.4	66.2	- 6.3
40.0	40.0	0.0
78.0	72.8	- 6.7
66.4	67.2	+ 1.2
92.5	88.3	- 4.8

Method F (a) appears the less reliable of the two, since the necessity for the removal of iron oxide stain deposited on the disc during the test introduces new sources of errors.

State of the Dissolved Species

Table IV shows the results of the two analytical techniques F (b) and F (c) used on identical samples, i.e. the reaction of molybdic acid with silicic acid in solution and the reaction of molybdic acid with silicic acid converted to sodium monosilicate. Although the comparison appears to be quite satisfactory, indicating absence of polymerized and colloidal silica in solutions, the method F (c) probably involves larger errors due to its complicated treatment procedure.

TABLE IV

THE STATE OF THE DISSOLVED SPECIES

Sample	mg/1 SiO_2 Method F (b)	mg/1 SiO_2 Method F (c)
1	149	154
2	181	186
3	186	188
4	169	166
5	148	139
6	47.6	43.3

Adsorption of Silica on Stainless Steel

Silicic acid is known to adsorb quite strongly in practically any surface and in order to avoid spurious results on succeeding runs, the silica adsorbed from a prior run had to be removed or the quantity adsorbed had to be determined.

In the platelet tests the amount of silica adsorbed on the stainless steel of the autoclave was determined by desorbing it during two consecutive runs with 10^{-2} M NaOH after the completion of each experiment. Care had to be taken to keep the temperature below 100°C in these two desorption tests, because above this temperature NaOH vigorously attacked the stainless steel itself. Following these two desorption runs, a third blank run with pure water had to be carried out to remove all traces of hydroxide; this also served as a final desorption to remove any traces of silica. Generally, no silica was detected in the water from the third run.

In the powder tests it was convenient to desorb the silica from the autoclave at the beginning of a successive run, while the autoclave was coming to operating temperature and while the powder sample was still out of the solution. To check this technique, a blank test was run to determine the length of time required to desorb the silica--the run succeeding the blank showed that the silica had been almost completely removed. Table V shows the results of these tests.

TABLE V

RATE OF DESORPTION OF SILICA FROM STAINLESS STEEL AT 470°F

Time since the Heater was on	mg/l SiO_2
155 minutes	0.86
190 "	0.82
220 "	0.74
280 "	0.76
Successive run	0.10

Note: Equilibrium temperature was reached at 155 minutes

Adsorption of silica at a solid/liquid interface is expected to be a function of surface area at the solid/liquid interface and the concentration of silica in solution. If the amount of adsorbate absorbed is plotted vs. the equilibrium concentration of adsorbate in solution, a plateau or series of plateaus may occur at certain concentrations of the adsorbate indicating monolayer or multilayer adsorption. The results for the adsorption of silica on stainless steel are tabulated in graphical form on Fig. 19, in the manner outlined above. A horizontal plateau (A) was obtained for the average of the points in the range 10-30 mg/l SiO_2 and a horizontal plateau (B) was obtained for the average of the points in the range 40-70 mg/l SiO_2. The surface area

available for adsorption can be assumed to be identical for all experiments. If we then interpret the results to be two separate plateaus (A) and (B), we might suppose (A) at 0.5 mg SiO_2 to be a monolayer of adsorbed silica and (B) at 1.0 mg SiO_2 to be a double layer of adsorbed silica since plateau (B) occurs at approximately twice the elevation of plateau (A).

Using these data, we can make a calculation for the surface area of the stainless steel reaction vessel:

$$A = C_s \times 6.02 \times 10^{23} \times a_m \times 10^{-16} \text{ cm}^2$$

where: A = surface area in cm^2

C_s = saturation concentration, i.e. amount of adsorbate needed to form a monolayer in grammols.

a_m = the area covered by a single molecule of the adsorbate in Å^2.

For C_s we will use 0.5 mg/60 x 10^3 mg/grammol. The maximum area covered by one molecule of solubilized silica has been calculated from a model of the SiO_4 tetrahedron in the plan view, Fig. 20,

where: a = Si - O distance x cos (90 - tetrahedral angle)

$= 1.62 \cos 16.7^\circ = 1.55$ Å

$b = O^{=}$ radius $= 1.40$ Å

From the diagram we can see that the area "a_m" is approximately three times the area of each oxygen "ion" $O^{=}$,

i.e. $a_m = 3\pi (O^{=})^2 = 3\pi (1.40)^2$

$= 18.47 \text{ Å}^2$

Holt and King in a similar calculation used $a_m = 12.3 \text{ Å}^2$ as the area of a silica "molecule".

Therefore,

$$A = \frac{0.5}{60 \times 10^3} \times 6.02 \times 10^{23} \times 18.47 \times 10^{-16}$$

$$= 9{,}265 \text{ cm}^2$$

The geometric surface area at the solid/liquid interface is about 700 cm^2; taking into account a roughness factor of 1.5, the actual surface area should be then about 1000 cm^2 which is about one-tenth the value calculated from adsorption data.

One explanation for this discrepancy is that the solubilized silica is adsorbing in the form of colloidal particles (each colloidal particle containing more than ten silica molecules) rather than in the form of discrete molecules, since the solid/liquid interface could be an environment suitable for the formation of colloidal silica. A second explanation for the discrepancy is that the silica may be adsorbing in the form of polycyclic silicic acid containing about ten silica molecules per radical.

Surface Area of the Quartz Powder

Many concerted attempts were made to measure the specific surface area of the quartz powder fraction used in the powder tests by the standard B.E.T. method and by the adsorption of surfactants on the powder at the quartz/solution interface; these methods failed because the small surface area of the powder put it below the range of determinations by these methods. The surface area was then calculated from random photomicrographs of mounted powder samples, Fig. 12. Inspection of eight slides showed the size fraction to be very uniform, the photomicrographs are thought to be truly representative of the whole sample.

An average particle size for the powder was obtained by measuring every particle shown on the photomicrographs on Fig. 12. The particles appear to be approximately rectangular with dimensions of 113 x 70 microns. Determinations of thickness to average screen size of quartz ore gives a value of 0.55 (35), thickness/average screen size ratio. The average screen size of quartz powder (-200#, +270#) is 62.5μ, therefore the thickness should be 0.55 x 62.5 = 34μ.

If we assume the particles are rectangular with dimensions of 113μ x 70μ x 34μ, we can calculate the surface area as follows:

Volume/particle:

$$V = 1 \times w \times t$$

$$= 113\mu \times 70\mu \times 34\mu$$

$$= 2.689 \times 10^{-7}\ cm^3$$

Surface area/particle:

$$A = (113x70x2) + (113x34x2) + (70x34x2)$$

$$= 2.826 \times 10^{-4}\ cm^2$$

Density of $SiO_2 = 2.65$

Therefore, mass of each particle

$$= 2.6 \times 2.689 \times 10^{-7}$$

$$= 7.12 \times 10^{-7}\ gm$$

Number of particles/gm

$$= 1 \div (7.12 \times 10^{-7})$$

$$= 1.41 \times 10^{6}$$

Therefore, total surface area

= No. particles/gm x S.A./Particle

$$= 1.41 \times 2.83 \times 10^{2}$$

$$= 399\ cm^2/gm \text{ or } 400\ cm^2/gm$$

This value for surface area could be too low by 100%.

The surface area of the powder during reaction is assumed to remain essentially constant, Fig. 18, since a very low percentage of the powder dissolves during a reaction.

The Data as Expressed by the First Order Rate Equation

The rate equation

$$\ln\left[1 - \frac{M_s}{M^e_s}\right] = -k_1 t \left[\frac{M'_w}{M^e_s}\right] A$$

derived in the theoretical section has been used on the experimental data and the actual calculations are shown in the calculation section. Tables VIII-1 to VIII-17 compile the experimental data and calculations for a first order reaction. These data are summarized as plots of $\ln\left[1-M_s/M^e_s\right]$ vs. t on Figs. 23 to 24, inclusive, and the effect of temperature on specific rate constant can be noted from these plots. The slopes of these curves were taken from Zone C of the rate data, since it is the object of this thesis to study the kinetics of the crystalline quartz-water system. The slopes of the first order rate curves were obtained by least squares analysis of the data from Zone C by computer, the program of which is shown on Table IX. The results of the least squares analysis are compiled on Table X, A and B. The specific rate constants were calculated as shown in the calculation section and are compiled on Table XI.

The reproducibility of the experimental data was compared on two identical experiments, 1 and 8, and the results are compiled graphically on Fig. 20. The slope of the two curves agree within 0.5% which is well within the

standard deviation of the slopes of either curve.

The first order dependence of the rate equation upon surface area is illustrated on Fig. 22.

Two parallel tests, 5 and 8, were run with different volumes of solution (700 ml and 500 ml) to test the validity of the rate equation with respect to solution volume. The slopes of the first order rate curves agree to within 0.5% which, again, is well within the standard deviation of the slopes of either curve. Furthermore, the half-life concentration relationship for the first order reaction is obeyed, which proves beyond a doubt that the quartz-water reaction is first order.

Surface Phenomena Observed on the Platelets

Microscopic examination of the disc surfaces before and after dissolution tests brought out rather startling differences in their appearance, Figs. 25 (a), (b) and (c). The heavily fissured surface, Fig. 25 (c), was obtained on two occasions, while all other specimens showed the surface to be etched non-uniformly as seen in Fig. 25 (b) but without evidence of fissures. The dissolution rate appeared to be not affected by the appearance of fissures--the results falling in line with those when no fissures were formed.

Experimental Errors

Since the system being studied was pressurized and the reaction temperatures were near the critical temperature

for water, also the quartz-water reaction is easily inhibited or accelerated by the appearance of minute quantities of impurities, it was very important to test the procedure to check for and eliminate systematic errors. These checks revealed that systematic error was absent and that in all cases random error was the only source of error. Table VI lists the sources of systematic errors and the comments on the measures taken to eliminate them.

The cumulative random error of this system is not readily calculated since the system is of changing concentration and since evaluation of the cumulative error involved in obtaining the specific rate constant from the first order rate equation

$$k_1 = -\ln\left[1 - \frac{M_s}{M^e_s}\right] \cdot \frac{1}{t} \cdot \frac{1}{A} \cdot \left[\frac{M^e_s}{M'_w}\right]$$

is both difficult and without significance, i.e. A could be in error by 100%. t and M^e_s, and M'_w are known to have less than 0.2% error.

The one appreciable source of error is in M_s and this error has to be estimated from the calibration curve, Fig.13, and the average dilution factor used in computing C_s and thus M_s. The maximum deviation of M_s is estimated to be $\Delta M_s = 0.04\ M_s$.

Table XIII shows a comparison between the maximum expected deviation of C_s and the standard deviation of C_s obtained from a statistical analysis of the data. The

TABLE VI

SOURCES OF SYSTEMATIC ERROR

Systematic Error	Comment on the Measures Taken To Eliminate Systematic Error
Loss of pressure due to leakage and water vapor due to imperfect sealing	Platelet Tests: Checked pressure with bourdon gage, 50% of the experiments were discarded due to this factor. Powder Tests: Pressure automatically recorded during a run. Experimental system virtually leak free. In both series, volume of solution checked at conclusion of each run. No fluid loss in powder tests; in the platelet tests fluid loss accompanies loss of pressure.
Temperature	Temperature was continuously recorded during each experiment and the recorder was frequently checked against a potentiometer. Temperature adjustments were made if necessary. The thermocouples were commercially calibrated but were checked against boiling water for confirmation.
Appearance of solubilized iron due to abrasion. Rate being controlled by diffusion from the bulk.	Preliminary investigations were made to obtain a stirring speed that avoided these two possibilities (Figs. 15 and 16).
Sample taken not representative of solution in autoclave.	Checked in every experiment by taking consecutive samples. Samples were representative.
Analytical technique not giving the correct value for total silica content.	Analytical technique checked by the methods previously outlined, found to be reliable.
Spurious results due to silica adsorbed on autoclave from previous experiment	Adsorbed silica desorbed and the quantity determined before each experiment was started.

standard deviation is always less than the maximum deviation of C_S, which is desirable. Table XII shows the standard deviation of the slope for each experiment in %, the platelet tests at ±1.95% having a smaller average standard deviation than the powder tests (±2.58%). Two identical runs, 1 and 8, gave a reproducibility of 99.67% in their slopes indicating that the experimental results had fairly good precision.

DISCUSSION OF RESULTS

Although the quartz-water system appears to be a simple one, many uncertainties exist as to the mechanism involved in dissolution and the state of the dissolved species. These uncertainties exist because only small quantities of quartz go into solution, even at high temperatures, and because soluble silica tends to form colloidal aggregates in supersaturated solutions. Frederickson and Cox(29) consider that the dissolution of quartz involves disintegration of mosaic elements to give a suspension of colloidal particles. They argue that the dissolved species exist as a large polyelectrolyte (and not as a simple ion) which titrates with molybdate ions stoichiometrically, in good agreement with gravimetric determinations of SiO_2. Work by O'Connor(30) confirms that polysilicic acids develop full color with molybdic acid in less than five minutes if the polysilicic acids are non-cyclic. The fact that after two minutes no increase in optical density was noted during titrations of the solutions obtained in this series of tests would suggest that monosilicic acid was the only species. Yet, despite the apparent confirmation of determinations by the conversion method, F (c) (Table IV), and the findings of Morey(31) who analyzed for "colorimetric" and total silica, there is no assurance that the polyelectrolyte species is definitely not present. Light scattering determinations on the dissolution samples would help to establish whether the nature

of the dissolved species is colloidal polyelectrolyte or monomeric silicic acid, but it is doubtful that light scattering determinations would yield any data because the concentration of dissolved quartz (even in saturated solutions) is very low and the diameter of the colloid if present would likely be too small.

A plot of log k_1 (specific rate constant) vs. 1/T (Fig. 26) for the powder and platelet tests gives the experimental activation energy of 18.21 ± 0.57 kcal/mole and 18.86 ± 0.43 kcal/mole for the platelet and powder tests respectively, although the specific rate constant for the platelet tests is seventy times that for the powder tests. The activation energies for both series of tests can be considered to be identical since the standard deviation of one is greater than the difference in activation energy. The magnitude of the activation energy suggests a surface reaction as the controlling step in the solution:

$$(SiO_2)_{quartz} + 2H_2O_{(1)} \rightleftharpoons Si(OH)_4 \text{ (in solution)}$$

although diffusion through a polymerized layer of silicic acid at the surface of the quartz cannot be excluded.

Comparison with activation energies obtained by other investigators on dissolution of quartz in alkaline media, Table VII, seems to imply that in all cases a surface reaction is the rate controlling step, although the actual rates of dissolution are very much higher in alkaline media.

In solutions of high pH the dissolution reaction involves OH^- ions and the formation of some ionized species like SiO_4^{4-} or $Si(OH)_6^{2-}$. Additional work is required to find out whether $Si(OH)_4$ species produced in distilled water is monomeric or polymerized, and ionized or unionized.

TABLE VII

COMPARISON OF ACTIVATION ENERGIES DETERMINED BY OTHER INVESTIGATORS

Temp.	Solvent	SiO_2 Species	$E_{(activation)}$	Reference
205-344°C	Water	Crystalline Quartz	18.8 kcal/mole	
150-170°C	In NaOH	Quartz Sand	17.5 kcal/mole	(4)
125-160°C	7.5N NaOH	Quartz Sand	22.6 kcal/mole	(4)
70- 90°C	2.73-10.3M NaOH	Quartz Cubes	18-25 kcal/mole	(11)
30- 60°C	Dilute Alkali	Sp. Bulky Silica	21 kcal/mole	(12)

The great difference in the specific rate constant between the dissolution of (0001) basal plane of the plates and the randomly oriented crystallographic planes of the powder is consistent with the observations of Kennedy(9) who found that plates cut parallel to basal (0001) plane appear to reach equilibrium in water in one-quarter to one-half the time required by a plate cut parallel to rhombohedral face

and those of Mugge(31) who found that the rate of dissolution for (0001) basal plane was one hundred times that of the hexagonal face. Since there is a 70-fold difference in rates (notwithstanding the error in surface area) one must assume that the greatest area of powder exposed to dissolution was on the hexagonal face. The weakest bonding in quartz crystals therefore appears to be parallel to the c-axis.

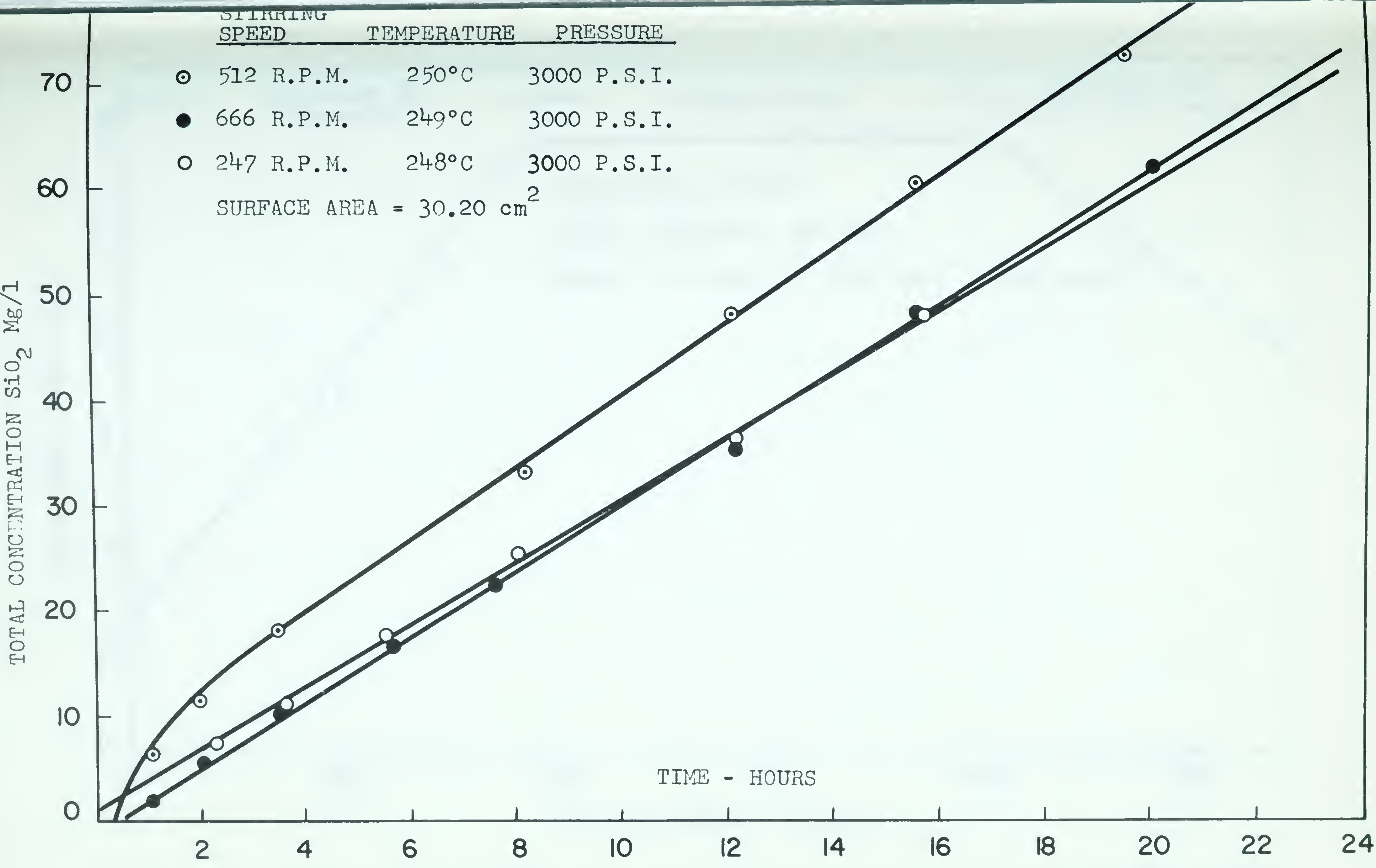

FIG. 15 THE EFFECT OF STIRRING ON THE RATE OF DISSOLUTION OF A QUARTZ PLATE IN WATER

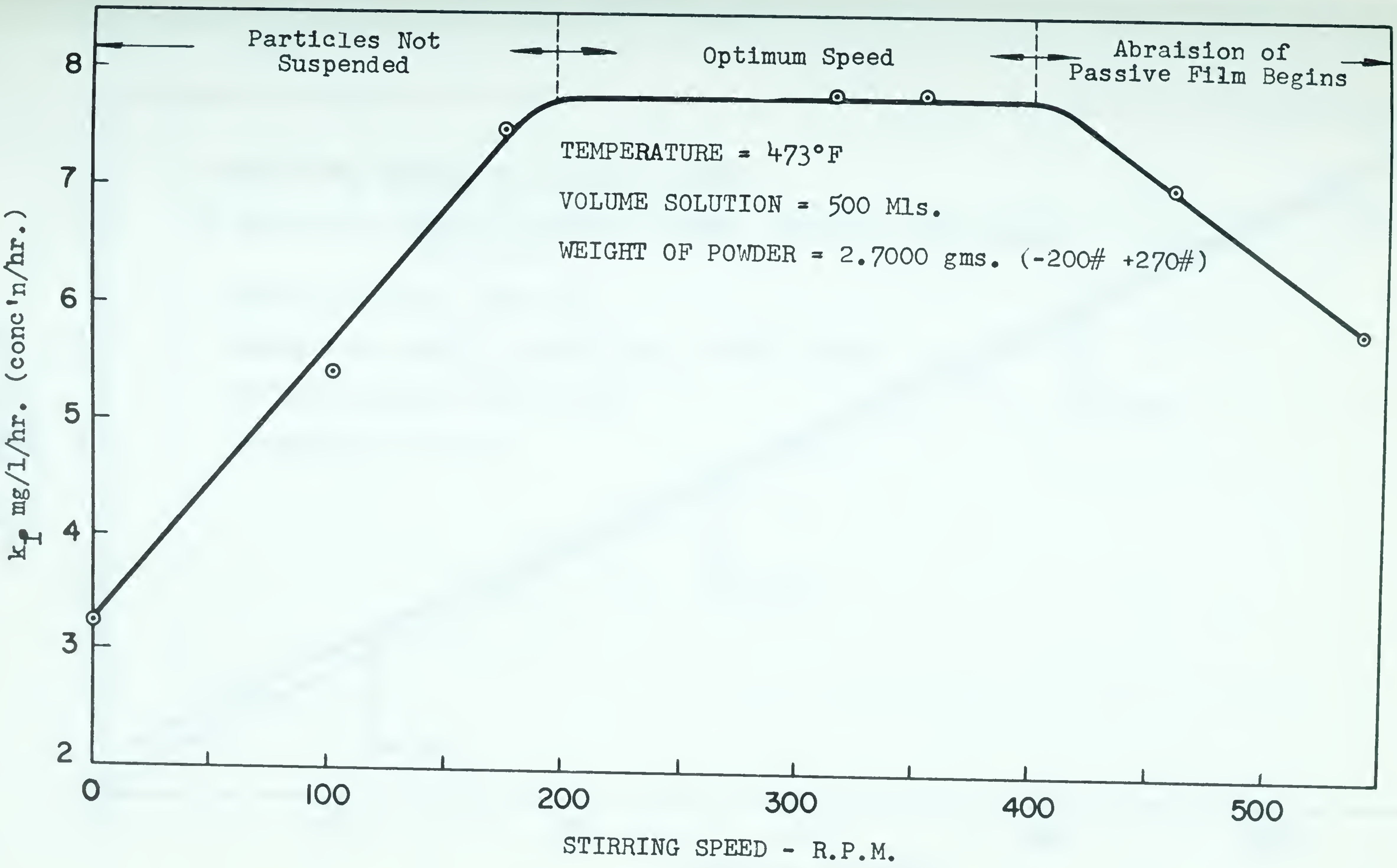

FIG. 16 THE EFFECT OF STIRRING SPEED ON THE RATE OF DISSOLUTION OF QUARTZ POWDER

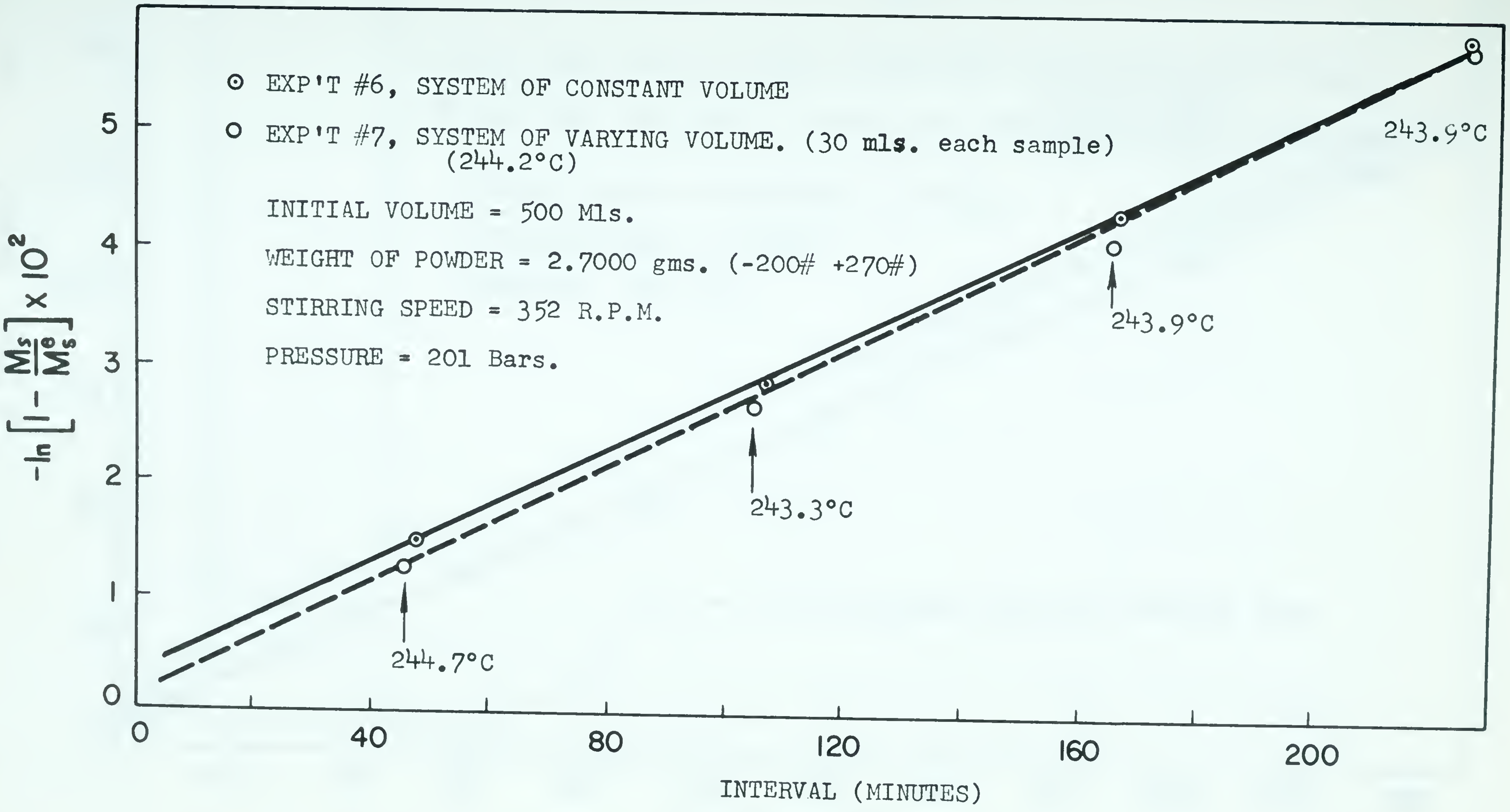

FIG. 17 A STUDY OF THE EFFECT OF VARYING VOLUME (DUE TO SAMPLING) ON RATE

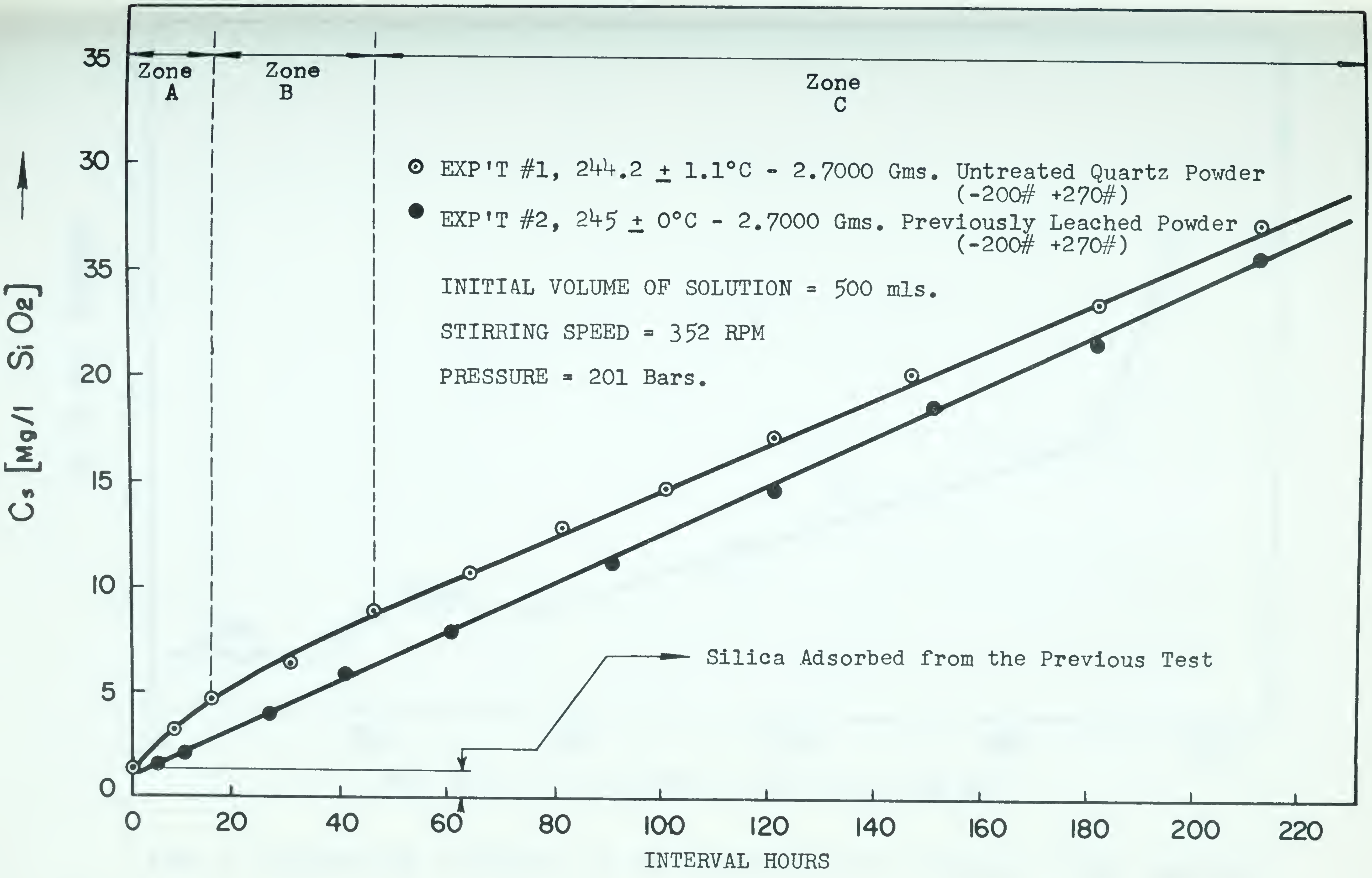

FIG. 18 TYPICAL PLOT OF CONCENTRATION vs. TIME EXHIBITING THE THREE REACTION ZONES FOR THE REACTION OF QUARTZ IN WATER

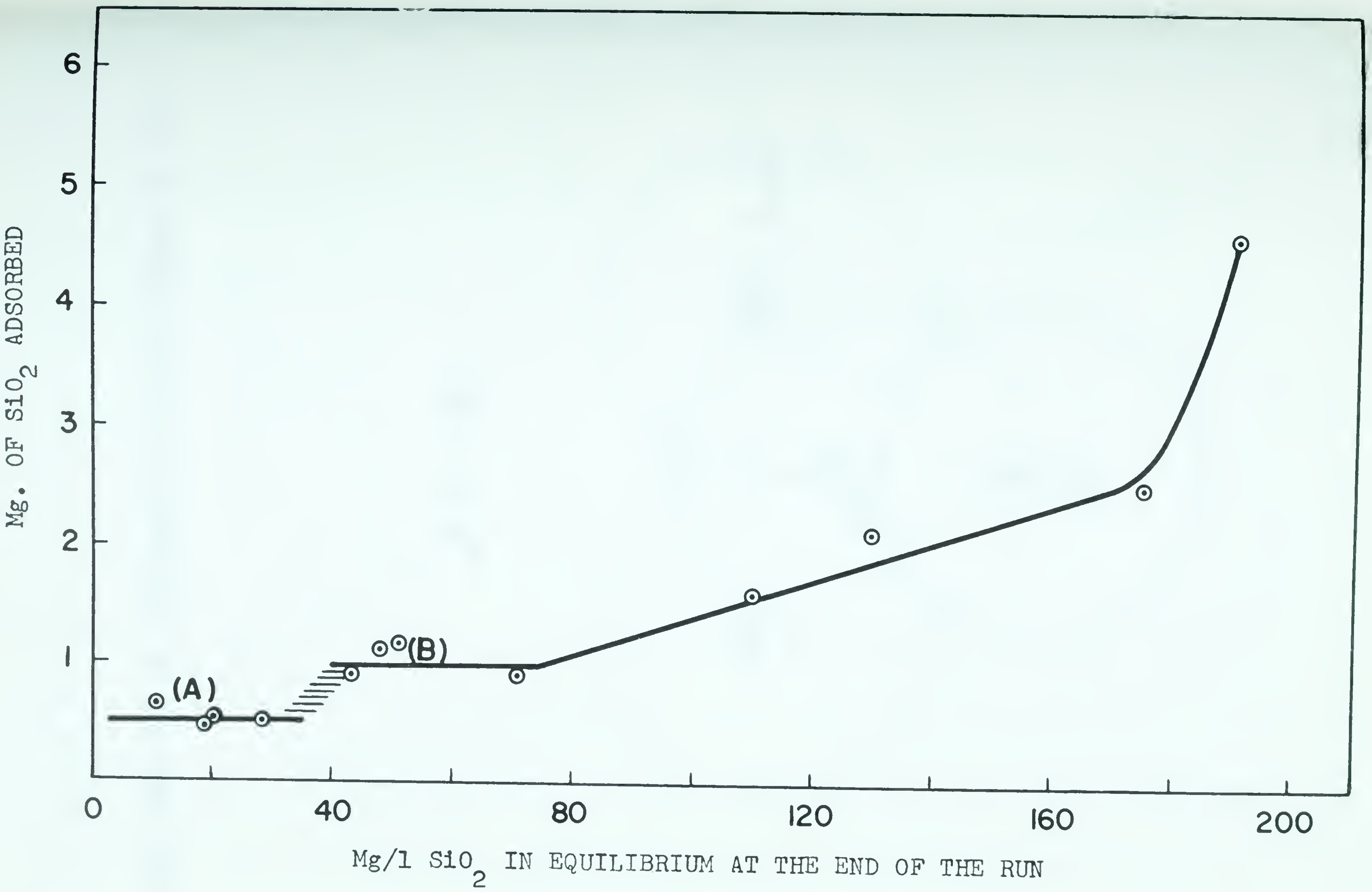

FIG. 19 ADSORPTION ISOTHERM FOR THE SOLUBLE SILICA / STAINLESS STEEL INTERFACE

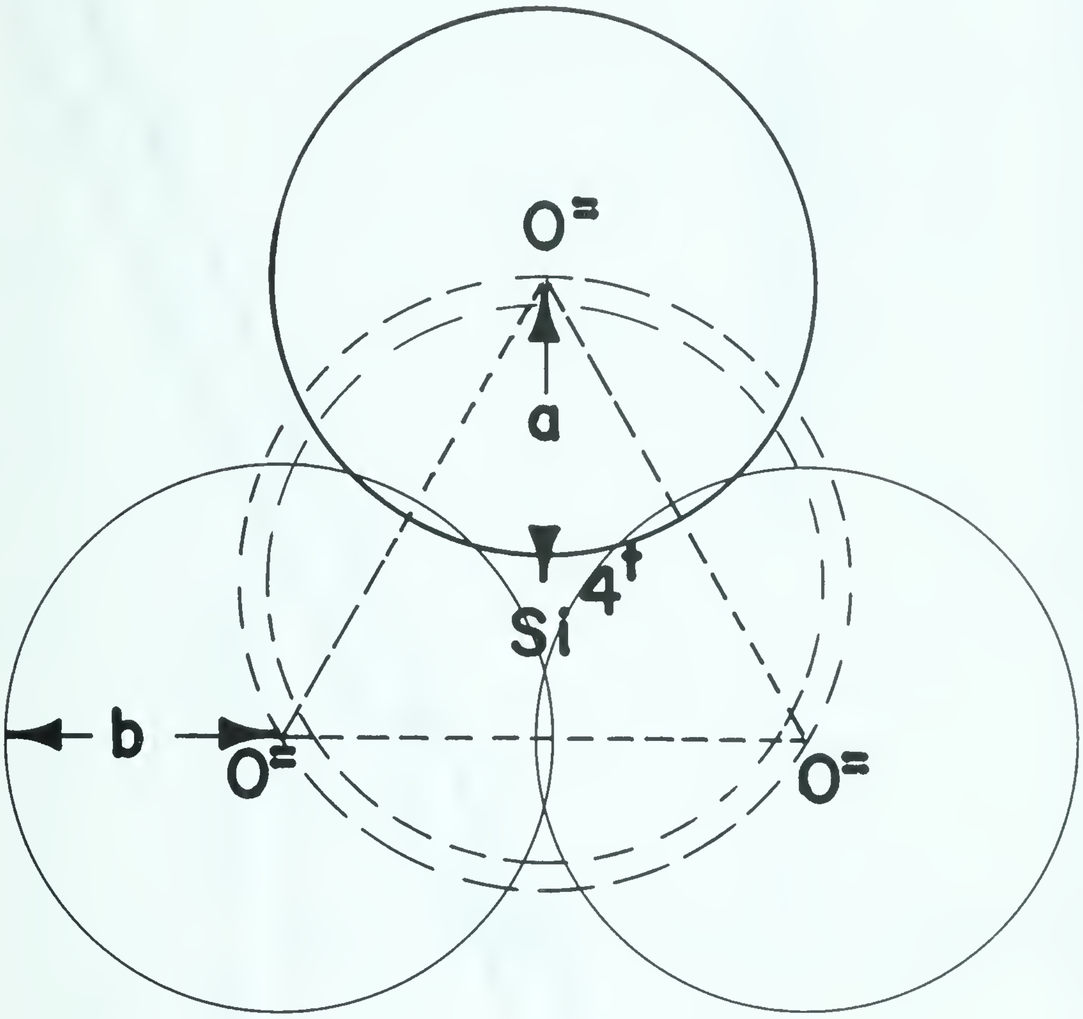

$1\,\text{Å} = 0.8''$

FIG. 20 MODEL OF SiO_4 TETRAHEDRON IN THE PLAN VIEW

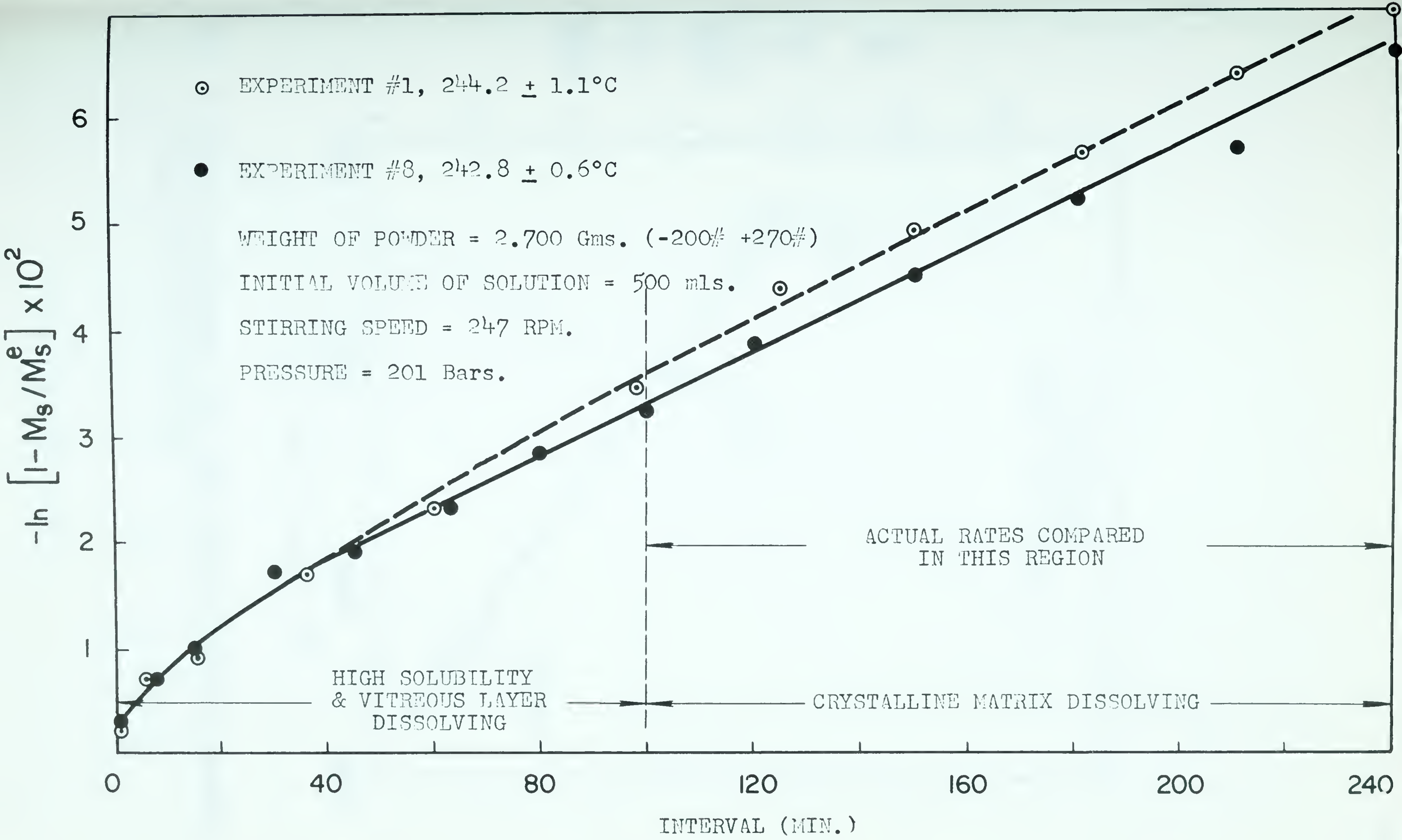

FIG. 21 REPRODUCIBILITY TEST

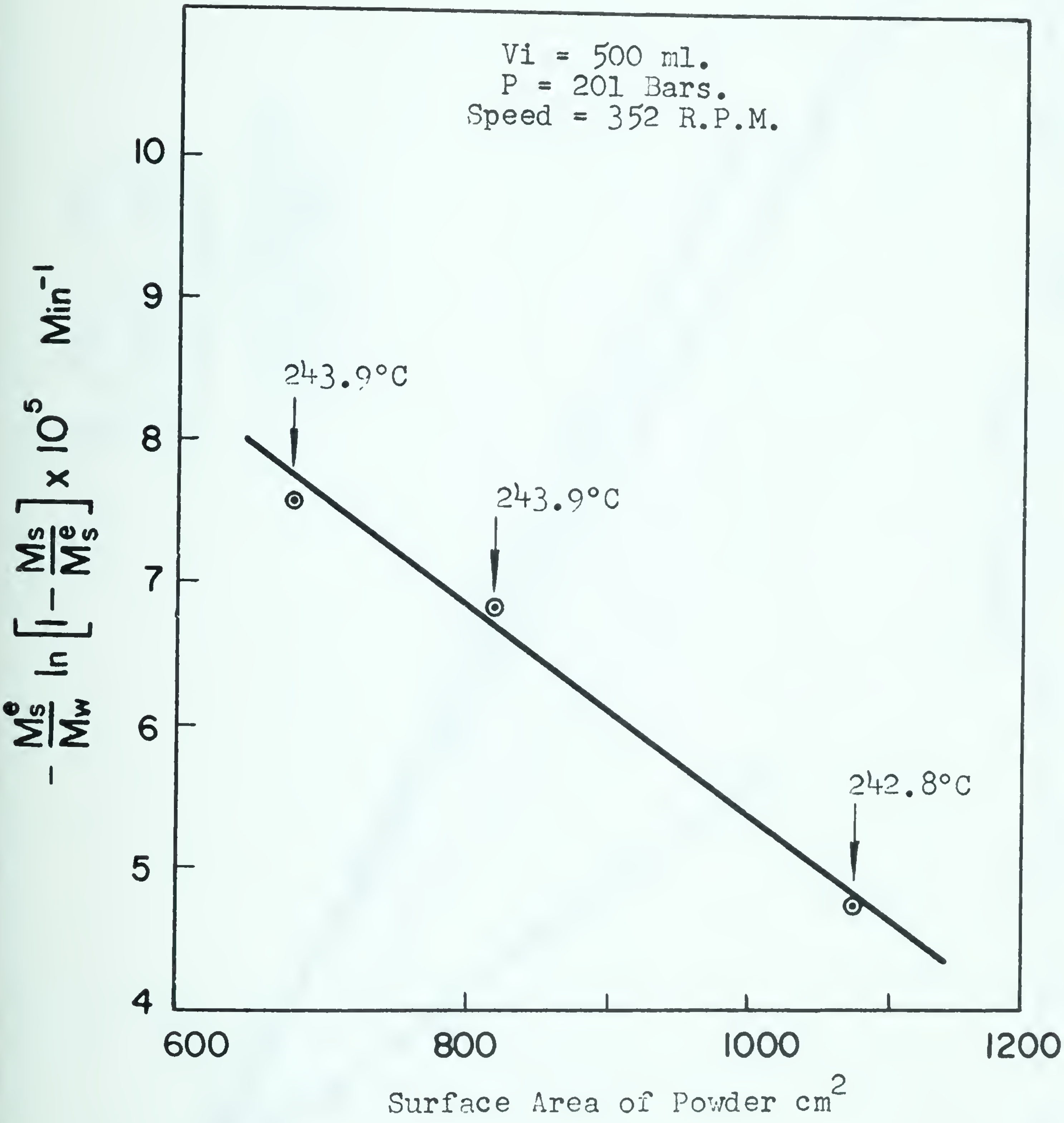

FIG. 22 RELATION BETWEEN RATE AND SURFACE AREA OF QUARTZ AVAILABLE FOR REACTION

[illegible]

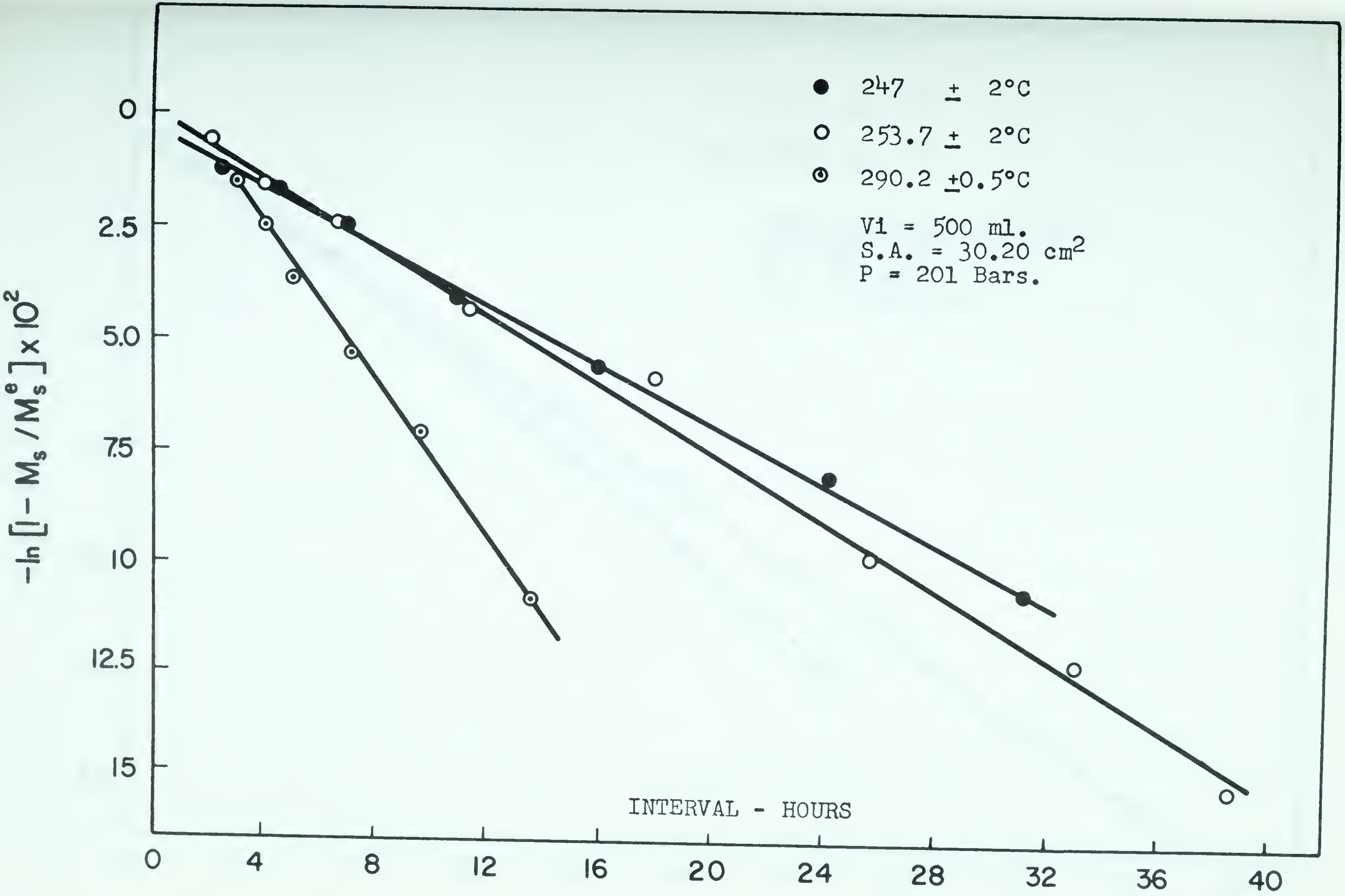

FIG. 23A EFFECT OF TEMPERATURE ON RATE AS EXPRESSED BY THE FIRST ORDER RATE EQUATION FOR THE REACTION OF A **QUARTZ PLATE WITH WATER**

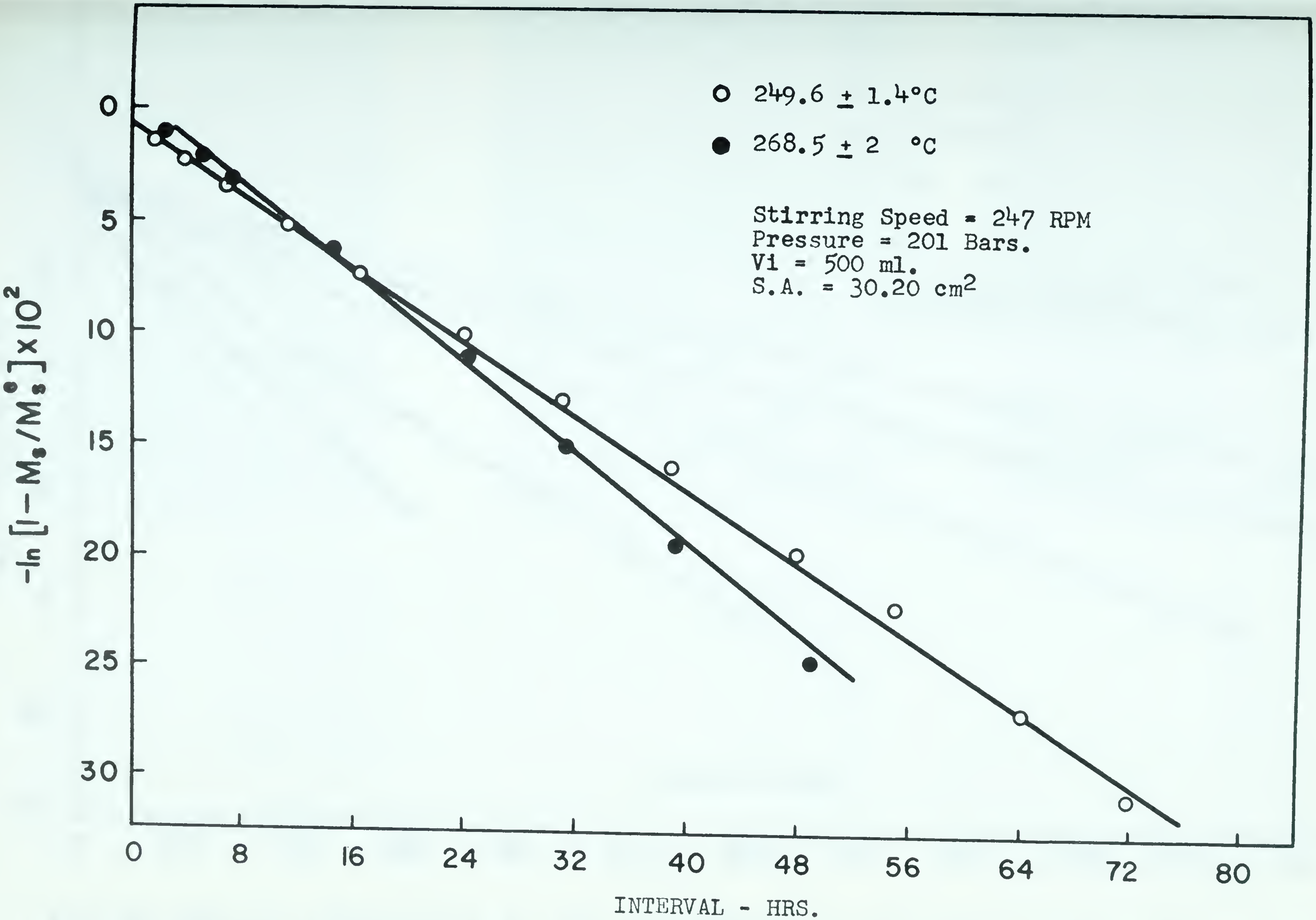

FIG. 23B EFFECT OF TEMPERATURE ON RATE AS EXPRESSED BY THE FIRST ORDER RATE EQUATION FOR THE REACTION OF A QUARTZ PLATE WITH WATER

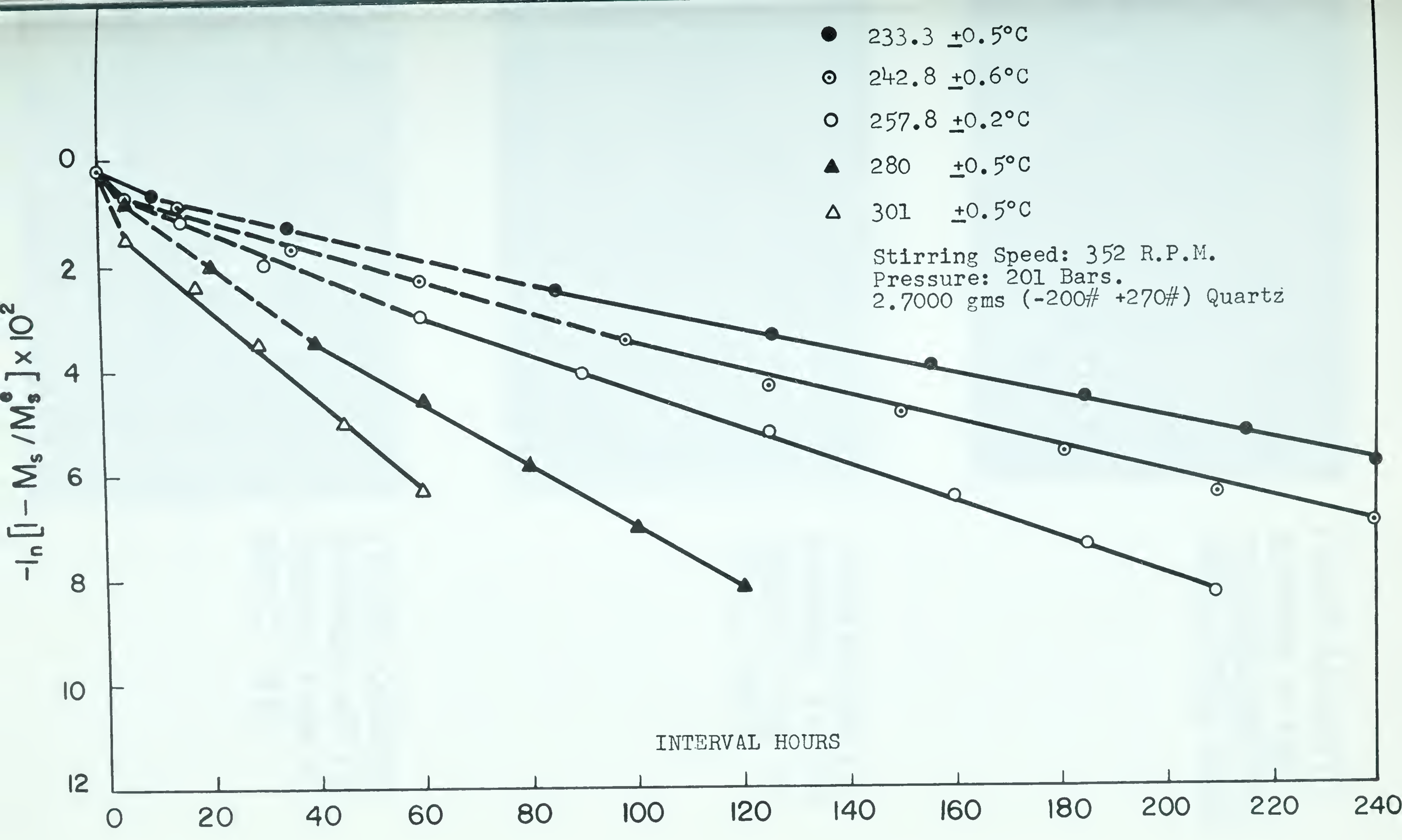

FIG. 24 EFFECT OF TEMPERATURE ON RATE AS EXPRESSED BY THE FIRST ORDER RATE EQUATION FOR THE REACTION OF QUARTZ POWDER WITH WATER

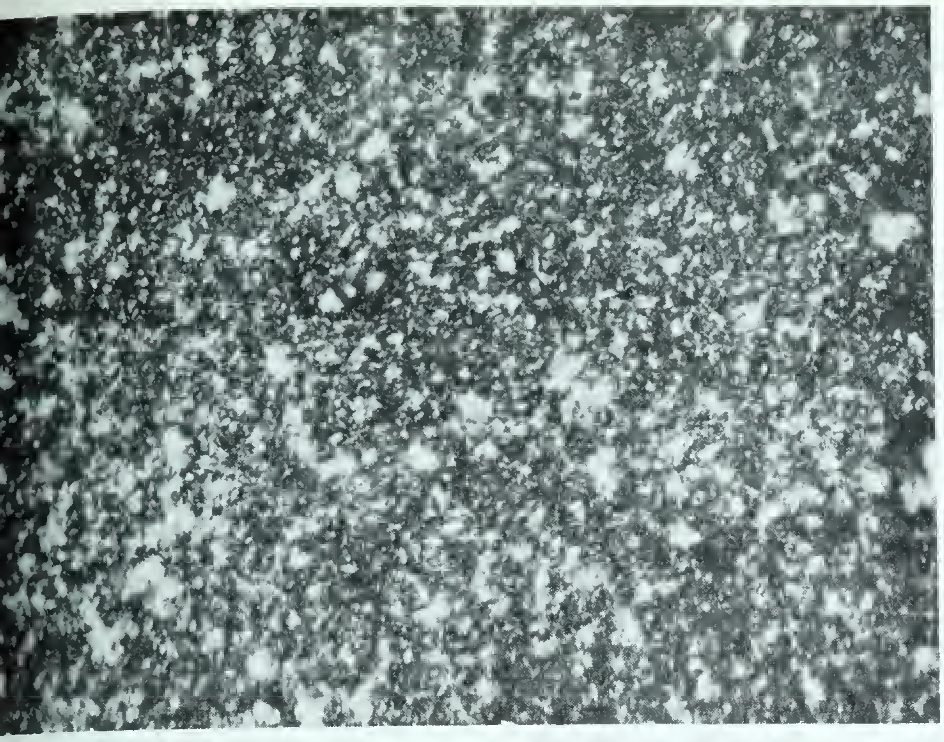

FIG.25 A QUARTZ SURFACE AFTER POLISHING, BEFORE DISSOLUTION. 380X

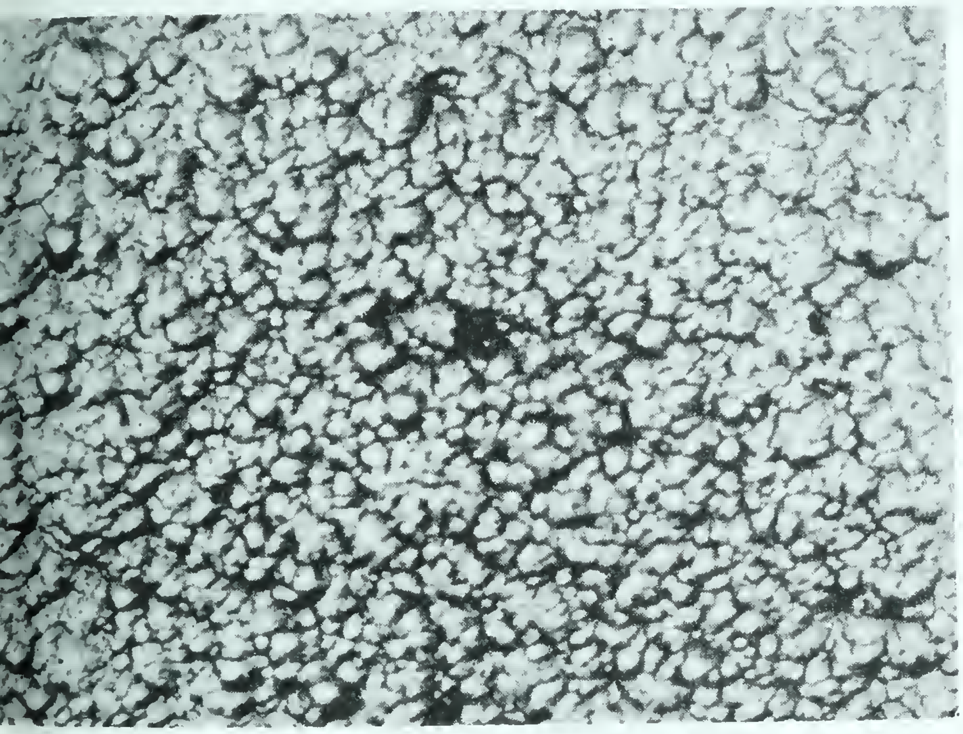

FIG.25 B QUARTZ SURFACE AFTER DISSOLUTION AT 315°C. 380X

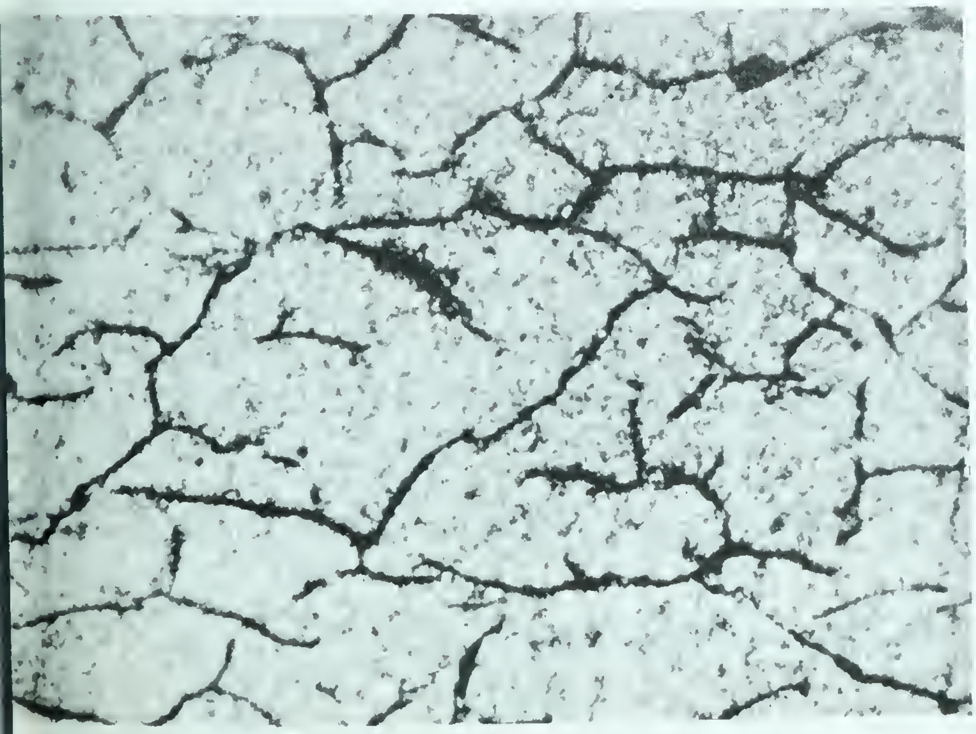

FIG.25 C QUARTZ SURFACE AFTER DISSOLUTION AT 219°C. 137X

CONCLUSIONS

The reaction of quartz with water can be stoichiometrically represented by:

$$SiO_{2\,(solid)} + H_2O_{(1)} \rightleftharpoons Si(OH)_{4\,(in\ solution)}$$

The mechanism by which it dissolves is most likely:

(1) disintegration of mosaic elements due to the dissolution of the higher solubility material cementing them together;

(2) the appearance in solution of colloidal particles 800 Å in diameter (from the elements forming the mosaic) and monomeric silica (from the material cementing the elements of the mosaic);

(3) further disintegration of the colloid to polysilicic acid and monosilicic acid.

The quartz-water reaction is first order and the rate equation is:

$$\ln \left[\frac{M^e_s - M_s}{M^e_s}\right] = -k_1 \,.\, A \,.\, t \,.\left[\frac{M'_w}{M^e_s}\right]$$

where: M_s = grammols of $Si(OH)_4$

M'_w = initial concentration of water

A = concentration of quartz expressed as surface area in cm^2

k_1 = rate of forward reaction.

M^e_s = concentration of $Si(OH)_4$ at equilibrium in grammols

t = time interval in seconds

This rate equation should be applicable over the whole range from initial dissolution to nearly equilibrium.

The activation energy for the dissolution of both quartz powders and platelets in water is of the order of 18.7 kcal/mole, suggesting a surface reaction as the controlling step in the dissolution of quartz in water for both basal and randomly oriented planes of quartz.

The basal (0001) plane of a quartz plate appears to dissolve at seventy times the rate at which the randomly oriented planes of quartz powders dissolve.

Both random and systematic errors appear to have been minimal during these experiments, even though the apparatus and experimental technique were complex.

Dissolved quartz appears to adsorb at the solution stainless steel interface as colloidal particles (each particle containing more than ten silica molecules) or as a polysilicic acid containing about ten silica units per acid radical, rather than in the form of discrete molecules.

A rapidly dissolving layer of high solubility quartz was found to exist on the ground quartz particles, the depth of which was calculated to be 206 Å.

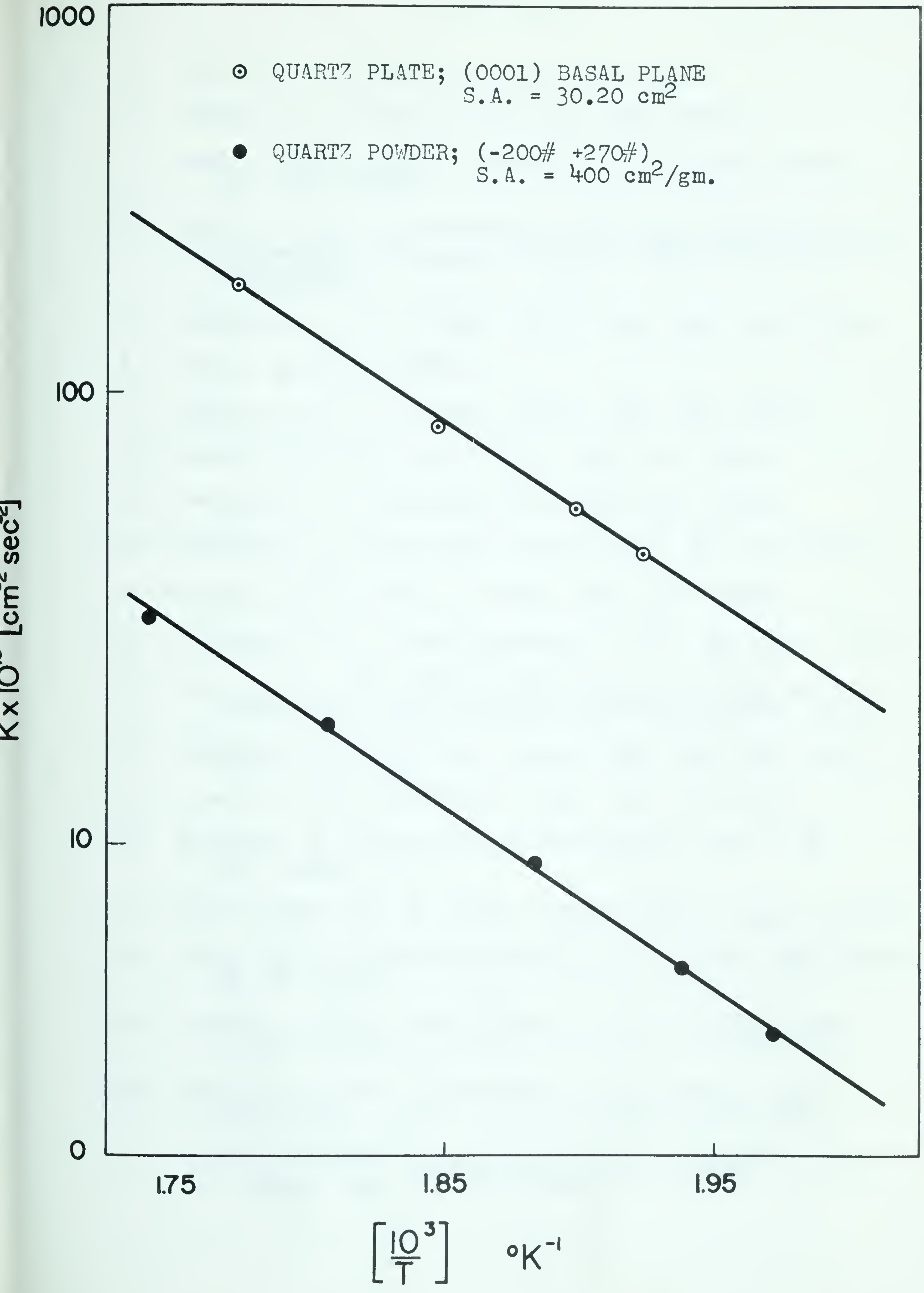

FIG. 26 ARRHENIUS PLOT FOR ACTIVATION ENERGY

REFERENCES

1. Van Lier, J. A. et al., 64, 1675 (1960).
2. Liberti, A., Chem. & Ind., 51, 1983 (1963).
3. Morey, G. W., et al., Geochim. et Cosmochim. Adtn., 26, 1029 (1962).
4. Burkin, A. R., Proceedings of the International Mineral Processing Congress, 6-9 April 1960, Inst. Min. & Metallurgy.
5. Kitahara, S., Rev. Phys. Chem. Japan, 30, 122 (1960).
6. Ibid., 30, 109 (1960).
7. Laudise, R. A., J. Phys. Chem., 65, 1396 (1961).
8. Wood, J. A. Jr., Am. J. Sci., 256, 40 (1958).
9. Kennedy, G. C., Econom. Geol., 45, 629 (1950).
10. Kitahara, S., Rev. Phys. Chem. Japan, 30, 122 (1960).
11. Hooley, J. G., Can. J. Chem., 39, 1221 (1961).
12. O'Connor, T. L., and Greenberg, S. A., 62, 1195 (1958).
13. Iler, R. K., The Colloid Chemistry of Silica and Silicates, pp. 13-14, Cornell University Press, 1955.
14. Kitahara, S., Rev. Phys. Chem. Japan, 30, 115 (1960).
15. Franck, E. U., Z. Physik. Chem., 6, 345 (1956).
16. Mosebach, R., Neues Jahrbuch Mineralog. Abb., 87, 351 (1955).
17. Brintzinger, H., Z. Anorg. Allgem Chem., 196, 44 (1931).
18. Kitto, P. H., and Patterson, H. S., J. Ind. Hyg. Toxicol, 24, 59 (1942).
19. Dempster, P. B., and Ritchie, P. D., J. Appl. Chem., 3, 182 (1953).
20. Dempster, P. B., and Ritchie, P. D., Nature, 169, 538 (1952).
21. Clelland, D. W., Cumming, W. W., and Ritchie, P. D., J. Appl. Chem., 2, 31 (1952).

22. Clelland, D. W., and Ritchie, P. D., J. Appl. Chem., 2, 42 (1952).

23. Gibb, J. G., Ritchie, P. D., and Sharpe, J. W., J. Appl. Chem., 3, 213 (1953).

24. Holt, P. F. and King, D. T., J. Chem. Soc., 773 (1955).

25. Laudise, R. A., J. Am. Chem. Soc., 81, 562 (1959).

26. Alexander, G. B., Heston, W. M., and Iler, R. K., J. Phys. Chem., 58, 453 (1954).

27. Alexander, G. B., J. Am. Chem. Soc., 75, 5655 (1953).

28. Govett, G. J. S., Anal. Chem. Acta., 25, 69 (1961).

29. Frederickson, A. F., Cox, J. E., American Mineralogist, 39, 886 (1954).

30. O'Connor, T. L., J. Phys. Chem., 65, 1 (1961).

31. Mugge, V. O., pp. 96-126, Festschrift Harry Rosenbusch, Stuttgart, 1906.

32. Jander, G., Jahr, K. F., 41, 48 (1934), Coll. Beihefte.

33. Heavens, O. S., Acta Cryst., 6, 571 (1953).

34. Puxley, P. A., Private Communication, Feb. 14, 1963.

35. Lilge, E. O., Clarke, D. R., The Hydrocyclone, Progress Report #3, Mar. 1961, University of Alberta, Dept. of Mining & Metallurgy.

36. Greenberg, S. A., J. Phys. Chem., 61, 960 (1957).

37. Chemistry 370, 372 & 470 Manual, 1959.

38. "The Kinetics of the Dissolution of Crystalline Quartz in Water at High Temperature and High Pressures--in Unit Processes in Hydrometallurgy," H. Siebert, W. V. Youdelis, J. Leja, E. O. Lilge, (Dallas, Feb. 25-28, 1963), Ed. by M. E. Wadsworth and F. T. Davis, Publ. Gordon and Breach, Science Publishers, N. Y.

39. "A Multiple-Bomb Leaching Unit," E. O. Lilge and H. Siebert. Presented at the Hydrometallurgy Symposium in Dallas, February 1963. Submitted for publication to A.I.M.E., February 10, 1964.

Rate Equation Calculations

The first order rate equation derived has the form:

$$\ln\left[\frac{M^e_s - M_s}{M^e_s}\right] = -k_1 tA\left[\frac{M'_w}{M^e_s}\right]$$

If $\ln\left[\frac{M^e_s - M_s}{M^e_s}\right]$ is plotted vs. t,

$$\text{the slope} = -k_1 A\left[\frac{M'_w}{M^e_s}\right]$$

and we can solve for k_1.

Therefore, we must first calculate

$$\ln\left[\frac{M^e_s - M_s}{M^e_s}\right]$$

(i) Calculation of $\ln\left[\frac{M^e_s - M_s}{M^e_s}\right]$

$$\ln\left[\frac{M^e_s - M_s}{M^e_s}\right] = \ln\left[1 - \frac{M_s}{M^e_s}\right]$$

Since we have the ratio $\frac{M_s}{M^e_s}$, we can use the values C_s/C^e_s in its place.

$$M_s = \frac{C_s}{60 \times 10^3} \times \frac{V}{1000}$$

$$\text{and } M^e_s = \frac{C^e_s}{60 \times 10^3} \times \frac{V}{1000}$$

where C_s and C^e_s are in mg/l.

Therefore,

$$\ln\left[1 - \frac{M_s}{M^e_s}\right] = \ln\left[1 - \frac{C_s}{C^e_s}\right]$$

Similarly, the reaction we are studying is

$$SiO_2 + H_2O \rightleftharpoons Si(OH)_4$$

but C_s and C^e_s are both in terms of weight of SiO_2, however the ratio again takes care of this.

Therefore, for C_s we use the experimental value; for C^e_s we get the value from the isobaric solubility curve (Fig. 1) on the 201 bar isobar and at the required temperature.

Example: (Run #1)

At 201 bars and 244.2°C

C_s = 6.21 mg/l at 30 minutes

Therefore,

$$\left[1 - \frac{C_s}{C^e_s}\right] = \left[1 - \frac{6.21}{455}\right]$$

$$\ln\left[1 - \frac{6.21}{455}\right] = -0.01715$$

(ii) Calculation of Rate Constant k_1 from Slope

$$k_1 = -\text{slope} \times \frac{1}{A} \times \frac{M^e_s}{M'_w}$$

$$\frac{M^e_s}{M'_w} = \frac{C^e_s \cdot \frac{V}{1000}}{55.5 \frac{V}{1000}} \times \frac{1}{6 \times 10^4}$$

$$= 3C^e_s \times 10^{-7}$$

Therefore,

$$k_1 = -\text{slope} \times 3\frac{C^e_s}{A} \times 10^{-7} \text{ sec}^{-1} \text{ cm}^{-2}$$

Example: (Experiment #1)

$$\text{Slope} = -24.65 \times 10^{-5} \text{ min}^{-1}$$

$$A = 400 \text{ cm}^2/\text{gm} \times 2.7 \text{ gm}$$

$$C^e_s = 45.5 \text{ mg/l}$$

Therefore,

$$k_1 = + \frac{24.65 \times 10^{-5} \times 455 \times 3 \times 10^{-7}}{400 \times 60 \times 2.7}$$

$$= 5.19 \times 10^{-13} \text{ sec}^{-1} \text{ cm}^{-2}$$

Note: All slopes were calculated by least squares analysis on a computer. The data is compiled on Table IX.

Calculation of Activation Energy

$$k_1 = Ae^{-Eact/RT}$$

$$\log k_1 = \log A' \frac{-Eact}{RT}$$

$$\log k'_1 - \log k''_1 = -\frac{Eact}{4.58}\left[\frac{1}{T_1} - \frac{1}{T_2}\right]$$

or $$Eact = \frac{-\log k'_1 - \log k''_1}{\frac{1}{T_1} - \frac{1}{T_2}} \times 4.58$$

The slope of a plot of $\log k_1$ vs. $1/T$ (Arrhenius plot) can be used to get Eact,

and $$Eact = -4.58 \times \text{slope}$$

The slope was calculated by least squares of a computer for both the powder and platelet runs, and the results are listed below:

	Slope	Std. Dev. Slope	Eact
Powder Tests	4.1176	± .0273	18.86 ± 0.13 kcal/mole
Platelet Tests	3.9768	± .1247	18.21 ± 0.57 kcal/mole

TABLE VIII - 1

EXPERIMENTAL DATA AND CALCULATIONS FOR A FIRST ORDER REACTION

Interval No.	Time Interval (Min.)	C_s Mg/L	C^e_s Mg/L	$-\ln(1-M_s/M^e_s)$
	0	1.24	455	0.00300
1				
	7.5	3.05	455	0.00702
2				
	15	4.54	455	0.01005
3				
	30	6.21	455	0.01715
4				
	45	8.73	455	0.01918
5				
	63	10.45	455	0.02327
6				
	80	12.58	455	0.02840
7				
	100	14.54	455	0.03252
8				
	120	17.12	455	0.03874
9				
	150	19.85	455	0.04500
10				
	180	23.20	455	0.05235
11				
	210	27.10	455	0.06188
12				
	240	29.30	455	0.06614

Pressure = 3000 psi or 201 Bars

Temperature = 244.2 ± 1.1°C

Weight of Powder = 2.700 Gms.

Initial Volume of Solution = 500 Mls.

Type of Sample = (-200#, +270#) Quartz Powder

TABLE VIII - 2

EXPERIMENTAL DATA AND CALCULATIONS FOR A FIRST ORDER REACTION

Interval No.	Time Interval (Min.)	C_s Mg/L	C^e_s Mg/L	$-\ln(1-M_s/M^e_s)$
	0	1.04	460	0.00200
1				
	6	1.54	460	0.00300
2				
	10	2.01	460	0.00401
3				
	26	3.86	460	0.00803
4				
	40	5.70	460	0.01207
5				
	60	7.75	460	0.01715
6				
	90	11.05	460	0.02429
7				
	120	14.50	460	0.03149
8				
	150	18.55	460	0.04082
9				
	180	21.60	460	0.04814
10				
	210	25.60	460	0.05763
11				
	240	27.90	460	0.06294

Pressure = 3000 psi or 201 Bars

Temperature = 245 ± 0°F

Weight of Powder = 2.700 Gms.

Initial Volume of Solution = 500 Mls.

Type of Sample = (-200#, +270#) Quartz Powder, previously leached for 12 hrs. @ 430°F

TABLE VIII - 3

EXPERIMENTAL DATA AND CALCULATIONS FOR A FIRST ORDER REACTION

Interval No.	Time Interval (Min.)	C_s Mg/L	C^e_s Mg/L	$-\ln(1-M_s/M^e_s)$
	0	0.96	455	0.00200
1				
	5	2.00	455	0.00401
2				
	15	3.36	455	0.00702
3				
	32	4.74	455	0.01106
4				
	50	6.28	455	0.01410
5				
	68	7.83	455	0.01715
6				
	111	11.09	455	0.02429
7				
	147	13.90	455	0.03046
8				
	177	16.00	455	0.03563
9				
	212	18.43	455	0.04082
10				
	240	19.35	455	0.04291

Pressure = 3000 psi or 201 Bars

Temperature = 243.9 ± 0°C

Weight of Powder = 1.700 Gms.

Initial Volume of Solution = 500 Mls.

Type of Sample = (-200#, +270#) Quartz Powder

TABLE VIII - 4

EXPERIMENTAL DATA AND CALCULATIONS FOR A FIRST ORDER REACTION

Interval No.	Time Interval (Min.)	C_s Mg/L	C^e_s Mg/L	$-\ln(1-M_s/M^e_s$
	0	0.85	455	0.00200
1				
	5	1.53	455	0.00300
2				
	15	3.49	455	0.00803
3				
	33	5.37	455	0.01207
4				
	48	6.67	455	0.01511
5				
	61	8.22	455	0.01816
6				
	98	11.74	455	0.02634
7				
	130	14.60	455	0.03252
8				
	161	17.90	455	0.03978
9				
	190	19.80	455	0.04395
10				
	220	22.70	455	0.05129

Pressure = 3000 psi or 201 Bars

Temperature = 243.9 ± .3°C

Weight of Powder = 2.0500 Gms.

Initial Volume of Solution = 500 Mls.

Type of Sample = (-200#, +270#) Quartz Powder

TABLE VIII - 5

EXPERIMENTAL DATA AND CALCULATIONS FOR A FIRST ORDER REACTION

Interval No.	Time Interval (Min.)	C_s Mg/L	C^e_s Mg/L	$-\ln(1-M_s/M^e_s)$
	0	1.85	455	0.00401
1				
	5	2.79	455	0.00602
2				
	15	4.06	455	0.00904
3				
	30	6.24	455	0.01410
4				
	45	8.15	455	0.01816
5				
	62	10.12	455	0.02225
6				
	92	13.11	455	0.02943
7				
	120	16.45	455	0.03666
8				
	150	18.85	455	0.04395
9				
	180	22.15	455	0.05024
10				
	220	27.30	455	0.06188

Pressure = 3000 psi or 201 Bars

Temperature = 243.9 ± 0.5°C

Weight of Powder = 2.7000 Gms.

Initial Volume of Solution = 700 Mls.

Type of Sample = (-200#, +270#) Quartz Powder

TABLE VIII - 6

EXPERIMENTAL DATA AND CALCULATION FOR A FIRST ORDER REACTION

Interval No.	Time Interval (Min.)	C_s Mg/L	C^e_s Mg/L	$-\ln(1-M_s/M^e_s)$	Volume Sample	Experiment No.
1	45	6.07	460	0.01309	0	6A
2	105	12.30	450	0.02737	0	6B
3	165	18.27	455	0.04082	0	6C
	225	25.74	455	0.05868	0	6D
		Avg.	455			

Pressure = 3000 psi or 201 Bars

Temperature = 6A 244.7 ± 0.5°C
6B 243.3 ± 2.0°C
6C 243.9 ± 0.5°C
6D 243.9 ± 0.5°C

Weight of Powder = 2.700 Gms.

Initial Volume of Solution = 500 Mls.

Type of Sample = (-200#, +270#) Quartz Powder

NOTE: All readings were referred to 15 minutes as zero time so that runs 6 and 7 could be compared to check the effect of sampling on the experimental system. This was found necessary because the amount of silica adsorbed on the autoclave walls was not constant for each experiment.

TABLE VIII - 7

EXPERIMENTAL DATA AND CALCULATIONS FOR A FIRST ORDER REACTION

Interval No.	Time Interval (Min.)	C_s Mg/L	C^e_s Mg/L	$-\ln(1-M_s/M^e_s)$	Volume Sample
	47	6.73	456	0.01511	30.58
1					
	107	12.88	456	0.02840	30.84
2					
	166	19.23	456	0.04291	30.08
3					
	225	25.53	456	0.05763	30.37

Pressure = 3000 psi or 201 Bars

Temperature = 244.2 ± 0.5°C

Weight of Powder = 2.7000 Gms.

Initial Volume of Solution = 500 Mls.

Type of Sample = (-200#, +270#) Quartz Powder

NOTE: All readings were referred to 15 minutes as zero time so that runs 6 and 7 could be compared to check the effect of sampling on the experimental system. This was found necessary because the amount of silica adsorbed on the autoclave walls was not constant for each experiment.

TABLE VIII - 8

EXPERIMENTAL DATA AND CALCULATIONS FOR A FIRST ORDER REACTION

Interval No.	Time Interval (Min.)	C_s Mg/L	C^e_s Mg/L	$-\ln(1-M_s/M^e_s)$
	0	0.84	450	0.00200
1				
	5	3.09	450	0.00702
2				
	15	4.12	450	0.00904
3				
	36	7.45	450	0.01715
4				
	60	10.25	450	0.02327
5				
	98	15.15	450	0.03459
6				
	125	19.48	450	0.04395
7				
	150	21.65	450	0.04919
8				
	181	24.90	450	0.05657
9				
	210	27.85	450	0.06401
10				
	240	30.45	450	0.07042

Pressure = 3000 psi or 201 Bars

Temperature = 242.8 ± 0.6°C

Weight of Powder = 2.7000 Gms.

Initial Volume of Solution = 500 Mls.

Type of Sample = (-200#, +270#) Quartz Powder

TABLE VIII - 9

EXPERIMENTAL DATA AND CALCULATIONS FOR A FIRST ORDER REACTION

Interval No.	Time Interval (Min.)	C_s Mg/L	C^e_s Mg/L	$-\ln(1-M_s/M^e_s)$
	0	0.63	370	0.00200
1				
	10	2.51	370	0.00702
2				
	35	4.96	370	0.01309
3				
	85	9.27	370	0.02532
4				
	126	12.12	370	0.03356
5				
	155	14.60	370	0.03978
6				
	185	16.55	370	0.04604
7				
	215	19.00	370	0.05235
8				
	240	21.10	370	0.05869

Pressure = 3000 psi or 201 Bars

Temperature = 233.2 ± 0.5°C

Weight of Powder = 2.700 Gms.

Initial Volume of Solution = 500 Mls.

Type of Sample = (-200#, +270#) Quartz Powder

TABLE VIII - 10

EXPERIMENTAL DATA AND CALCULATIONS FOR A FIRST ORDER REACTION

Interval No.	Time Interval (Min.)	C_s Mg/L	C^e_s Mg/L	$-\ln(1-M_s/M^e_s)$
	0	2.29	533	0.00401
1				
	6	4.10	533	0.00803
2				
	15	6.18	533	0.01207
3				
	31	10.55	533	0.02020
4				
	60	16.10	533	0.03046
5				
	90	21.55	533	0.04082
6				
	125	27.45	533	0.05235
7				
	160	33.35	533	0.06507
8				
	185	38.05	533	0.07365
9				
	210	42.80	533	0.08338

Pressure = 3000 psi or 201 Bars

Temperature = 257.8 ± 0.5°C

Weight of Powder = 2.700 Gms.

Initial Volume of Solution = 500 Mls.

Type of Sample = (-200#, +270#) Quartz Powder

TABLE VIII - 11

EXPERIMENTAL DATA AND CALCULATIONS FOR A FIRST ORDER REACTION

Interval No.	Time Interval (Min.)	C_s Mg/L	C^e_s Mg/L	$-\ln(1-M_s/M^e_s)$
	0	1.92	642	0.00300
1				
	5	5.67	642	0.00904
2				
	20	12.55	642	0.01980
3				
	40	21.92	642	0.03490
4				
	60	29.10	642	0.04604
5				
	80	36.60	642	0.05869
6				
	100	43.55	642	0.07042
7				
	120	50.60	642	0.08230

Pressure = 3000 psi or 201 Bars

Temperature = 280 ± 0.5°C

Weight of Powder = 2.7000 Gms.

Initial Volume of Solution = 500 Mls.

Type of Sample = (-200#, +270#) Quartz Powder

TABLE VIII - 12

EXPERIMENTAL DATA AND CALCULATIONS FOR A FIRST ORDER REACTION

Interval No.	Time Interval (Min.)	C_s Mg/L	C^e_s Mg/L	$-\ln(1-M_s/M^e_s)$
	0	2.18	732	0.00300
1				
	5	10.90	732	0.01511
2				
	18	17.50	732	0.02429
3				
	30	25.95	732	0.03563
4				
	45	36.30	732	0.05129
5				
	60	44.60	732	0.06294

Pressure = 3000 psi or 201 Bars

Temperature = 301 ± 0.5°C

Weight of Powder = 2.7000 Gms.

Initial Volume of Solution = 500 Mls.

Type of Sample = (-200#, +270#) Quartz Powder

TABLE VIII - 13

EXPERIMENTAL DATA AND CALCULATIONS FOR A FIRST ORDER REACTION

Interval No.	Time Interval (Hrs.)	C_s Mg/L	C^e_s Mg/L	$-\ln(1-M_s/M^e_s)$
	0	0	490	0.000
1				
	2.08	6.21	490	0.01309
2				
	4.00	11.1	490	0.02327
3				
	7.00	18.2	490	0.03770
4				
	11.00	25.3	490	0.05340
5				
	16.33	36.0	490	0.07580
6				
	24.08	47.8	490	0.10314
7				
	31.00	60.0	490	0.13011
8				
	39.00	72.0	490	0.15900
9				
	48.00	87.6	490	0.19723
10				
	55.00	97.5	490	0.22189
11				
	64.00	116.0	490	0.27050
12				
	72.00	129.8	490	0.30788

Pressure = 3000 psi or 201 Bars

Temperature = 249.6 ± 1.4°C

Initial Volume of Solution = 600 Mls.

Type of Sample = (0001) Basal Plane of Quartz Crystal, Surface Area = 30.20 cm^2

TABLE VIII - 14

EXPERIMENTAL DATA AND CALCULATIONS FOR A FIRST ORDER REACTION

Interval No.	Time Interval (Hrs.)	C_s Mg/L	C^e_s Mg/L	$-\ln(1-M_s/M^e_s)$
	0	0	471	0.00
1				
	2.5	5.02	471	0.01106
2				
	4.5	7.6	471	0.01613
3				
	7.0	11.3	471	0.02429
4				
	10.8	18.3	471	0.03978
5				
	15.8	25.6	471	0.05551
6				
	24.1	36.2	471	0.08013
7				
	31.1	47.6	471	0.10536

Pressure = 3000 psi or 201 Bars

Temperature = 247 ± 2°C

Initial Volume of Solution = 600 Mls.

Type of Sample = (0001) Basal Plane of Quartz Crystal, Surface Area = 30.20 cm^2

TABLE VIII - 15

EXPERIMENTAL DATA AND CALCULATIONS FOR A FIRST ORDER REACTION

Interval No.	Time Interval (Hrs.)	C_s Mg/L	C^e_s Mg/L	$-\ln(1-M_s/M^e_s)$
	0	0	586	0.0
1				
	2.5	4.72	586	0.00904
2				
	5.0	12.00	586	0.02020
3				
	7.0	17.50	586	0.03046
4				
	12.0	28.9	586	0.05024
5				
	14.5	35.7	586	0.06294
6				
	24.0	61.5	586	0.11093
7				
	31.0	82.4	586	0.15199
8				
	39.0	103.2	586	0.19358
9				
	48.6	129.1	586	0.24846

Pressure = 3000 psi or 201 Bars

Temperature = 268.5 ± 2°C

Initial Volume of Solution = 600 Mls.

Type of Sample = (0001) Basal Plane of Crystalline Quartz, Surface Area = 30.20 cm^2

TABLE VIII - 16

EXPERIMENTAL DATA AND CALCULATIONS FOR A FIRST ORDER REACTION

Interval No.	Time Interval (Hrs.)	C_s Mg/L	C^e_s Mg/L	$-\ln(1-M_s/M^e_s)$
	0	0	687	0.0000
1				
	3.0	10.0	687	0.01511
2				
	4.0	16.4	687	0.02429
3				
	5.0	24.6	687	0.03666
4				
	7.0	35.4	687	0.05235
5				
	9.5	47.6	687	0.07150
6				
	13.5	70.5	687	0.10870

Pressure = 3000 psi or 201 Bars

Temperature = 290.2 ± 0.5°C

Initial Volume of Solution = 596 Mls.

Type of Sample = (0001) Basal Plane of Crystalline Quartz, Surface Area = 30.20 cm^2

TABLE VIII - 17

EXPERIMENTAL DATA AND CALCULATIONS FOR A FIRST ORDER REACTION

Interval No.	Time Interval (Hrs.)	C_s Mg/L	C^e_s Mg/L	$-\ln(1-M_s/M^e_s)$
	0	0	510	0.000
1				
	2.0	2.70	510	0.00501
2				
	4.0	7.48	510	0.01511
3				
	6.6	11.68	510	0.02327
4				
	11.3	21.82	510	0.04395
5				
	17.8	31.3	510	0.06294
6				
	25.5	47.7	510	0.09761
7				
	33.0	58.4	510	0.12104
8				
	38.5	70.4	510	0.14850

Pressure = 3000 psi or 201 Bars

Temperature = 253.7 ± 2°C

Initial Volume of Solution = 607 Mls.

Type of Sample = (0001) Basal Plane of Crystalline Quartz, Surface Area = 30.20 cm^2

TABLE IX

LEAST SQUARES COMPUTER PROGRAM

```
..I H. SIEBERT LEAST SQUARES ANALYSIS 922107
..I SAVE OUTPUT CARDS
..I RUN A MAXIMUM OF 2 HOURS SAVE CARDS
..LOAD FORTRAN EXECUTE
      DIMENSION X(100),Y(100)
 20   READ 2,N,L,P95,P99
 2    FORMAT(2I5,2F10.5)
      SX=0.0
      SX2=0.0
      SXY=0.0
      SY=0.0
      SY2=0.0
      READ 3,(X(I),Y(I),I=1,N)
 3    FORMAT(2F10.5)
      DO 1 I=1,N
      SX=X(I)+SX
      SY=Y(I)+SY
      SXY=X(I)*Y(I)+SXY
      SX2=X(I)*X(I)+SX2
 1    SY2=Y(I)*Y(I)+SY2
      FN=N
      CMX=SX*SX/FN
      SMX=SX2-CMX
      CMY=SY*SY/FN
      SMY=SY2-CMY
      CMXY=SX*SY/FN
      SPM=SXY-CMXY
      B=SPM/SMX
      SSR=B*B*SMX
      SSAR=SMY-SSR
      VAR=SSAR/(FN-2.0)
      VRC=VAR/SMX
```

TABLE IX (Continued)

```
8     SDRC=VRC**0.5
9     CL95=P95*SDRC
      CL99=P99*SDRC
      XA=SX/FN
      YA=SY/FN
      A=YA-B*XA
      J=FN
      SDEV2=0
      DO 11 I=1,J
      DEV=Y(I)-A-B*X(I)
      DEV2=DEV*DEV
11    SDEV2=SDEV2+DEV2
      FJ=J
      PUNCH 14,L
14    FORMAT(10X,3HNO.I4)
      STDV=(SDEV2/(FJ-1.0))**0.5
      PUNCH 12,STDV
12    FORMAT(10X,13HST.DEV. OF Y=1F15.9)
      PUNCH 5,A,B
5     FORMAT(10X,10HINTERCEPT=1F15.9,3X,6HSLOPE=1F15.9)
      PUNCH 6,CL95,CL99
6     FORMAT(3X,26HCONFIDENCE LIMITS OF SLOPE2F15.9)
      PUNCH 7,SDRC
7     FORMAT(10X,17HST.DEV. OF SLOPE=1F20.9)
      PUNCH 16
16    FORMAT(1H )
      GO TO 20
      END
```

TABLE X - A

COMPILATION OF DATA FROM LEAST SQUARES COMPUTER ANALYSIS OF EXPERIMENTAL DATA FOR DISSOLUTION OF QUARTZ POWDER IN WATER

Test No.	-Slope x 10^{-4}	Confidence Limits of Slope x 10^{-4}		Std. Dev. Slope x 10^{-4}	Y-Intercept x 10^{-4}	Std. Dev. of "Y" x 10^{-4}
		*95% ±	99% ±	±		±
1	2.465	.153	.232	.063	83.22	9.705
2	2.607	.067	.095	.030	12.33	7.967
3	1.545	.203	.336	.0731	72.75	9.349
4	2.018	.243	.447	.076	65.25	6.366
5	2.466	.097	.152	.038	68.93	5.346
6	2.504	.486	1.121	.113	11.86	12.383
7	2.400	.202	.466	.047	33.74	5.082
8	2.474	.242	.400	.087	117.23	9.272
9	2.136	.096	.158	.034	68.02	3.949
10	3.508	.108	.179	.039	90.89	4.471
11	5.959	.180	.330	.056	107.98	3.092
12	8.960	1.027	1.886	.323	95.39	12.130

* 95% Confidence Limits means that 95 of 100 points would fall within the specified range.

TABLE X - B

COMPILATION OF DATA FROM LEAST SQUARES COMPUTER ANALYSIS OF EXPERIMENTAL DATA FOR DISSOLUTION OF QUARTZ PLATES IN WATER

Test No.	-Slope x 10^{-4}	Confidence Limits of Slope x 10^{-3}		Std. Dev. Slope x 10^{-3}	Y-Intercept x 10^{-3}	Std. Dev. of "Y" x 10^{-3}
		95%	99%			
13	4.0714	±.1870	±.2720	±.0810	+6.0821	±5.1822
14	3.2968	.1404	.2202	.0546	+2.3468	1.2994
15	5.1887	.2048	.3037	.0868	-8.314	3.7281
16	8.7570	.5969	.9860	.2144	-9.8642	1.6878
17	3.8273	.1841	.2787	.0751	-1.677	2.5320

TABLE XI

SLOPES, SPECIFIC RATE CONSTANTS AND RECIPROCAL KELVIN TEMPERATURES FOR EACH EXPERIMENT

No.	-Slope x t^{-1}	k = Slope $\frac{M_s^e}{M'_w} \times \frac{1}{A}$ $sec^{-1} cm^{-2}$	1/T °K
1	$24.65 \times 10^{-5} min^{-1}$	5.19×10^{-13}	1.933
2	$26.08 \times 10^{-5} min^{-1}$	5.55×10^{-13}	1.931
3	$15.46 \times 10^{-5} min^{-1}$	5.17×10^{-13}	1.935
4	$20.18 \times 10^{-5} min^{-1}$	5.60×10^{-13}	1.935
5	$24.66 \times 10^{-5} min^{-1}$	5.20×10^{-13}	1.935
6	$25.04 \times 10^{-5} min^{-1}$	5.24×10^{-13}	--
7	$23.96 \times 10^{-5} min^{-1}$	5.06×10^{-13}	--
8	$24.74 \times 10^{-5} min^{-1}$	* 5.15×10^{-13}	* 1.940
9	$21.36 \times 10^{-5} min^{-1}$	* 3.66×10^{-13}	* 1.975
10	$35.08 \times 10^{-5} min^{-1}$	* 8.66×10^{-13}	* 1.884
11	$59.59 \times 10^{-5} min^{-1}$	*17.71×10^{-13}	* 1.808
12	$89.60 \times 10^{-5} min^{-1}$	*30.36×10^{-13}	* 1.742
13	$40.71 \times 10^{-4} hrs^{-1}$	5.51×10^{-12}	1.914
14	$32.97 \times 10^{-4} hrs^{-1}$	* 4.29×10^{-12}	* 1.923
15	$50.52 \times 10^{-4} hrs^{-1}$	* 8.17×10^{-12}	* 1.847
16	$87.57 \times 10^{-4} hrs^{-1}$	*16.60×10^{-12}	* 1.776
17	$38.37 \times 10^{-4} hrs^{-1}$	* 5.39×10^{-12}	* 1.898

* denotes data used for Arrhenius Plot

TABLE XII

STANDARD DEVIATION OF SLOPE COMPUTED AS PER CENT

A. Powder Tests		B. Platelet Tests	
Test No.	Std. Dev. of Slope %	Test No.	Std. Dev. of Slope %
1	± 2.54	13	± 1.99
2	1.15	14	1.66
3	4.73	15	1.67
4	3.79	16	2.45
5	1.52	17	1.96
6	4.51		
7	1.96		
8	3.52		
9	1.59		
10	1.11		
11	0.94		
12	3.60		
Average	± 2.58%	Average	± 1.95%

TABLE XIII

STANDARD DEVIATION OF C_s COMPARED TO MAXIMUM DEVIATION OF C_s

Test No.	Std. Dev. Y^{I} x 10^{-4}	Std. Dev. C_s^{II} mg/l	Max. Dev. C_s^{III} mg/l
1	± 9.705	± 0.44	± 1.17
2	7.967	0.73	1.12
3	9.349	0.42	0.71
4	6.366	0.29	0.91
5	5.346	0.24	1.09
6	12.383	0.56	1.03
7	5.082	0.73	1.02
8	9.272	0.42	1.22
9	3.949	0.15	0.84
10	4.471	0.24	1.71
11	3.092	0.19	2.02
12	12.130	0.89	1.78
13	51.822	2.53	5.19
14	12.994	0.61	1.90
15	37.281	2.17	5.16
16	16.878	1.16	2.82
17	25.320	1.29	2.82

I - Obtained from the least squares computer analysis of the results

II - $Y = -\ln\left[1 - \frac{M_s}{M^e_s}\right] = -\ln\left[1 - \frac{C_s}{C^e_s}\right]$

Therefore,

$C_s = (1 - \ln Y)C^e_s$ since C^e_s = constant at a given temperature and pressure

TABLE XIII - Continued

III - Error here is in reading values of O.D. from the colorimeter; all other quantities involved can be read so accurately that error due to them is negligible.

Therefore,

Average error of colorimetric method = .04 C_s

Use maximum value of C_s obtained in each run.

B29823